UNIVERSITÄTSKLINIKUM HAMBURG-EPPENDORF

III. Department of Medicine

Professor Dr. med. Tobias B. Huber

Establishment of a membranous nephropathy model in transgenic rats expressing human PLA_2R on podocytes

Dissertation

for the academic degree of Doctor of Human Biology (Dr. rer. biol. hum.)
at the
Medicine Faculty of the University of Hamburg

Submitted by

Nicoletta Ferru
from
Italy

Hamburg 2025

Angenommen von der

Medizinischen Fakultät der Universität Hamburg am: 05.06.2026

Veröffentlicht mit Genehmigung der

Medizinischen Fakultät der Universität Hamburg.

Prüfungsausschuss, der/die Vorsitzende: Prof. Dr. Elion Hoxha

Prüfungsausschuss, zweite/r Gutachter/in: Prof. Dr. Thorsten Wiech

Table of contents

1. Introduction 6

1.1 Kidney anatomy and functions 6
1.1.1 Glomerular filtration barrier 7

1.2 Membranous nephropathy 9
1.2.1 Epidemiology and clinical presentation 10
1.2.2 Diagnosis 10
1.2.3 Treatment 11
1.2.4 Clinical trials 12

1.3 Membranous nephropathy pathogenesis 14
1.3.1 Patho-mechanisms and predisposing genetic factors 14
1.3.2 Major endogenous antigens: PLA_2R and THSD7A 16
1.3.3 Anti PLA_2R antibodies 17
1.3.4 Potential new antigens associated with MN 18

1.4 Established animal models for PLA_2R associated MN 19
1.4.1 Heymann nephritis 19
1.4.2 PLA_2R-induced MN model in Göttingen minipigs 21
1.4.3 Mice transgenic models of PLA_2R associated MN 22

1.5 Project aim 23

2. Materials and methods 24

2.1 List of materials, reagents, consumables, machines and solutions 24

2.2 Animals 29

2.3 Genotyping 30
2.3.1 Hemizygous rats 30
2.3.2 Homozygous rats 32

2.4 Animal experiments 34
2.4.1 Active immunisation 34
2.4.2 Passive immunisation 35

2.5 Samples collection 36
2.5.1 Kidney perfusion 36
2.5.2 Glomeruli isolation 37
2.5.3 Kidney preparation for histology 38

2.6 Rat plasma 38
2.6.1 Detection of anti PLA_2R antibodies by western blot 38

2.6.2 Detection of anti PLA_2R antibodies by commercial ELISA 39

2.7 Rat kidney 40
2.7.1 Tissue preparation for histology 40
2.7.2 Periodic acid Schiff staining 40
2.7.3 Immunofluorescence staining 40
2.7.4 Rat glomerular extract production 41
2.7.5 Quantification of total protein concentration 41
2.7.6 Western blot analysis of RGE 42
2.7.7 Anti PLA_2R antibody elution 43

2.8 Rat urine 43
2.8.1 Albumin ELISA and creatinine assay 43
2.8.2 Urine analysis by Western blot 44

3. Results 45

3.1 Validation of PLA_2R transgene expression vectors 45

3.2 Genotyping of PLA_2R transgenic rats 48

3.3 Phenotyping of PLA_2R transgenic rats 51

3.4 Passive immunisation 54
3.4.1 Hemizygous rats 54
3.4.2 Homozygous rats 62

3.5 Active immunisation 70
3.5.1 Hemizygous rats 70
3.5.2 Homozygous rats 77

4. Discussion 87

5. Summary 94

6. List of abbreviations 97

7. List of figures 100

8. Bibliography 102

9. Note of thanks 114

10. Curriculum Vitae 115

11. Statutory declaration 116

1. Introduction

1.1 Kidney anatomy and functions

Kidneys are retroperitoneal paired organs located between the transverse processes of thoracic (T12) and lumbar (L3) vertebrae. Each kidney weighs 150-200 gr in males and 120-135 gr in females, has a length of 10 to 12 cm, a width of 5 to 7 cm and a thickness of 3 to 5 cm (Soriano et al., 2018). The median side of each kidney is concave and present a chamber, called the renal pelvis, which hosts the renal artery, vein and the ureter. The blood vessels supply oxygen and nutrients to the parenchyma and return the filtered blood to the circulation; the ureter branches into major and minor calyxes and conveys the urine to the bladder (Soriano et al., 2018). Two regions, medulla and cortex compose the renal parenchyma. The cortex is the peripheral part of the kidney, which extends towards the renal pelvis forming columns interposed in the medulla. Cortex and medulla share the structural and functional unit of the kidney called nephron (Arnold and Brown, 1966). An adult has approximately 2 million nephrons per kidney (Soriano et al., 2018). Each nephron consists of a filtration system, represented by the glomerulus, and a renal tubule adept to reabsorption and secretion. The glomerulus is essentially a capillary tuft surrounded by the Bowman's capsule which is in charge of collecting the glomerular filtrate. A system of aggregated cells, called mesangium, guarantees structural stability to the glomerular vascular loops and plays the role of scavenger removing protein aggregates and pathogens from the glomerulus (Ebefors et al., 2022). The capsule is in continuation with the renal tubule system, which is made up of proximal convoluted tubule, loop of Henle and distal convoluted tubule. Different distal convoluted tubules merge into common collecting ducts, delimiting the end of the nephron (Betts et al., 2013). Each kidney is encased by a connective tissue, named capsule. This inflects to enclose the pelvis and becomes one with the connective tissue of the calyxes wall (Betts et al., 2013). Kidneys are the organs responsible for the urine production, a process that involves the glomerular filtration, tubular reabsorption and secretion (Banerjee, 2005). The kidneys of a healthy adult filter 180 L of blood per day with a renal plasma flow (RPF) of 600-720 mL/min (Kaufman et al., 2018). The glomerular filtration occurs in the capillary network of the glomerulus and produces a plasma ultra-filtrate depleted of large proteins and cells. The volume and composition of the plasma ultra-filtrate will change in the following processes of reabsorption and secretion that take place in the renal tubule through active and passive transports as well as endocytosis (Banerjee, 2005). By means of these processes, kidneys contribute to regulate the body fluids composition. Majority of water and valuable solutes like glucose, amino acids and electrolytes are reabsorbed through trans-epithelial transports along the

proximal tubule (Gallardo et Vio, 2022). The loop of Henle includes a descending limb that is permeable to water but not to sodium chloride; vice versa the ascending part reabsorbs sodium chloride but no water. This part of the tubule plays an important role in the concentration of urine by creating a concentration gradient for water reabsorption (Banerjee, 2005). The distal part of the nephron is dedicated to fine adjustments with sodium, calcium, water reabsorption and potassium and hydrogen ions secretion (Gallardo et Vio, 2022). The tubular secretion, passage of compounds from the blood to the tubular fluid, involves different organic anions and cations such as bile salts, prostaglandins, catecholamine, histamine (Gallardo et Vio, 2022). Fine adjustments in sodium and water intake/excretion along the renal tubule are fundamental to regulate blood volume and pressure; this is made possible through systems such as the renin-angiotensin-aldosterone system (RAAS), the antidiuretic hormone (ADH), the atrial natriuretic peptide (ANP) (Gallardo et Vio, 2022). Another important role of the kidneys is the regulation of acid-base balance through the secretion of hydrogen and reabsorption of bicarbonate ions. The acid-base regulation, which occurs in the tubule cells, involves the glutamine catabolism that aim to regenerate the bicarbonate spent to neutralize hydrogen ions deriving from fixed acid. As a result of the glutamine catabolism, ammonium and bicarbonate ions are produced; Ammonium ions are then excreted in the urine while bicarbonate ions are transported to the plasma (Gallardo et Vio, 2022). Kidneys have an endocrine function which imply the release of erythropoietin, 1.25-dihydroxycholecalciferol and renin essential for the blood cell production, bone health and the regulation of blood pressure (Gallardo et Vio, 2022).

1.1.1 Glomerular filtration barrier

When the blood arrives to the glomerulus, by means of the afferent arteriole, it goes through a multi-layered filtration barrier (Figure 1) whose first components are the capillaries fenestrated endothelium and its glycocalyx in the luminal side. The glycocalyx is a negatively charged layer of proteoglycans and glycoproteins that selects the passage of molecules accordingly to their charge (Reitsma et al., 2007). The glycocalyx lays on a fenestrated endothelium, characterized by 60-80 nm transcellular holes not provided with a diaphragm (Satchell and Braet, 2008). These trans-cytoplasmic holes have a physiologic significance, in fact they allow a high rate of fluid and solutes exchanges without the need of endocytosis or receptor mediated mechanisms of transport (Finch et al., 2023). Immediately under the endothelium, there is the glomerular basement membrane (GBM), which gives structural support to the filter.

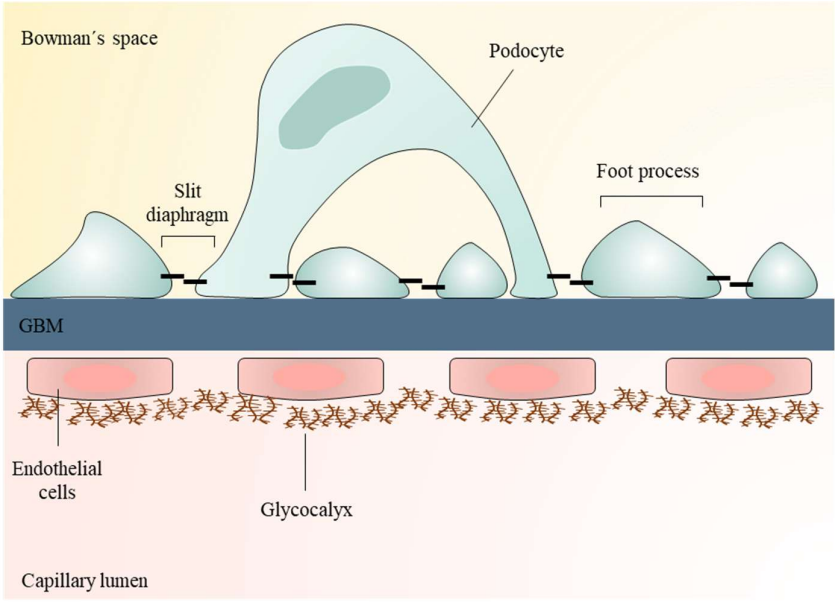


Figure 1: Schematic representation of the glomerular filtration barrier. *The glomerular filtration barrier (GBM) is composed by glycocalyx, fenestrated endothelium, glomerular basement membrane and podocytes. Created with BioRender.com.*

The GBM is made of laminin, type IV collagen, nidogen and heparin sulphate proteoglycan. All these components are synthetized by the endothelial cells and podocytes (Arif and Nihalani, 2013). Analogously to the endothelium, also the GBM exhibits a negative charge, mainly given by the presence of agrin sulphated glycosaminoglycan chains. However, the GBM contribution to the charge selectivity of the filter is conflicting. Different studies that aimed to reduce the GBM anionic properties showed in fact that no significant changes are seen in the functionality of the glomerular filtration barrier (Harvey et al., 2007; van den Hoven 2008).

The third component of the filtration barrier, facing towards the urinary space and wrapping up the capillary loops, is represented by highly differentiated epithelial cells denominated podocytes (Arif and Nihalani, 2013). Long extroflexions, called primary foot processes, develop from the cell body and branch out in further smaller secondary and tertiary foot processes (Pavenstädt et al., 2003). Podocytes have an important role in assuring structural stability to the glomerular filtration barrier. In order to guarantee adhesion to the GBM, podocyte receptors bind to specific GBM proteins such as integrins (Adler, 1992; Lennon et al., 2014). Podocytes select the passage of molecules in a size dependent manner, via a porous zipper-like structure (width= 40 nm; pores radius= 46-87 Å) that connects the space between adjacent foot processes (Ohlson et al., 2000). This structure is known as slit-diaphragm (Patrakka et al., 2009). The proteins that constitute the slit-diaphragm (nephrin, NEPH1–3, podocin, Fat1, VE-cadherin, and P-cadherin) are connected to the podocytes actin cytoskeleton and are essential for the functionality of the glomerular filtration barrier (Tryggvason et al., 2006).

All three components described above, contribute to carry out an important function of the glomerulus, which is the blood filtration, by selecting the passage of solutes according to size and charge (Sörensson et al., 2001). Low molecular weight solutes such as electrolytes, glucose, urea, creatinine and small plasma proteins with a radius smaller than 18 Å (Gallardo and Vio, 2022) can cross the filtration barrier and reach the Bowman's capsule where they become part of the glomerular ultra-filtrate. Above this radius, filterability is reduced and the anionic net charge of the molecules oppose the passage. Another important factor that regulates the dynamics of the glomerular filtration is the contraction tone of the smooth muscle of afferent and efferent arterioles (Gallardo and Vio, 2022). This resistance translates in hydrostatic pressure, which makes possible to push fluids and solutes through the glomerular filtration barrier (Ogobuiro et al., 2019). Changes in hydrostatic pressure modulate the volume of plasma, which passes from the glomerular capillaries towards the Bowman's capsule, and the glomerular filtration rate (GFR). The GFR is approximately 100-125 mL/min (Gallardo et Vio, 2022). Once in the tubule system, composition and volume of the ultra-filtrate change thanks to diffusion and active transport (ion, water channels) leading to the urine formation (Gallardo and Vio, 2022). The malfunction of the glomerular filtration process, characterized by increased permeability to macromolecules, can result from the damage of basement membrane, endothelium surface and podocytes (Verma et Patil, 2024). This leads to nephrotic syndrome, a clinical condition defined by massive loss of protein in the urine (>3 gr/24h), hypoalbuminemia, followed by hyperlipidaemia, decline in plasma colloid osmotic pressure and oedema (Tapia et Bashir, 2017). Despite membranous nephropathy representing the most common cause of nephrotic syndrome in adults, this syndrome can also occur in patients with congenital infections, diabetes, systemic lupus erythematosus, or neoplasia.

1.2 Membranous nephropathy

Membranous nephropathy (MN) is an antibody mediated glomerular autoimmune disease that represents the most frequent cause of nephrotic syndrome in adults (Ronco et al., 2021). Historically MN was classified in primary and secondary form according to the underlying cause of the disease development. In primary MN, circulating autoantibodies, predominantly belonging to IgG4 subclass, are produced against antigens expressed on the podocytes. In secondary MN concomitant diseases are present, such as systemic lupus erythematosus, cancer and infections (Hoxha et al., 2022).

1.2.1 Epidemiology and clinical presentation

Data collected from 40 studies conducted in different geographic areas (Europe, North and South America, Australasia, Middle East) showed that MN is a rare disease with an incidence rate of 1.2/100 000 per year (McGrogan et al., 2011). The occurrence in the paediatric population is lower and most of the cases are associated with co-morbid illnesses (Chen et al., 2007). MN can occur at all ages, in average it is diagnosed in 50-60 years old people with a male prevalence at a 2 to 1 ratio (Ronco et al., 2021). Most patients affected by primary MN develop autoantibodies against PLA_2R (Phospholipase A2 receptor) which account for 70-80% of cases (Beck et al., 2009; Hoxha et al., 2022). Independently from the classification into primary and secondary, MN is characterised by the accumulation of immune complexes in the sub epithelial space of the glomerular filtration barrier; these deposits, containing immunoglobulins, antigens and complement components, eventually lead to podocytes injury and impairment of the glomerular filter structure (Ronco et al., 2021; Hoxha et al., 2022). Consequently to this, patients develop the main clinical manifestation, which is proteinuria. Among the patients, an 80% develop nephrotic range proteinuria (>3.5 g/d), while the remaining 20% shows low levels of proteinuria (Couser, 2017). In case nephrotic syndrome occurs, other symptoms are observed alongside the loss of proteins in the urine, such as hypoalbuminemia (<30 g/L), hyperlipidemia and edema (Tapia, 2017).

1.2.2 Diagnosis

The diagnosis is made with the observation of the clinical symptoms, with laboratory tests and autoimmune screening for the detection of PLA_2R antibodies in patients' serum; the detection of PLA_2R antibodies in the serum can be done with commercially immunofluorescence test (IFT) and enzyme linked immunosorbent assay (ELISA) or by western blot (Rovin et al., 2021). Kidney biopsy is the gold standard to make the diagnosis of glomerular diseases, however it can be avoided in the presence of specific clinical situations such as positivity for PLA_2R antibodies, eGFR> 60, no diabetes and no causes of secondary MN (Rovin et al., 2021). In the examination of the renal biopsy, different microscopy techniques (light microscopy, immunofluorescence, and electron microscopy) are applied to search for the morphological characteristics of the disease (Glassock, 2003). At the early stage of the disease, when analysed by light microscopy using conventional staining such as methenamine and periodic acid Schiff, the capillary walls appear normal. Only in the later stages, the capillary walls become thicker and reveal spike-like projections of the GBM (Glassock, 2003). By immunofluorescence it is possible to observe the

IgG deposition along the outer aspect of the capillary wall; the deposits show a granular appearance during the early stage of the disease and a more uniform depositions as the disease proceeds into a later stage (Glassock, 2003). Immunofluorescence can also be used to show the co-localisation of antigen, IgG and complement components such as C3, C4d, C5b-9 and C1q (Zhang et al., 2018; Seifert et al., 2023). The characteristic morphologic features visible by electron microscopy are: electron dense areas that represent the deposits in the sub-epithelial space beneath the podocytes foot processes, GBM projections (spikes) between deposits and podocyte feet effacement with slit pore membrane obliteration (Glassock, 2003).

1.2.3 Treatment

The observation of laboratory and clinical criteria (eGFR, proteinuria, PLA_2R-ab levels etc.), helps to assign patients diagnosed with MN to different levels of risk for progressive loss of kidney function (Figure 2). In order to assess treatment response and to guide adjustments to therapy, this evaluation needs to be repeated periodically every 3 and 6 months after the diagnosis (Rovin et al., 2021).

Low risk	Moderate risk	High risk	Very high risk
• Normal eGFR, proteinuria <3.5 g/d and serum albumin >30 g/l OR • Normal eGFR, proteinuria <3.5 g/d or a decrease >50% after 6 months of conservative therapy with ACEi/ARB	• Normal eGFR, proteinuria >3.5 g/d and no decrease >50% after 6 months of conservative therapy with ACEi/ARB AND • Not fulfilling high-risk criteria	• eGFR <60 ml/min/1.73 m²* and/or proteinuria >8 g/d for >6 months OR • Normal eGFR, proteinuria >3.5 g/d and no decrease >50% after 6 months of conservative therapy with ACEi/ARB AND at least one of the following: • Serum albumin <25 g/l† • PLA2Rab >50 RU/ml‡ • Urinary α_1-microglobulin >40 µg/min • Urinary IgG >1 µg/min • Urinary β_2-microglobulin >250 mg/d • Selectivity index >0.20§	• Life-threatening nephrotic syndrome OR • Rapid deterioration of kidney function not otherwise explained

Figure 2: Criteria to assess risk for loss of kidney function.
Glomerular filtration rate, proteinuria, serum albumin, urinary biomarkers and PLA_2R antibody titer are criteria used to assign patients to one of the four risk category and choose the most appropriate therapy. (Rovin et al., 2021). eGFR: estimated glomerular filtration rate. ACEi/ARB: angiotensin converting enzyme inhibitor/angiotensin II receptor blocker. PLA_2Rab: phospholipase A2 receptor antibody.

All patients with MN should receive a supportive therapy (Rovin et al., 2021). This includes the administration of angiotensin converting enzyme inhibitors or angiotensin receptor blockers to

reduce proteinuria, statins to treat hyperlipidaemia and lower the cholesterol levels in the blood, diuretics and a dietary plan poor of salt to treat oedema. (Couser, 2017). Immunosuppressive treatment can be implemented in patients from “moderate to “high” and “very high” risk of progressive loss of kidney function (Figure 3) (Rovin et al., 2021).

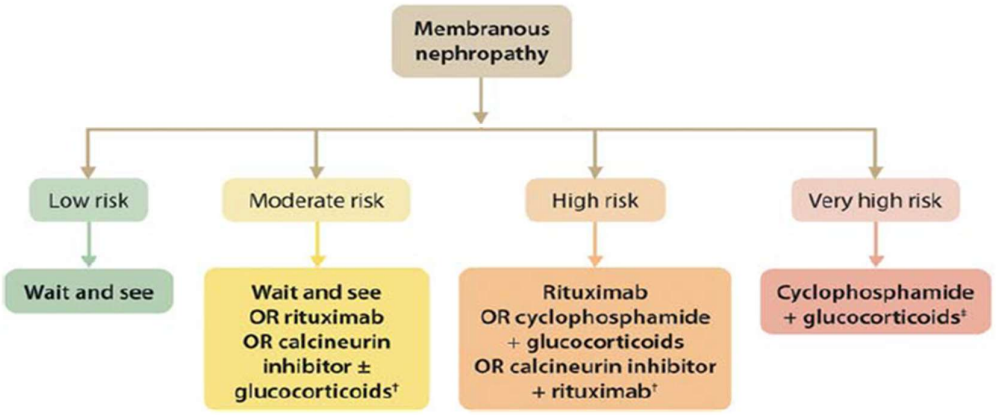


Figure 3: Therapy assignment according to risk category.
Low risk patients receive only supportive care and are kept under observation. Depending on the patient´s risk category, different immunosuppressive regimen are given (Rovin et al., 2021).

The immunosuppressive treatments applied nowadays include 3 regimen options, alkylating agents/steroids (cyclophosphamide, chlorambucil), calcineurin inhibitors/steroids (cyclosporine, tacrolimus), and monoclonal antibodies (rituximab). Among the effects on the immune system, the administration of alkylating agents reduces the cellular response including a decrease in the number of B cells and thus in the autoantibodies production (Quan et al., 2022; Cupps et al., 1982). The mechanism of action of calcineurin inhibitors relies on inhibition of calcineurin, an enzyme essential in the T cells signalling and genes activation such as the gene codifying interleukin-2 which promotes T cells proliferation; moreover, it has an antiproteinuric effect due to the stabilization of actin cytoskeleton of the podocyte (Faul et al., 2014). Rituximab, a mouse/human IgG1k chimeric monoclonal antibody specific for CD20 cell surface receptor, acts depleting B cells (Marinaki et al., 2013).

1.2.4 Clinical trials

One of the first standardized immunosuppressive treatments widely adopted for membranous nephropathy was the “Ponticelli regimen” which consists in the monthly alternating cyclic administration of steroids and alkylating agents over a six months period. The first clinical trial showed that the regimen favours remission of the nephrotic syndrome and preserves the renal function compared to patients that receive a symptomatic treatment only (Ponticelli et al., 1984).

A second trial was done to investigate the long-term effect of the regimen in which patients were followed between two to eleven years (Ponticelli et al., 1989). It was confirmed that the remission rate is higher in the treated group compared to the patients who received supportive treatment only. Side effects of this treatment included weight gain, infections, leukopenia and tumours. The efficacy of Ponticelli regimen was also studied in patients with deteriorating excretory renal function (Howman et al., 2013). This trial concluded that the risk of a further 20% decline in renal function was significantly lower in the patients treated with Ponticelli regimen compared to the other two groups: patients receiving supportive treatment and patients treated with cyclosporine. Serious adverse effects were observed in all these three groups: in 48% of patients treated with the Ponticelli regimen, in 32% of patients treated with cyclosporine and in 21% of patients that received only the supportive treatment.

In early 2000, rituximab was used to treat MN and succeeded in inducing complete or partial proteinuria remission in 60% of patients with nephrotic syndrome (Remuzzi et al., 2002; Fervenza et al., 2008). Considering the potential of these first results that showed rituximab minimal side effects, mainly infusion related, new trials were designed to confirm the efficacy of this monoclonal antibody and to compare it with the conventional treatments.

GEMRITUX was a randomized controlled trial meant to test the efficacy of rituximab versus non-immunosuppressive anti-proteinuric treatment (NIAT) in nephrotic MN patients (Dahan et al., 2017). It was observed that the addition of rituximab compared to the NIAT treatment alone decreased PLA_2R antibodies level and lead to an increase of serum albumin already after three months. This result was important to prove the possibility of using PLA_2R antibodies and serum albumin as markers to monitor the treatment. The beneficial effect of adding rituximab was confirmed after six months; the proteinuria remission rate in the NIAT-rituximab group was higher (64, 9%) compared to the patients treated with NIAT only (37, 5%). Overall, addition of rituximab didn’t show effects on safety.

The randomized trial MENTOR was designed to compare rituximab with the calcineurin inhibitor cyclosporine (Fervenza et al., 2019). Twelve months after treatment started, the percentage of partial or complete proteinuria remission was similar between the two groups (60% rituximab, 52% cyclosporine). However, at twenty four month the remission rate was 60% in the rituximab group and 20% in the cyclosporine. A further limitation of cyclosporine was the higher number of relapses after treatment withdrawal compared to rituximab (60% vs 29%). According to these results rituximab resulted superior in maintaining long term proteinuria remission. Serious non-fatal adverse effects occurred in 17% of rituximab treated patients and in 31% of cyclosporine group.

RI-CYCLO trial was planned to make a comparison between rituximab and the cyclic corticosteroid-cyclophosphamide regimen (Scolari et al., 2021). After twelve months, 62% of patients receiving rituximab and 73% receiving the cyclic regimen had partial or complete remission; at thirty six months, the percentage of patients that developed partial or complete remission was again similar between the two groups. Adverse severe effects were observed equally in both groups. The outcome of this trial showed that rituximab doesn't differ in terms of harm or benefit when compared to the Ponticelli regimen.

These immunosuppressive treatments are all accompanied by short and long term side effects. Adverse events observed in the cyclic regimen are leukopenia, infections, cardiovascular/thrombotic events and malignancies (Ponticelli et al., 1989; van den Brand et al., 2014). Infusion reactions are common in rituximab treated patients (van den Brand et al., 2017; Scolari et al., 2021) while gastrointestinal pain, nephrotoxicity and infections are some of the adverse effects associated with cyclosporine (Howman et al., 2013; Farenza et al., 2019). A limiting factor of rituximab lies in the 20-40% of unresponsive patients (Saha et al., 2023). Rituximab may display a reduced bioavailability and under-dosing because of excretion through the nephrotic urine and by internalization/destruction due to polymorphisms of the neonatal Fc receptor (Jacobs et al., 2017; Passot et al., 2013).

The disease outcome of MN patients is variable. Spontaneous remission of proteinuria occurs in 30-40% of patients (Polanco, 2010), the other two thirds of patients persist with proteinuria and among these ~ 40% progress to end stage renal disease (ESRD) within ten years from the diagnosis (Sinico, 2016). Predictor factors of poor renal outcome are male gender, increasing age, high proteinuria, elements such as interstitial fibrosis and sclerosis, elevated serum creatinine and high PLA_2R antibodies (Cattran, 2005). At the time of diagnosis, high levels of proteinuria represent a risk for loss of kidney function, however, patients with non-nephrotic proteinuria not always have a good prognosis (Hoxha et al., 2014). Monitoring PLA_2R antibodies can help to predict the clinical outcome, in fact serological remission precedes clinical remission while persistence of the antibodies is associated with resistant disease (Bech et al., 2014; Ramachandran et al., 2018; Hoxha et al., 2014).

1.3 Membranous nephropathy pathogenesis

1.3.1 Patho-mechanisms and predisposing genetic factors

70-80% of MN patients produce antibodies against PLA_2R. This protein is expressed on the podocyte of healthy human glomeruli and it is found in the immune deposits of MN patients (Beck et al., 2009). The pathogenicity of PLA_2R antibodies has been proven in an animal model

of PLA_2R specific MN (Reinhard et al. 2023). Besides PLA_2R, also other proteins can be targeted by autoantibodies. Among these are proteins expressed on the podocyte (PLA_2R, THSD7A, NTNG1) and potential exogenous antigens (NELL-1, NCAM1, EXT1/EXT2) planted in the sub epithelial space (Xu et al., 2024; Hoxha et al., 2022). It is challenging to study the development of the disease at its early stage, before the diagnosis is made. A longitudinal study (Burbelo et al., 2020) conducted on samples from the serum repository of the U.S Department of defence, showed in fact that PLA_2R antibodies can be detected months or even years (median = 274 days) before symptoms appear and the renal biopsy is performed. The binding of the autoantibodies, mainly IgG4, to the antigen induces complement activation and the assembly of the membrane attack complex C5b-9 which then leads to podocyte injury, impairment of glomerular filtration barrier and consequent proteinuria (Baker et al., 1989). The key role of the complement was at first investigated in Heymann nephritis, an experimental model of MN developed in rats (Couser, 2017). Complement components from the three activation pathways have been found in biopsies from MN patients; immunofluorescence and mass spectrometry analysis performed on MN kidney biopsies revealed positivity for C3-C9 and C1q (Zhang et al., 2018; Ravindran et al., 2020; Ayoub et al., 2021; Seifert et al., 2023). A crucial event following the complement activation is the assembly of the membrane attack complex (C5b-9) on the podocyte membrane; this induces damage through different mechanisms such as overproduction of reactive oxygen species (ROS), cytoskeletal alterations, upregulation of tumour growth factor β (TGF-β) and matrix metalloproteinase-9 (MMP9) (Pavenstadt et al., 2003). ROS are produced locally and initiate lipid peroxidation and the degradation of collagen-IV in the GBM (Neale et al., 1993; Kerjaschki et Neale, 1996). Disruption of actin cytoskeleton impairs the podocyte anchoring system to the GBM, which results in displacement of the slit diaphragm and effacement of foot processes (Beck et Salant, 2014). Eventually, the structural rearrangement of the GBM through matrix overproduction and breakdown occurs as result of TGF- β and MMP9 action respectively (McMillan et al., 1996; Shankland et al., 1996).

Primary MN is a non-hereditary disease; however, genome wide association studies (GWAS) discovered significant association with specific loci. One of these studies (Stanescu et al., 2011), performed on primary MN patients belonging to three European populations, identified significant alleles in the PLA_2R locus and in the HLA-DQ (human leukocyte antigen, class II) region. The significantly associated single nucleotide polymorphisms (SNPs) are located in non-coding regions of PLA_2R and HLA-DQ and don't impact with the proteins structure. The HLA, human equivalent of the generic MHC (Major Histocompatibility Complex), is a region of chromosome 6 dense with genes that have a key role in the immune response. HLA can be

subdivided in class I, II and III. Class I (HLA-A, B, C) and class II (HLA-DR, DP, DQ) genes encode for cell surface glycoproteins that present endogenous and exogenous antigens to $CD8^+$ cytotoxic T cells and to $CD4^+$ T helper cells, while class III encode for complement components, cytokines and lymphotoxin (Janeway et al., Immunobiology, 2009) .

A more recent GWAS (Xie et al., 2020) was extended to a bigger cohort of primary MN patients including not only European but also East Asian ancestries. This study defined ancestry specific HLA alleles and reported two new loci: nuclear factor Kappa B subunit-1 (NF-kB1) and interferon regulatory factor-4 (IRF4). NF-kB and IRF4 genes encode for transcriptional regulators of inflammation. NF-kB family is represented by dimeric transcription factors involved in the regulation of inflammatory responses, innate and adaptive immunity, cellular differentiation and proliferation (Mitchell et al., 2016). An inappropriate regulation of NF-kB can cause abnormal T-cell activation which associates with autoimmune and inflammatory responses (Liu et al., 2017). An increased NF-kB activity in podocytes was also shown to contribute to proteinuria development in passive Heymann Nephritis model (Mudge et al., 2001). NF-kB complex regulates the expression of different genes, one of these is IRF4 (Grumont et Gerondakis, 2000). IRF4 is a transcription factor expressed in immune T and B cells, macrophages and dendritic cells, that has a central role in the regulation of innate and adaptive immune system and whose activation is induced by Toll-like receptor, T-cell receptor and tumour necrosis factor signalling (Lu et al., 2023).

Despite the male predominance of MN, no sex-specific risk loci where found (Sekula et al., 2017). Finding genetic variants it is important for several reasons such as: understanding the mechanisms involved in podocyte damage and proteinuria development, identifying risk factors that predispose some individuals more than others to the disease, design targeted therapies and personalize treatments to improving patient's outcome.

1.3.2 Major endogenous antigens: PLA_2R and THSD7A

The major podocyte antigens that are targeted by autoantibodies are the proteins PLA_2R and THSD7A (thrombospondin type 1 domain containing protein 7A) which account for 70-80% and 2.5-5% of MN patients respectively (Beck et al., 2009; Tomas et al., 2014). PLA_2R is a 185 kDa transmembrane glycoprotein, belonging to the mannose receptor family, abundantly expressed on podocytes but also found in lungs, pancreas and placenta (Q13018-Uniprot, 2023). Its extracellular structure consists of a cysteine rich domain (Cys-R), a fibronectin II domain and 8 C-type lectin domains (CTLD). PLA_2R presents different post translational modifications, among which various disulphide bonds and three N-glycosylations. This receptor is responsible

for binding and internalising secreted phospholipase A2 ($sPLA_2$) suggesting that its role could be to inhibit $sPLA_2$ action (release of arachidonic acid, cell adhesion and signalling) or to produce second messengers upon $sPLA_2$ internalisation and degradation (Ancian et al., 1995). Even though the exact role of PLA_2R in the podocyte is still not fully clear a study conducted in vitro showed that $sPLA_2$ induces podocyte apoptosis in a time and dose dependent manner (Pan et al., 2014).

In 2014 Tomas et al discovered THSD7A, the second most common endogenous antigen targeted by antibodies in MN patients. This 250 kDa transmembrane glycoprotein is characterized by a big extracellular portion composed by a tandem string of 21 thrombospondin type 1 (TSP-1) domains, which has structural homology to the TSP-1 domains of thrombospondin 1 (THBS1), complement component 6 and F-spondin. The first 3 N-terminal TSP-1 domains are separated by a coiled coil domain (Seifert et al., 2018). Similarly to PLA_2R, various disulphide bonds and N-glycosylations characterize it (Q9UPZ6-Uniprot, 2023). THSD7A was found to be expressed on the foot process of podocytes, where it stabilizes the membrane dynamics (Herwig et al., 2019). Expression of THSD7A was also observed in lung bronchioles and several malignancies (Stahl et al., 2017; Von Haxthausen et al., 2018).

1.3.3 Anti PLA_2R antibodies

In 2009, antibodies against PLA_2R were identified for the first time in the serum of patients affected by primary MN (Beck et al., 2009). The circulating autoantibody against PLA_2R, as well as the antibodies found in the sub-epithelial deposits, belonged predominantly to the IgG4 subclass. At baseline, all patients with primary MN tested positive for PLA_2R-specific IgG4; moreover, 99%, 75%, and 28% showed positivity for PLA_2R-specific IgG3, IgG1, and IgG2, respectively (Von Haxthausen et al., 2018). Even though IgG4 are poor activators of the complement compared to the other subclasses (IgG1, IgG2, IgG3), total serum as well as purified IgG4 derived from PLA_2R antibody positive patients resulted to be able to activate the lectin complement pathway and induce podocyte injury in vitro through synaptopodin (SYNPO) and podocin (NEPH1) degradation (Haddad et al., 2021). This unexpected IgG4 ability was explained by the antibodies glycosylation, which made possible the IgG4 binding to mannose binding lectin (MBL) and the C4d and C5b-9 complement deposition. Among MN patients, 97% develop PLA_2R antibodies that target the Cys-R domain, followed by 52%, 38% and 10% of patients recognising the CTLD1, CTLD7 and CTLD8 domain respectively (Fresquet et al., 2015; Seitz-Polsky et al., 2016; Reinhard et al., 2020). Different studies came to the same conclusion that the PLA_2R antibodies recognise the protein only under non-reducing conditions. This

testifies the importance of the disulphide bonds in keeping the antigenic epitope conformation (Beck et al., 2009). A study suggested that patients positive to PLA_2R antibodies recognizing only the dominant Cys-R epitope have a better prognosis compared to patients whose antibodies have spread to other epitopes (Seitz-Polski et al., 2016). According to this hypothesis, the spreading of PLA_2R antibodies to different epitopes in the follow up time points is associated with disease worsening and vice versa a reverse spreading of the antibodies to the Cys-R domain only hints a positive outcome. Later on, this hypothesis was rebutted and it was shown that at baseline all patients develop PLA_2R antibodies recognising at least two epitopes and that only the total PLA_2R antibody levels correlate with the disease outcome (Reinhard et al., 2020). The detection of circulating autoantibodies is not only important for the diagnosis of the disease but also for monitoring the clinical activity. Prospective studies carried out in primary MN patients showed in fact the correlation of PLA_2R antibody levels with the occurrence of remission and relapse (Hoxha et al., 2014; Mahmud et al., 2019). It was observed that patients that have lower PLA_2R antibody levels at the time of the diagnosis, responded more quickly to the treatment. In fact, the lower the PLA_2R antibody levels, the faster the remission was reached. On the other hand, patients that didn't attain remission from proteinuria kept high levels of circulating PLA_2R antibodies. The use of PLA_2R antibody levels as a clinical activity marker can be exploited to select the treatment strategy that brings to a better outcome and avoid side effect of an unnecessary immunosuppressive treatment (Hoxha et al., 2014).

1.3.4 Potential new antigens associated with MN

PLA_2R and THSD7A are well-established antigens associated with MN, however new candidate antigens have been discovered by means of glomerular laser microdissection and through antigen precipitation with antibodies eluted from kidney biopsy, each followed by mass spectrometry analysis (Ronco et al., 2021; Hoxha et al., 2022). To discriminate if these are actual antigens and not biomarkers, some criteria have to be met; sub epithelial staining of the new antigen along the capillary walls, detection of antigen specific IgG in circulation, co-localization of antigen with IgG in the sub-epithelial deposits and correlation between antibodies levels and clinical course (Ronco et al., 2021). The newly discovered antigens include endogenous or exogenous proteins on regard of their expression on the podocytes. Among the endogenous antigens are serine protease high temperature requirement A (HTRA1) (Al-Rabadi et al., 2021), netrin G1 (NTNG1) (Reinhard et al., 2022), contactin (CNTN1) (Le Quintrec et al., 2021; Santoro et al., 2022) and semaphorin-3B (SEMA3B) (Sethi et al., 2020). Analogously to PLA_2R and THSD7A, these candidate antigens are expressed in the podocytes where they co-localize with the respective

antibodies, forming sub-epithelial immune deposits. Apart from HTRA1 and SEMA3B, which are secreted proteins, the others are anchored to the podocyte membrane. The predominant subclass involved with these antigens is IgG4 except for SEMA3B which is characterized by IgG1. Similarly to THSD7A, patients affected by MN mediated by CNTN1-ab can be associated with other pathologies such as Guillain-Barré syndrome and chronic inflammatory demyelinating polyneuropathy (Fehmi et al., 2023). Interestingly majority (72%) of SEMA3B cases occur in paediatric patients, suggesting that these cases could be a distinct type of disease and that more studies need to be carried out to confirm it as a new antigen (Sethi et al., 2020). Belonging to the category of antigens not expressed on the glomeruli is the second most common antigen after PLA_2R, NEL-like protein 1 (NELL-1) (Sethi et al., 2019). NELL-1 is a secreted protein mostly expressed in neural tissue, while in the kidney it is found in the tubules and it's almost absent in the glomeruli (The Human Protein Atlas, 2025). Cases of NELL-1 associated MN have no IgG4 dominance but instead present mainly circulating IgG1. NELL-1 is a target antigen in malignancy-associated MN as well as associated with exposure to different drugs such as lipoid acid, mercury-containing creams, bucillamine etc (Caza et al., 2021).

1.4 Established animal models for PLA_2R associated MN

Animal models are fundamental to study the characteristics of MN such as pathogenic molecular mechanisms, morphological features, complement activation and proteinuria development.

1.4.1 Heymann nephritis

The first animal model established to replicate the morphological traits of primary MN was Heymann nephritis (Heymann et al., 1959). Among the typical MN features that could be reproduced with this model are: IgG deposition in the sub epithelial space, complement activation, thickening of the glomerular basement membrane around the immune deposits, podocyte foot effacement, and proteinuria. Heymann nephritis could be achieved both by active and passive immunisation. According to the active immunisation protocol, rats received intraperitoneal injection of blood free rat kidney suspension in saline mixed 1:1 with Freund´s complete adjuvant. Six weeks after the first injection, majority of animals developed proteinuria (200 mg/24h) hypoproteinaemia and hyperlipidemia; periodic acid Schiff staining (PAS) of the kidney, performed at the end of the experiment, revealed thickening of the glomerular capillaries. Control animals, which received liver or lung suspensions, did not develop proteinuria and only showed mild structural alteration of the glomerulus (Heymann et al., 1989).

The passive immunisation protocol was carried out using heterologous antibodies raised against rat Fx1A (crude extract of the renal cortex) (Couser et al., 1978). Accumulation of IgG, deposition of C3 and proteinuria appeared 4 days after the intravenous immunisation. The nephritogenic antigens better characterized in Fx1A are two. One is a glycoprotein called megalin (gp330), which is a low-density lipoprotein receptor, and the second is the receptor associate protein (RAP) which binds to megalin (Kerjaschki et a., 1982; Farquhar et al., 1995). The Heymann nephritis model has provided fundamental insights into the patho-mechanisms of MN, such as:

- In situ formation of immune complexes, through IgG binding to the antigen on the podocyte surface, subsequently shed into the GBM (Kerjaschki et. al, 1987)
- Induction of glomerular injury through complement activation (Salant et al., 1980) and recruitment of $CD4^+$ and $CD8^+$ cytotoxic T cells (Quiza et al., 1992; Penny et al., 1998)
- Assembly of the membrane attack complex (C5b-9) on the podocytes, leading to transmembrane channels formation, membrane lipids rearrangement and of loss of membrane integrity (Perkinson et al., 1985; Cybulsky et al., 2005)
- Upregulation of endoplasmic reticulum (ED) stress proteins (bip, grp94) to suppress protein synthesis and reduce C5b-9-induced injury (Cybulsky et al., 2005, Cybulsky et al., 2002)
- Release of arachidonic acid by cytoplasmic phospholipase A_2, subsequently metabolised by cyclooxygenase 1 and 2 to generate prostaglandin E_2 and thromboxane A_2 (Cybulsky et al., 1987; Katano et Cybulsky, 2000)
- Increased intracellular Ca^{2+} (Cybulsky et al., 1989)
- Increased protein ubiquitination and impairment of the ubiquitin-proteasome system (Meyer-Schwesinger et al., 2011; Kitzler et al., 2012)
- Accumulation of reactive oxygen species (ROS) with consequent lipid peroxidation, modification of collagen IV in the GBM and impaired glomerular perm selectivity (Neale et al., 1994)
- Activation of NF-κB transcription factor, driving expression of pro-inflammatory cytokines (eg. IL-1β), proteases and enzymes involved in ROS and prostaglandin production (Mudge et al., 2001)
- DNA damage associated with upregulation of p53, p21, growth-arrest DNA damage-45 (GADD45) and checkpoint kinases-1 and -2 (Pippin et al., 2003)
- Upregulation of MMP-9, TGF-β2, TGF-β3, promoting the development of a disorganized GBM (McMillan et al., 1996; Shankland et al., 1996)

- Actin cytoskeleton condensation with altered adhesion to the GBM (Topham et al., 1999; Liu et al., 2010)
- Loss of slit diaphragm integrity due to dissociation of nephrin from the actin cytoskeleton (Saran et al., 2003).

Despite the contribution of Heymann nephritis to understand the patho-mechanisms involved in the primary MN, there are important limitations that don't allow the complete translation of the human disease into the animal model. The challenges of this experimental model reside in important differences such as the antigen and the IgG subclasses involved. The human equivalent of megalin (Uniprot P98164: LRP-2) is mainly expressed in proximal tubular brush border and has only 77% homology with rat megalin. To overcome some of these limitations, other animal models for primary MN were generated using Göttingen minipigs and transgenic animals.

1.4.2 PLA_2R-ab induced MN in Göttingen minipigs

The podocytes in minipigs show a PLA_2R expression pattern very similar to that in humans. In 2023, Reinhard et al used this advantage to establish an animal model that proved the pathogenicity of human anti PLA_2R antibodies. As prerequisite, sera from MN patients positive for PLA_2R-ab had been shown to bind porcine PLA_2R ($pPLA_2R$). The passive immunisation resulted in podocyte foot effacement, resembling an early stage of MN. Sub epithelial electron dense deposits were detectable by electron microscopy. A granular deposition of human IgG and porcine complement C3 was observed on the glomerular basement membrane; porcine complement C1q, complement factor B, C3, C5-C9 were detected by mass spectrometry in sieved glomeruli. The predominant role of the IgG4 subclass was confirmed. In fact, majority of the PLA_2R specific antibodies eluted from isolated pig glomeruli, belong to IgG4 subclass. Using immunofluorescence staining, IgG4 co-localize with $pPLA_2R$. The pathogenic effect of the PLA_2R-ab was visible 7 day after the immunisation when the minipig became proteinuric. Despite the use of a unilateral nephrectomy, to amplify the kidney exposure to the human antibodies, a nephrotic range proteinuria was never achieved. A limitation of this model was the necessity of large amounts of human sera which are not available to immunize animals with considerable body weight ($\geq$ 50 Kg).

However, this model was crucial to demonstrate the pathogenic role of PLA_2R antibodies in causing podocyte damage with complement activation and proteinuria. Minipigs present physiological and immunological similarities to humans and have already being used to evaluate

immunosuppressive treatments before clinical trials in humans (Golbus et al., 2022). This PLA_2R induced MN model in minipigs thus represent a good translational tool to test efficacy and safety of novel treatments.

1.4.3 Mice transgenic models of PLA_2R associated MN

The lack of PLA_2R expression on the podocyte of mice as well as of rats (Rinschen et al., 2018; UniProt 2023), required the generation of genetically modified animals. The first transgenic mice to be developed consisted of Bagg albino mice (BALB/c) expressing murine PLA_2R ($mPLA_2R$) specifically on the podocyte (Meyer-Schwesinger et al., 2020). A strong $mPLA_2R$ expression was detected on both the membrane and cytoplasm of positive mice. No structural disturbance was observed in untreated animals. Confocal microscopy analysis showed no interference with nephrin expression and a normal morphology of foot processes, glomerular basement membrane and endothelium. The maintenance of physiological permeability in the filtration barrier of positive mice was assessed by measuring the urinary albumin to creatinine ratio; this assay showed that $mPLA_2R$-positive mice did not indeed developed proteinuria before treatment. MN disease traits were induced in $mPLA_2R$-positive animals with passive immunisation. Purified rabbit anti-$mPLA_2R$ IgG (experimental group) or rabbit unspecific IgG (control group) were injected intraperitoneally in $mPLA_2R$-positive and/or negative mice. Only the $mPLA_2R$-positive mice treated with rabbit anti-$mPLA_2R$ IgG developed hypercholesterolemia and proteinuria (albumin to creatinine ratio: 100 g/g) in an IgG dose dependent manner. Heavy proteinuria was confirmed also with periodic acid-Schiff staining in which it was displayed as protein casts in dilated tubules. At 5 to 7 days after the immunisation, immunofluorescence and electron microscopy analysis showed all the MN morphological characteristics in $mPLA_2R$-positive mice belonging to the experimental group, as well as C3 complement deposition in partial co-localization with rabbit IgG. Oxidative stress was also observed by an increase of superoxide dismutase in podocytes.

The immunisation of $mPLA_2R$ mice with human anti-PLA_2R IgG was not successful. This outcome was explained by the incapacity of the human IgG to bind $mPLA_2R$, which has only a moderate amino acid identity (72%) with $hPLA_2R$ (Catherine Meyer-Schwesinger et al., 2020). Another transgenic mouse line was established to express human PLA_2R ($hPLA_2R$) on the podocytes (Tomas et al., 2023). These BALB/c transgenic mice expressed $hPLA_2R$ specifically on the podocyte membrane and cytoplasm and this expression didn't induce major disturbance in the podocyte structure during the first weeks of life. However, after 3 to 7 weeks, $hPLA_2R$-positive mice started to produce spontaneously antibodies against $hPLA_2R$, developed ascites

and had to be euthanized. Mouse hPLA$_2$R-IgG specifically bind hPLA$_2$R but not mPLA$_2$R and co-localize with GMB protein laminin. Interestingly mouse anti hPLA$_2$R-IgG recognise the same PLA$_2$R regions recognised by human PLA$_2$R-IgG: Cys-R, CTLD1, CTLD7-8 domains. Another analogy observed was the abundance of murine IgG1 in the sub-epithelial deposits; this IgG subclass resemble human IgG4 in its limited capacity to bind C1q and activate the complement. Complement deposition was positive for C1q, C4d, CFB, CFH, C3 and C5-b9. Sign of oxidative stress was verified by increase of superoxide dismutase in podocytes. At 4 weeks, exclusively hPLA$_2$R positive mice, developed proteinuria along with a drop of serum albumin and increase of serum lipids.

1.5 Project aim

The aim of this project was to establish a new animal model of PLA$_2$R induced MN. Considering that rodents don't express PLA$_2$R on the podocytes, a transgenic rat line expressing human PLA$_2$R specifically on this cell type was created. Before undergoing any treatment, the transgenic animals were phenotyped to: confirm the presence of PLA$_2$R expression, assess its cell specific localisation in the glomerulus, rule out the spontaneous production of rat anti hPLA$_2$R antibodies and spontaneous development of proteinuria. The rat tolerance for the transgenic hPLA$_2$R, prior the immunisation, was an important requisite to be able to induce MN starting from non proteinuric healthy animals. The strategies adopted to phenocopy PLA$_2$R induced MN consisted of both passive and active immunisation. Each experiment round was organized as experimental vs control study. The passive immunisation comprised the transfer of human plasma from MN patients with PLA$_2$R antibody positivity. The control counterpart received human plasma from a healthy donor. In the active immunisation protocol, the experimental group was treated with extracellular domain of human PLA$_2$R protein to induce the immune system to produce antibodies against it. The control group received the immunisation buffer without protein.

Blood and urine samples were collected at different time points and at the end of the experiments. Both kidneys were collected directly after the euthanization. Blood was used to detect the presence of anti PLA$_2$R antibodies in circulation; urine was used to monitor proteinuria through albumin quantification; kidney tissue was used for isolating glomeruli and carry out histology analysis. An hPLA$_2$R expressing rat model was established to better define the patho-mechanisms of membranous nephropathy, such as immune deposits formation, complement activation, immune mediators´ role in proteinuria development and lastly to have a mean for testing less toxic and more specific therapies.

2. Materials and methods

2.1 List of materials, reagents, consumables, machines and solutions

Materials/Reagents			
Application	**Product**	**Manufacturer**	**Cat. No.**
Hemizygous genotyping	Agarose	Thermo Fisher Scientific	16500500
	Ethidium bromide	Roth	7870.1
	Extract-N-Amp Tissue PCR Kit	Sigma Aldrich	XNAT2
	GeneRuler 100-bp DNA ladder	Thermo Fisher Scientific	SM0241
	Glacial acetic acid ≥ 99 %	Sigma Aldrich	A6283
	m-ywhae-001, 002 primers	Integrated DNA Technologies	-
	STA5-21, 22 primers		-
	TriTrack DNA loading dye (6x)	Thermo Fisher Scientific	R1161
Homozygous genotyping	Monarch gDNA isolation kit	New England Biolabs	NEB #T3010
	Nuclease free H2O	Qiagen	1299117
	PLA_2R-F/R primers	Integrated DNA Technologies	-
	PowerUp™ SYBR™ Green Master Mix	Thermo Fisher Scientific	A25742
Rat immunisation	Dulbecco's Phosphate Buffered Saline w/o Calcium and Magnesium	Anprotec	AC-BS-0002
	Freund's adjuvant compelte	Sigma Aldrich	F5881-10ML
	Freund's adjuvant inompelte	Sigma Aldrich	F5506-10ML

	PLA_2R(ec)-HIS	Euroimmun	FB190430.2
Histology	Alexa Fluor 488 AffiniPure™Donkey anti rat IgG (H+L)	Jackson ImmunoResearch	712-545-150
	Cy™2 AffiniPure™Donkey anti mouse IgG (H+L)	Jackson ImmunoResearch	715-225-150
	Cy™3 AffiniPure™Donkey anti goat IgG (H+L)	Jackson ImmunoResearch	705-165-147
	Cy™2 AffiniPure™Donkey anti rabbit IgG (H+L)	Jackson ImmunoResearch	711-225-152
	Cy™3 AffiniPure™Donkey anti guinea pig IgG (H+L)	Jackson ImmunoResearch	706-165-148
	eBioscience™DRAQ5™	Thermo Fisher Scientific	65-0880-92
	Ethanol ≥ 99,8 %	Roth	9065.1
	Fluoromount-G medium	Thermo Fisher Scientific	00-4958-02
	Goat anti collagen IV	SouthernBiotech	1340-01
	Goat anti rat C3c	Nordic-MUbio	GARa/C3c
	Guinea pig anti nephrin	OriGene	BP5030
	Hematoxylin	Thermo Fisher Scientific	NC9220898
	5 % Normal horse serum blocking solution	Vector Laboratories	S-2000
	Proteinase 24	Sigma Aldrich	P8038
	Rabbit anti human IgG	Agilent Technologies	A0423
	Rabbit anti Laminin	Sigma Aldrich	L9393
	Rabbit anti PLA_2R	Sigma Aldrich	HPA012657
	Schiff´s reagent	Thermo Fisher Scientific	50-301-27

	Tissue-Tek O.C.T. Compound	Sakura	4583
Glomerular extract	DC protein assay	Biorad	5000112
	Glycerol	Sigma Aldrich	49767
	10 % Octagam	Octapharma	05373935
	Protein G resin	GeneScript	L00209
	Triton X-100	Merck	T8787
Antibody elution	PierceTM IgG elution buffer	Thermo Fisher Scientific	21004
Western Blot	Glycin	Roth	3908.2
	Goat anti rabbit IgG	Merck	A9169
	Goat anti rat IgG	Thermo Fisher Scientific	A10549
	4x Laemmli sample buffer	Biorad	1610747
	Methanol ≥ 99.9%	Merck	1.06009
	Mouse anti GAPDH	Santa Cruz	Sc-32233
	Mouse anti human IgG4	Southern Biotech	9200-05
	Mouse anti human IgG total	Southern Biotech	9040-05
	Pierce ECL substrate	Thermo Fisher Scientific	32106
	Precision plus protein standards	Biorad	161-0374
	Rabbit anti goat IgG	Merck	A8919
	Rabbit anti HIS tag	Antikorper online	ABIN1573881
	Rabbit anti mouse IgG	Merck	A9044
	TG-SDS buffer	VWR	0147
ELISA	Anti PLA_2R ELISA (IgG)	Euroimmun	EA 1254G
	Carbonate-Bicarbonate buffer	Sigma Aldrich	C3041
	H_3PO_4	Sigma Aldrich	W290017

	Rat albumin	Sigma Aldrich	A6272
	Sheep anti rat albumin	Thermo Fisher Scientific	A110-134A
	Sheep anti rat albumin-HRP	Thermo Fisher Scientific	A110-134P
	TMB ELISA Peroxidase substrate	Biozol	OORA01684
	Tris Buffered Saline with BSA, pH 8,0	Sigma Aldrich	T6789
	Tris Buffered Saline with Tween20, pH 8,0	Sigma Aldrich	T9039
Creatinine assay	Creatinine	Sigma Aldrich	C4255-10G
	Creatinine Jaffe' (fluid 5+1)	Hengler analytik	0621211
Various	cOmplete EDTA free protease inhibitor cocktail	Merck	11873580001
	EDTA	Merck	324504-100ML
	Milk powder	Roth	T145.3
	NaCl	Roth	3957.1
	PBS (1x Dulbecco)	PanReacAppliChem	A0964.9050
	Trizma Base	Sigma Aldrich	T6066
	Tween 20	Roth	9127.1
Machines/Consumables			
Amicon ultra-4 centrifugal filter, 30 KDa MWCO		Merck	UFC803024
Confocal laser scanning microscope		Zeiss	Lsm-800 Axio Observer
Corning® microscope slides		Merck	CLS294875X25
Corning Spin-X UF concentrator		Merck	CLS431480
Costar® Spin-X® Centrifuge Tube Filters, 0.45 µm Pore CA		Corning	8163
Electrophoresis power supply		Amersham	EPS 3501 XL
Epredia™ STP 120 Tissue Processor		Fisher Scientific	813150

Heraeus Fresco™ 21 micro centrifuge	Thermo Fisher Scientific	75002555
Heraeus megafuge 8R centrifuge	Thermo Fisher Scientific	75007214
Amersham Imager 600	Cytiva	29-0834-61
Infinite M200 Pro microplate reader	Tecan	30213624
Mersilene (polyester) suture	Ethicon	XJR665.P31
Microcon-10 kDa Centrifugal filter unit	Merck	MRCPRT010
Mini centrifuge Sprout	Heathrow Scientific	1HAC.1
4-15% mini protean TGX precast protein gels	Biorad	4561086
Microtome	Histo-Line laboratories	IHISMR3000LIBRA
Multistix 10SG test strips	Siemens	01526748
NanoQuant plate™	Tecan	379483
PCR plate half skirt LP transparent	Sarstedt	721981
pH meter	SI Analytics	Lab 855
PVDF membrane (0,45 µm)	Sigma Aldrich	IPVH00010
QuantStudio™ 3 Real-Time PCR System	Thermo Fisher Scientific	MAN0010408
Rocking platform	Witeg	RK-2D
Safety multifly needle	Sarstedt	85.1642.235
Thermal cycler	Techne	GZ-93945-19
Tissue embedding cassettes	Merck	Z672122
Tissue Tek cryomold	Sakura	4566
Tissue-Tek® TEC™ 6 Embedding Console System	Sakura	5110
Trans-blot turbo transfer system	BioRad	1704150
TS-100 thermo shaker (SC-24N)	BioSan	BS-010120-AAI
Tubes rotator	LABINCO	L29150716
UV transilluminator	Vilber Lourmat	V037179

96 Well high affinity binding plate	Sarstedt	82.1581.200
96 Well plate	Sarstedt	82.1581
Solutions		
Solution	**Ingredients**	**Concentration**
Blocking solution (Western Blot)	Milk in PBS-T	3,5 % (w/v)
Citrate buffer, pH 6.2	Sodium citrate dehydrate Citric acid	87,4 mM 12,6 mM
Neutralisation buffer, pH 8.5	Tris base HCl	1 M -
Non denaturing lysis buffer	Tris base pH 8 Glycerol Triton X-100 Protease inhibitor	50 mM 20 % (v/v) 1 % (v/v) 1x
PBS-T	Potassium Phosphate Sodium Chloride Tween-20	20 mM 150 mM 0,1 % (v/v)
1x Running buffer	Tris base Glycine SDS	25 mM 192 mM 0,1 % (w/v)
1x TAE, pH 8	Tris base Glacial acetic acid EDTA	40 mM 20 mM 1 mM
1x Transfer buffer	Tris base Glycine	25 mM 200 M

2.2 Animals

All animal experiments related to this project were approved by the Veterinarian Agency of Hamburg (government body approval numbers: N21/007, N20/070) and were carried out according to the national animal care and ethical guidelines. Sprague Dawley transgenic rats (SD-Tg(NPHS2-PLA$_2$R/tdTomato)) expressing human PLA$_2$R on the podocytes were generated in collaboration with GenOway (Lyon, France). To create the transgenic animals, purified PLA$_2$R transgene and CRISPR/Cas9 were microinjected into the male pro-nucleus of fertilized oocytes. The insertion of the transgene occurred in a random region of the rat genome. Viable two-cell embryos were re-implanted into a foster mother. All pups were screened by polymerase chain reaction (PCR) and sequenced to verify the insertion and the integrity of the transgene. Subsequently, the hemizygous founders were mated with wild type animals to confirm the vertical transmission of the transgene. Wild types outbred Sprague Dawley rats, used for mating, were ordered from Envigo. All animals were kept at the animal facility of the University Medical

Center Hamburg-Eppendorf in accordance with the local and international research animal husbandry regulations. Here, they were housed in open cages with light/dark phases of 12/12 hours' length, receiving food and water ab libitum.

2.3 Genotyping

2.3.1 Hemizygous rats

For the genotyping of the hemizygous rats, "Extract-N-Amp Tissue PCR" Kit (Sigma Aldrich) and two primer sets were used. One primer targeted the PLA_2R gene while the other was a quality control specific for m-ywhae, a gene that codifies for "mouse tyrosine 3-monooxygenase/tryptophan 5-monooxygenase activation protein epsilon".

Direct PCR lysis extraction

Ear punches (2 mm diameter), from fifteen days old rats, were collected to extract genomic DNA. The ear tissue was incubated for 10 minutes at room temperature with 100 µl of "Extraction solution" and 25 µl of "Tissue preparation solution". A second incubation followed for 3 minutes at 95°C. The tissue lysate, containing free genomic DNA (gDNA), was neutralized adding 100 µl of "Neutralization solution B", mixed well and stored at -20°C ready to be used for the amplification step. The PCR was executed directly on the tissue lysate without a prior DNA isolation. Separate master mixes for each primer were assembled at room temperature mixing the following components: 10 µL of "Extract-N-Amp PCR reaction mix", forward and reverse primers (PLA_2R: 0.4 µM F/R; m-ywhae: 0.8 µM F/R), 4 µL of tissue extract and PCR grade water up to a final volume of 20 µL. The PCR master mix was distributed into 0.2 mL PCR stripe. After being pulsed vortexed, the PCR stripes were spin down and placed into a gradient thermal cycler, which carried out the amplification applying the following profile:

Step	Temperature (°C)	Time (s)	Number of Cycles
Initial denaturation	94	180	1
Denaturation	94	30	
Annealing	60	30	30
Extention	72	60	
Final extention	72	600	1
Hold	10	∞	

Figure 4: PCR profile.
PCR parameters used for the amplification of PLA_2R and m-ywhae.

Primers were purchased from “Integrated DNA Technologies” using the following sequences:

	Primer name	Sequence	Product size (bp)	
			Wild type	Transgenic
Transgenic PLA_2R	sta5-21	CCTGAAGGATTATGGCAGCTATCCCC	-	343
	sta5-22	CCACCTTGAGTCCAATGATTGCACC		

	Primer name	Sequence	Product size (bp)	
			Wild type	Transgenic
YWHAE	m-ywhae-001	GAGGTGTTTTGGGGGAGTTT	172	172
	m-ywhae-002	GGCTTCCATACCACCTTCAA		

Figure 5: Primers used for the genotyping of hemizygous rats.
Sequence of primers used for PLA_2R and ywhae amplification with relative product size.

At their arrival, each primer was reconstituted adding the required amount of PCR grade water (Qiagen) to reach a stock concentration of 100 µM. Primers stocks were split into 50 µl aliquots and stored at -20°C to avoid repeating freezing and thawing cycles.

Agarose gel electrophoresis

To determine rat’s genotype, the PCR products resulting from PLA_2R and m-ywhae amplification were visualized with an agarose gel electrophoresis. A 2% gel was prepared in a glass flask solubilising 0.8 gr of agarose powder (Thermo Fisher Scientific) with 40 ml of 1x tris-acetate-ethylenediaminetetraacetic acid buffer (TAE). The agarose solution was melted in a microwave. To allow the visualisation of the DNA, 0.8 µl of 10 mg/ml ethidium bromide (Roth) were added into the flask and gently mixed avoiding the formation of bubbles. The molten solution was poured into the gel tray of the casting apparatus together with the well combs. The gel was left at room temperature for approximately 45 min to solidify. The electrophoretic chamber was prepared for the run adding 200 ml of running buffer (1x TAE). DNA samples were prepared mixing 10 µl of PCR product with 2 µl of “TriTrack DNA loading dye” (Thermo Fisher Scientific). Ten microliters of this mix were loaded for the run. To track the DNA migration height, 4 µl of “GeneRuler 100-bp DNA ladder” (Thermo Fisher Scientific) were used. Power supply parameters were set at 90 V, 400 mA to let the DNA run for 40 min. The results of the run were determined exposing the gel to UV light in a transilluminator (Vilber Lourmat).

2.3.2 Homozygous rats

Genomic DNA isolation

High purity gDNA was extracted from 15 days old rat ear punches (2 mm diameter) following the protocol recommended by "Monarc genomic DNA purification" kit (New England Biolabs). Sample digestion was carried out incubating the tissues for 2h at 56°C in 200 µl of "Tissue lysis buffer" and 3 µl of "proteinase K" with agitation at full speed (1400 rpm). The incubation continued for 5 more minutes at 56°C adding 3 µl of "RNase A" to the lysate. The gDNA was prepared for the binding to the purification column by mixing the lysate with 400 µl of "gDNA binding buffer". The lysate/binding buffer mix was transferred to the purification column pre-inserted in a collection tube and centrifuged for 3 min at 1000x g. A further centrifugation step of 1 min at 12000x g was done to clear the membrane. The flow through was discarded and the purification column was inserted in a new collection tube. The contaminants present in the purification column were removed with two washings rounds made with 500 µl of "gDNA washing buffer" followed by 1 min of centrifugation at 12,000x g. The flow through was discarded after each washing step. The purification column was inserted in a 1.5 ml tube and 100 µl of preheated (60°C) "gDNA elution buffer" were added on top of the filter. After a 1 min incubation at room temperature, the purification column was centrifuged for 1 min at 12,000x g to collect the eluate. All centrifugation steps were done at 4°C. DNA concentration and purity were determined with "Infinite M200 Pro" microplate reader: 1.5 µl of DNA were added to a "Nano Quant plate" and the absorbance was read at 260 and 280 nm. Elution buffer was used as a blank.

Primer design

The set of primer specific for m-ywhae was used as endogenous control while the primers for PLA_2R amplification had to be redesigned to obtain a smaller amplicon size. The human sequence of PLA_2R extracellular domain was entered into "Primer3web 4.1.0" online service to design primer sequence according to the guidelines recommended by the "PowerUp SYBR Green Master Mix": amplicon size (70-180 bp), prime length, CG composition (40-60%), melting temperature (58-60°C), absence of internal secondary and primer-primer structures. The selected primer set (Figure 6) was then purchased from "Integrated DNA Technologies".

Gene	Primer probe	Sequence	Product size (bp)
Human PLA_2R-ec	3-PLA_2R Forward	CCT GAA GGA TTA TGG CAG CTA TCC	147
	3-PLA_2R Reverse	TAT CAG TGT CAG TAC AAC CGC AAG AGG	

Figure 6: PLA_2R primer used for the genotyping of homozygous rats.
Sequence of the PLA_2R primer, belonging to the human extracellular domain, used for the amplification with relative product size. Ec: extracellular

Real Time PCR

Analogously to the hemizygous genotyping, the isolated gDNA was used for the amplification of sequences located in two genes: PLA_2R (target gene) and m-ywhae (housekeeping gene or endogenous control). Two separate master mixes, one for each of the above-mentioned primers, were prepared in 0.2 ml PCR tube stripes by mixing 15 µl of "PowerUp SYBR Green mastermix", PLA_2R F/R primers (0.5 µM), m-ywhae 001/002 primers (0.5 µM; 0.6 µM), 3 µl of gDNA and nuclease free water up to a final volume of 30 µl. The samples/primer mixes were distributed as triplicates of 10 µl into a 96 well PCR plate. The PCR plate was covered with a plastic foil carefully sealed to avoid evaporation of the samples during the amplification. Together with the test samples, whose genotype was unknown, one wild type and one PLA_2R transgenic rat DNA were included in the assay respectively as negative and positive controls. A no template control for both primer mixes, consisting of all PCR reagents except the gDNA, was used to detect eventual contaminations. All samples were run in triplicates. The PCR plate layout and the RT-PCR profile were created using "Quant studio design & analysis" software. The PCR plate layout and the information relative to the amplification were loaded in a "Quant studio 3 Real-Time PCR" (Thermo Fisher Scientific), system in which the amplification was carried out according to the following profile:

Step	Temperature (°C)	Time (s)	Number of Cycles
UDG activation	50	120	1
Dual-Lock DNA polymerase	95	120	
Denaturation	95	15	40
Annealing	57	15	
Extention	72	60	

Figure 7: RT-PCR profile.
RT-PCR parameters used to amplify PLA_2R and m-ywhae. UDG: uracil-DNA glycosylase.

After the amplification, a dissociation curve was also performed:

Step	Temperature (°C)	Time (s)	Number of Cycles
1	95	15	
2	60	60	1
3	95	15	

Figure 8: RT-PCR dissociation curve.

To determine the relative quantification (RQ) of the PLA_2R transgene, and thus the rats' genotype, a comparative Ct (cycle threshold) approach was used. According to this strategy, the amplification of the PLA_2R transgene and of an endogenous control (gene solidly expressed within the samples) were measured in a reference sample (rat with known genotype) and in the test samples (rats with unknown genotype). The software compares the Ct normalized with the endogenous control gene between reference and test sample to calculate the copies of the PLA_2R transgene.

2.4 Animal experiments

2.4.1 Active immunisation

Eight to ten weeks old PLA_2R transgenic animals were selected for an active immunization experiment designed to stimulate the development of PLA_2R-specific rat antibodies. Rats' minimum body weight at the experiment start was 150 gr. Animals with comparable body weight and same sex were divided into experimental and control groups. The experimental group was immunised with human PLA_2R protein solubilized in an immunisation buffer composed by sterile phosphate buffered saline (PBS) and Freund's adjuvant. The control group received only the immunisation buffer without any protein. The immunisation protocol lasted a total of 27 weeks and included 9 immunisation shots carried out each 3 weeks (Figure 9). At every time point a total of 200 µl of immunisation mix were administered with two subcutaneous injections of 100 µl each, executed in two different points of the animal's back. The immunisation mix for the first time point (week 0) was prepared adding 10-20 µg of extracellular domain of human PLA_2R (Euroimmun), solubilized in PBS, to an equal volume (100 µl) of complete Freund's adjuvant (Sigma Aldrich). The solution was vortexed until the formation of an emulsion and collected with a 1 ml Injekt-F SOLO syringe. The following immunizations were done using the same amount of PLA_2R protein used at week 0 but emulsified with incomplete Freund's adjuvant (Sigma Aldrich). Before every immunisation, urine, blood and body weight information

were collected. At week 27, after urine collection, the animals were euthanized to collect blood and kidneys.

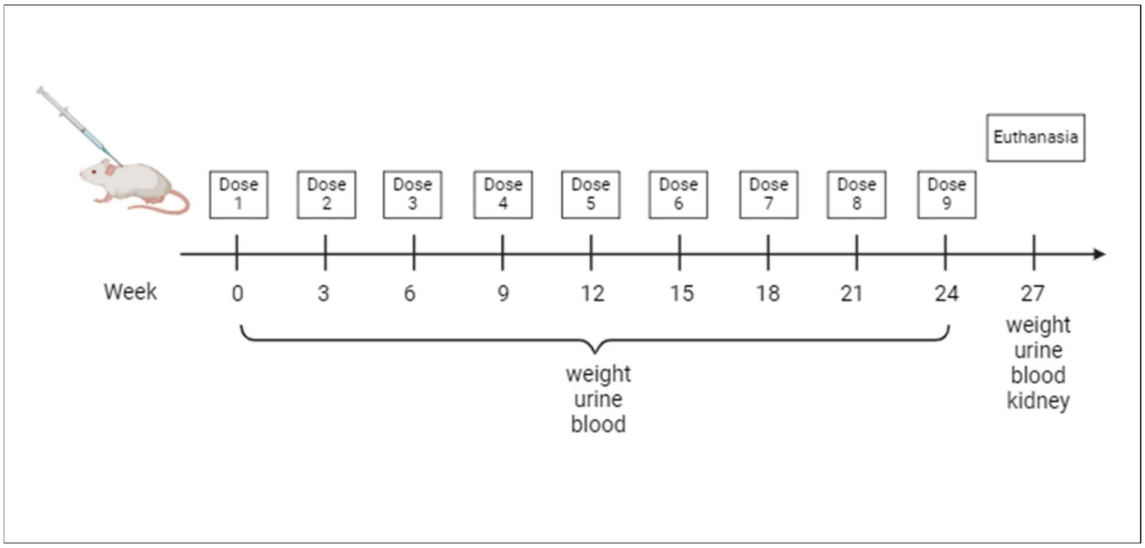


Figure 9: Schematic representation of active immunisation.
(Picture created with BioRender.com)

2.4.2 Passive immunisation

As in the active immunization experiments, passive immunization was performed on PLA_2R transgenic rats between seven and nine weeks of age, with a minimum body weight of 150 gr. Sibling animals, comparable in body weight and sex, were divided into experimental and control group. The experimental group received a pool of human plasma from 100 patients with PLA_2R antibody-positive MN (PLA_2R-ab level measured by ELISA: 460 RU/ml) while the control group was treated with plasma deriving from one healthy donor. Both plasma were concentrated to half volume using "Amicon ultra-4 centrifugal filter" (Merck, 30 KDa MWCO). The concentration protocol consisted in the centrifugation of 2 ml plasma per rat at 3000x g for a minimum of 30 min or until it was concentrated to half volume. The PLA_2R antibody positive plasma pool and the healthy plasma used for the immunisations, were analysed by western blot as primary antibodies with a dilution of 1:500 and 1:100 respectively. To test the binding capacity and specificity of the anti PLA_2R antibodies present in the plasma pool, rat glomerular extract from transgenic and wild type rats were used as antigen in non-reducing conditions. Moreover, the binding of the anti PLA_2R antibodies present in the plasma pool was tested towards the domains CysR, CTLD1-2, CTLD7-8 and CTLD8 (expressed in HEK293 cells), all run in non-reducing conditions. The passive immunisation experiment lasted 9 days. For each animal it was decided to administer a total of 1 ml of concentrated plasma via intravenous tail infusion. Infusions were performed on consecutive days: the first 500 µl of plasma were given at

day 0 and the other 500 µl 24h later at day1 (Figure 10). Before the infusions, the tail vessels were dilated submerging the tail in warm water (37-40°C). Urine, blood and body weight were collected at day 0, 2 and 6. At day 9, urine and blood were collected with the kidneys.

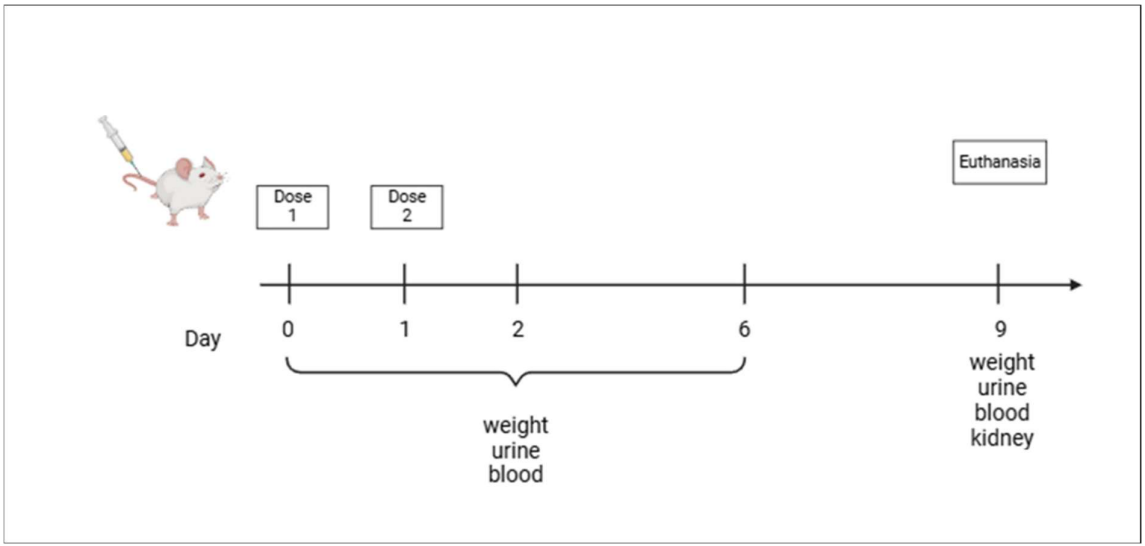


Figure 10: Schematic representation of passive immunisation.
(Picture created with BioRender.com)

2.5 Samples collection

During the immunisation experiments and before euthanizing the animals, a minimum volume of 1.5 ml urine was collected. Urine samples were kept on ice until their arrival at the laboratory where they were processed through centrifugation at 3000 rpm for 3 min to eliminate dirt particles. Supernatant was collected and evenly distributed in 0.5 ml tubes. Blood was withdrawn from the rats 'tail previously soaked in warm water to dilate the vessels. The amount of blood taken depended on the frequency of the sampling. A maximum volume of 200 µl was taken in the passive immunisation and 1 ml in the active immunisation. Following the euthanization with a CO_2/O_2 mixture, all blood was drawn up from the animal by cardiac puncture using a 1 ml syringe and 20 G needle. Blood was immediately collected in 0.5-2 ml tubes containing EDTA (Merck) (dilution 1:100) and kept at room temperature until a centrifugation step done at 3000 rpm for 10 min to separate plasma from cells. After the perfusion, both kidneys were collected and placed inside falcons tubes containing ice cold PBS.

2.5.1 Kidney perfusion

The perfusion of the kidneys was done to flash out the blood from the kidney's vessels immediately after the animals were euthanized. Less blood in the glomerulus helps to improve

the quality of histology and molecular analysis. Two ligatures were placed around the abdominal aorta and the inferior vena cava, directly above the renal arteries and near to the iliac arteries. Polyester suture thread (Ethicon) was used to make the ligatures. Prior to the vessel cannulation, a 25 G Safety multifly needle (Sarstedt) was prepared by filling it with PBS and removing air bubbles. The aorta was then cannulated in the portion between the two ligatures, around 1 cm below the kidneys' arteries ramification. The syringe needle was clumped together with the aorta to avoid the PBS to flush out from the puncture site. PBS was injected into the aorta with a 10 ml syringe until complete whitening of both kidneys. A small incision was made on the vena cava next to the needle to facilitate the PBS flow. To perfuse both kidneys of one rat ~ 100-150 ml of room temperature PBS were used.

2.5.2 Glomeruli isolation

To isolate glomeruli and renal tubules, the kidney tissue was placed inside a petri dish in contact with a cold plate where it was finely cut with a scalpel until completely homogenized. Subsequently the cut tissue was poured on a 106 µm sieve, pre-moistened with PBS implemented with 0.1% bovine serum albumin (PBS-BSA), and pushed through the meshes with the help of a small volumetric flask. A 50 ml syringe and a 20 G needle were used to flush abundant ice-cold PBS-BSA and push the glomeruli to the sieve below. In this way, glomeruli were collected inside the 53 µm sieve where they were washed with plenty of cold PBS-BSA to remove blood cells and other debris. After washing, the 53 µm sieve was tilted to gather all the glomeruli on one side. The glomeruli were pushed with flushes of cold PBS-BSA in a plastic weigh boat and eventually collected in a 50 ml falcon. The falcon containing the glomeruli was left for 10 min inside an ice box to let the isolated material to settle. In the same way, the tubules were washed and retrieved from a 20 µm sieve. All the 50 ml falcons containing glomeruli and tubules were centrifuged at 1200x g for 10 min at room temperature to form a pellet. All the supernatant was removed except for ~4 or 2 ml, respectively for glomeruli and tubules. The pellet and the left-over supernatant were pulse vortexed to re-suspend. Even volume aliquots of the suspended glomeruli or tubules were prepared in 1.5 ml tubes. All these aliquots were further centrifuged at 1200x g for 10 min at 4°C. After all centrifugation step, the supernatant was removed using a 1 ml tip overlapped to a thin western blot loading tip and substituted with 1 ml more of cold PBS-BSA. A total of three washing rounds were done using the above mentioned settings. At the last washing step, the supernatant was completely removed and the aliquots were blast frozen in liquid nitrogen to be subsequently stored at -80°C.

2.5.3 Kidney preparation for histology

All organs biopsies were kept in cold PBS (4°C) until they were processed for histology. Part of them were paraffin embedded, while the rest was preserved in cryo-embedding matrix. The samples intended to be paraffin embedded underwent a preparation process that included the steps of fixation, dehydration, paraffin infiltration and embedding. For the fixation, the biopsies were incubated in 4 % formalin at 4°C for 24h. The excess of formalin was removed with three washing steps, each in cold PBS and lasting 30 min, and then the biopsies where moved to a plastic tissue embedding cassettes (Merck). The dehydration, carried out in an automated system (Fisher scientific), involved the incubation of the samples with a series of solutions with increasing ethanol (EtOH) concentrations. The dehydration sequence included the incubation with 70 % EtOH (15 min), 90 % EtOH (15 min) and 100 % EtOH (30 min). The last incubation in 100 % EtOH was repeated for three times. Eventually, ethanol was cleared incubating the samples two times in 100% xylene, for 20 min and 45 min. The process of infiltration with molten paraffin was carried out at 58°C in the same automated system used for the dehydration. Finally the paraffin impregnated samples were embedded in paraffin blocks using a tissue embedding console (Sakura). The organ sections intended to be preserved by cryo-embedding where gently placed on top of laboratory cellulose wipes to remove the excess of PBS, laid inside a cryo-mold (Sakura) filled with Tissue-Tek medium (Sakura) and blast frozen in liquid nitrogen. The cryo-preserved tissues were stored at -80°C, while the paraffin preserved were left at RT. Small tissue pieces of the kidney were kept at 4°C in 4 % formalin to be subsequently analysed by electron microscopy.

2.6 Rat plasma

2.6.1 Detection of anti PLA_2R antibodies by western blot

To carry out the Sodium Dodecyl Sulfate–Polyacrylamide Gel Electrophoresis (SDS-PAGE): 10 ng of full length human PLA_2R, produced in human embryonic kidney 293 (HEK-293) cells, were added to 4x SDS loading dye, boiled at 95°C for 3 min and separated on a 4-15 % mini protean TGX precast protein gel (Biorad). The electrophoretic run was set at 160 V, 400 mA and lasted 45 min. Precision plus protein standards marker (Biorad; 250-10 kDa) was used to track the protein migration. For the transfer, a 0.45 µm PVDF (polyvinylidene fluoride) membrane (Merck) was activated for 30 sec in methanol and incubated for 5 min in transfer buffer (1x Tris-Glycin, 10 % methanol). Filter pads and gel were also incubated for 5 min in the transfer buffer. To convey proteins onto the PVDF membrane, a semi dry transfer was performed using “Trans-blot turbo” transfer system (BioRad) set at 25 V, 1 A, for a total of 30 min run. After the transfer,

the membrane was blocked 1 hour in 3.5 % milk solubilised in 0.1 % PBS-Tween (PBS-T), shaking on a rocking platform at RT. The PVDF membrane was probed with rat plasma diluted 1:100 in 0.5 % milk PBS-T. The incubation in primary antibody was performed overnight at 4°C on a rocking platform. The following day, the membrane was washed 3 times with PBS-T for 3 min at RT and incubated with the horseradish peroxidase (HRP) conjugated secondary antibodies: "goat anti rat IgG" (Thermo Fisher Scientific; 1: 5000), "mouse anti human IgG4" (Southern Biotech; 1:10 000), "mouse anti human IgG total (Southern Biotech; 1:20 000). All secondary antibodies above listed were prepared in 3.5 % milk-PBST and left in incubation for 1 hour at RT. After the incubation with the secondary antibody, the membrane was further washed 3 times with PBS-T at RT. The membrane was incubated with Pierce enhanced chemiluminescence (ECL) substrate (Biorad) for 3 min in the dark and developed with the "Imager 600" chemiluminescence system (Amersham) to detect the immuno-positive signals.

2.6.2 Detection of anti PLA_2R antibodies by commercial ELISA

The commercial "Anti PLA_2R-IgG" ELISA kit (Euroimmun) was used to determine the relative amount of PLA_2R specific rat IgG in the plasma of animals immunised against human PLA_2R. In order to quantify and compare the amount of PLA_2R specific rat IgG among different samples, a standard curve was set up making 15 serial dilutions (1:2) of rat plasma collected at week 27, belonging to a reference animal which showed a high amount of circulating PLA_2R-ab by western blot. All samples were diluted in "sample buffer" applying a factor (1:100; 1:150; 1:300) which was assigned considering the results of the previous western blots also made to evaluate the amount of circulating PLA_2R antibodies. One hundred µl/well of standards and samples were loaded into the 96 well plate (Sarstedt) and incubated for 30 min at RT. Subsequently, the samples were discarded and the plate was washed 3 times using 300 µl/well of "washing buffer". Incubation with 100 µl/well of the secondary antibody "goat anti-rat IgG" (Thermo Fisher Scientific; 1:1000), diluted in "sample buffer", proceeded for 30 min at RT. After removing the secondary antibody, the plate was washed as described above. For the detection, 100 µl/well of substrate were distributed into each well and let in incubation in the dark for 12 min at RT. The reaction was stopped with 100 µl/well of "stop reagent". Photometric measurement of the colour intensity was done with "Infinite M200 Pro microplate reader" (Tecan) exposing the plate to a wavelength of 450 nm.

2.7 Rat kidney

2.7.1 Tissue preparation for histology

Tissue sections, 1.5 µm thick, were cut from kidney paraffin blocks using a manual microtome (Histo-Line laboratories) and mounted on microscope slides. To remove the paraffin, tissue sections were incubated in xylene for 10 min, replacing the solution two times. The following step, tissue rehydration, was performed by incubating the sections for 10 min in a series of ethanol solutions with decreasing concentrations: 100% (solution replaced twice), 95%, and 70%. Eventually the slides were rinsed in distilled water for 3 min, changing water twice, until they were ready for the staining procedure.

2.7.2 Periodic acid Schiff staining

Tissue sections were first oxidized in 1% periodic acid solution for 5 min. They were then rinsed three times in tap water and one time in distilled water. An incubation with Schiff reagent (Thermo Fisher Scientific) followed at RT for 1 hour to develop a magenta colouration. Afterwards, the sections were placed under running tap water for 5 min and counterstained with hematoxylin (Thermo Fisher Scientific) for 1 min to visualize nuclei. A final 3 min wash in running water and a rinse in distilled water were done before dehydrating the tissue section and mounting the coverslip.

2.7.3 Immunofluorescence staining

All immunofluorescence stainings were performed on paraffin preserved kidney tissue sections. Following paraffin removal and rehydration, two different antigen retrieval methods were used: heat induced and enzymatic. For heat induced antigen retrieval, sections were incubated at 120°C in citrate buffer (pH 6.2) for 15 min in an autoclave, then cooled in ice for 10 min. For enzymatic antigen retrieval, tissue sections were incubated with proteinase 24 (Sigma Aldrich, 227mg/ml) for 30 min in a water bath at 37°C. Both reactions were stopped with 99% ethanol. Afterward, sections were washed 3 times for 3 min, first in distilled water and then in PBS. The blocking step followed, performed by incubating the tissue sections with 5% horse serum-PBS-BP (Vector Laboratories) for 30 min at RT. The blocking solution was then replaced with 150 µl of primary antibody, prepared in blocking solution, and incubated overnight at 4°C. The following primary antibodies were used: rabbit anti PLA_2R (Sigma Aldrich; 1:75), donkey anti rat IgG (Jackson ImmunoResearch; 1:2500), rabbit anti human IgG (Agilent technologies; 1:250), goat anti rat C3 (NordicYMUbio; 1:800), rabbit anti laminin (Sigma Aldrich; 1:200), goat anti collagen IV (Southern Biotech; 1:200), guinea pig anti nephrin (OriGene; 1:50). The next day, tissue sections

were washed 3 times with PBS for 5 min each and incubated for 30 min at room temperature with fluorochrome conjugated secondary antibodies. The following secondary antibodies, diluted in 5% horse serum, were used: donkey anti rabbit IgG (Jackson Immuno Research; 1:100), donkey anti-guinea pig IgG (Jackson Immuno Research; 1:100), donkey anti mouse IgG (Jackson Immuno Research; 1:100), donkey anti goat IgG (Jackson Immuno Research; 1:100). After 3 washing steps with PBS, cell nuclei were counterstained with Deep Red Anthraquinone 5 (DRAQ5) (Thermo Fisher Scientific; 1:1000) at RT for 10 min. A final 5 min wash in running tap water and a rinse in distilled water were performed before mounting the coverslips with "Fluoromount-G Mounting" medium (Thermo Fisher Scientific). Images were acquired using a LSM-800 Axio Observer confocal microscope in Airyscan mode and analyzed with ZEN 2.3 (Carl Zeiss microscopy GmbH) software.

2.7.4 Rat glomerular extract production

A Tris-HCl/glycerol lysis buffer supplemented with 1% triton X-100 (Merck) and 1x protease inhibitor (Merck) was used to extract total proteins from frozen isolated glomeruli pellet. For 1 gr of pellet, 165 µl of lysis buffer were added. The tissue was then homogenized with a plastic pestle and incubated 1 hour on a tube's rotator. In order to remove residual rat IgG from the tissue lysate, protein G resin (GeneScript) was used. Two hundred microliters of resin slurry were spun and pelleted in a mini centrifuge sprout. The resin was then equilibrated performing two washes with lysis butter deprived of triton X-100. After the incubation with lysis buffer, the glomeruli pellet was centrifuged at 14000 rpm for 10 min. Supernatant was retrieved and added to the pre equilibrated protein G resin. Sample and resin were let in incubation for 2 hours on a tube rotator. Resin was spun down to recover the lysate which was then transferred to a 0.45 µm Spin-X column (Costar) and centrifuged at 4000 x g for 2 min to filter remaining resin beads. All incubations and centrifugation steps were carried out at 4°C. The lysate or rat glomerular extract (RGE) was split in 20 µl aliquots, blast freeze in liquid nitrogen and stored at -20°C until being analysed by western blot.

2.7.5 Quantification of total protein concentration

The "DC protein assay" kit (Biorad) was used to determine the total protein concentration in the rat glomerular extract. A standard curve was made using four dilution points [0.2 mg/ml – 1.5 mg/ml] of "10% Octagam" human IgG (Octapharma) prepared in the same lysis buffer used to produce rat glomerular extract. Five microliters of standard and undiluted rat glomerular extract were loaded into a 96 well plate (Sarstedt). To prepare the working reagent, 20 µl of "Reagent S" were mixed with 1 ml of "Reagent A". Twenty-five microliters of working reagent were pipetted

into each well containing samples and standards. Two hundred microliters of "Reagent B" were added to the wells and let in incubation for 15 min at RT on a rocking platform. Absorbance was read in an "Infinite M200 Pro" (Tecan) microplate reader with a wavelength of 650 nm. Samples absorbance was interpolated onto the standards regression line whose slope and intercept were used to calculate the unknown concentration of the RGE samples.

2.7.6 Western blot analysis of RGE

To prepare the sample master mix, 8 µl (~ 5 µg) of rat glomerular extract were added to 4 µl of 4x Laemmli sample buffer and 3 µl of distilled water. The master mix was heated at 95°C for 3 min and 12 µl were loaded onto a "4-15% Mini-PROTEAN TGX" precast protein gel (Biorad). To analyse the samples under reducing conditions, 8 µl of rat glomerular extract were mixed to 4 µl of 4x Laemmli sample buffer and 3 µl of β-mercaptoethanol (700 mM). Three microliters of "Precision plus" protein standard (Biorad) were used to estimate the molecular weight of the separated proteins. The electrophoretic run was performed in 0.25x SDS running buffer at 160 V for 45 min. Proteins were transferred to a 0.45 µm PVDF membrane (Sigma Aldrich), pre-activated in methanol. Before the transfer, gel, membrane and filer pads were equilibrated in transfer buffer (10% methanol, 1x TG) for 5 min. Transfer was carried out under semi-dry conditions using Trans-blot Turbo (Bio-Rad) at constant 25 V for 25 min. Following transfer, the membrane was blocked in 3.5% milk PBS-T for 1 hour at RT with gentle shaking, then cut horizontally at approximately 75 KDa. The upper portion of the membrane, above 75 KDa, was incubated overnight at 4°C with either human PLA_2R positive plasma (1:100) or rabbit anti PLA_2R antibody (Sigma Aldrich; 1:200). The lower portion was incubated with mouse anti glyceraldehyde-3-phosphate dehydrogenase (GAPDH) antibody (Santa Cruz; 1:10k) as a control to normalise the PLA_2R signal intensity to protein loaded. After primary antibody incubation, the membranes were washed three times in PBS-T for 3 minutes each and incubated for 1 hour at RT with the following HRP conjugated secondary antibodies: mouse anti human IgG4 (Southern Biotech; 1:10k), mouse anti-human IgG total (Southern Biotech; 1:20k), rabbit anti-mouse IgG (Merck; 1:20k), goat anti-rabbit IgG (MERCK, 1:20k). All secondary antibodies were prepared in blocking buffer. Membranes were washed again in PBS-T, then incubated with Pierce ECL substrate (Thermo Fisher Scientific) for 3 min in the dark. Immuno-reactive bands were visualized using the Amersham Imager 600 (Cytiva).

2.7.7 Anti PLA_2R antibody elution

Elution of anti PLA_2R antibodies was performed on 1 gr of frozen isolated glomeruli pellet. The pellet was let to thaw and re-suspended with 500 µl of IgG elution buffer (pH 2.6) (Thermo Fisher Scientific) supplemented with protease inhibitor (1x). The pellet resuspension was carried out with the help of a plastic pestle. Incubation in elution buffer proceeded for 2 hours at RT on a tube rotator. Eluate was collected centrifuging the sample at 21000 x g for 10 min at 4°C. To remove the remaining tissue contaminants, the eluate was transferred to a 0.45 µm Spin-X column (Costar) and centrifuged at 4000 x g for 2 min. Lastly, 50 µl of neutralisation buffer (1 M Tris-HCl, pH 8.5) were added to the eluate. The eluate was diluted 1:2 in 1% milk-PBST and analysed by western blot where it was used as primary antibody. Twenty-five ng of full length human PLA_2R, expressed in transfected HEK-293 cells, were loaded under non-reducing conditions onto a 4-15% Mini-PROTEAN TGX precast protein gel (Bio-rad). Following the semi-dry transfer and blocking in milk, membrane sections above 75 KDa were cut and incubated with the eluate overnight at 4 °C. For the detection, the following antibodies were used: mouse anti-human IgG4 (Southern Biotech, 1:10k), mouse anti-human IgG total (Southern Biotech; 1:20K), goat anti-rat IgG (Thermo Fisher Scientific; 1:5k). Signals were visualized using chemiluminescent substrate (ECL, Thermo Fisher Scientific) and were acquired with the Amersham Imager 600.

2.8 Rat urine

2.8.1 Albumin ELISA and creatinine assay

High affinity binding 96 well plate (Sarstedt) was coated with 100 µl/well of sheep anti-rat albumin (Thermo Fisher Scientific; 1:500) prepared in 50 mM carbonate-bicarbonate buffer (pH 9.6). The incubation was carried out overnight at 4°C. The next day, the plate was washed 3 times with 200 µl/well of washing buffer (Sigma Aldrich; Tris Buffered Saline-Tween20, pH 8.0) and incubated with 300 µl/well of blocking buffer (Sigma Aldrich; 1 % BSA-Tris saline buffer) for 30 min. Rat urine was diluted (1:100; 1:200) in blocking buffer implemented with 10 % Tween-20. The standard curve was prepared with eleven dilution points of rat albumin (Sigma Aldrich; 5 µg/mL – 1.95 ng/mL) prepared in the same buffer as urine samples. After the incubation in blocking buffer, the ELISA plate was washed 3 times with 200 µl/well of washing buffer. Subsequently, 100 µl/well of urine samples and albumin standards were loaded and incubated for 1 hour on a shaker. The plate was washed 4 times with 300 µl/well of washing buffer and incubated with 100 µl/well of sheep anti-rat albumin HRP conjugated (Thermo Fisher

Scientific;1:50k) prepared in 10 % Tween-20 implemented blocking buffer. After 1 hour of incubation, the plate was washed 4 times with 300 µl/well of washing buffer. To develop the signal, a 3 min incubation followed in the dark with 100 µl/well of 5.5′-Tetramethylbenzidine (TMB) Peroxidase substrate (Biozol). The oxidation reaction was stopped adding 100 µl/well of 1 M H_3PO_4. Absorbance was measured at 450 nm using "Infinite M200 Pro" microplate reader (Tecan). To compare urine samples with different grades of concentrations, albumin values were standardized against urine creatinine. Creatinine levels were measured with Creatinine Jaffe' kit (Hengler analytic). Urine samples were diluted (1:5; 1:10) in 0.9 % NaCl. The creatinine standard curve was prepared with five creatinine dilution points (Sigma Aldrich; 0.5 g/L – 0.1 g/L) prepared in 0.9 % NaCl. Ten microliters of each sample were loaded on a 96 well plate (Sarstedt) and mixed with 50 µl of reagent 1 mixed with reagent 2 (ratio 5:1 ml). After 1 min of incubation, the plate was loaded on "Infinite M200 Pro" microplate reader (Tecan) and absorbance was measured at 492 nm. All ELISA and creatinine steps were performed at room temperature, except for the ELISA plate coating step.

2.8.2 Urine analysis by Western blot

Rat albumin and rat IgG content in urine were assessed by western blot using rat concentrated urine. To concentrate the urine, each sample was loaded in "Microcon-10 kDa" centrifugal filter units (Merck) and centrifuged at 10,000 x g for 20-30 min. The loading volume and the concentration factor were calculated individually for all samples considering the urinary creatinine concentration. After concentration, the samples were retrieved inverting the filter unit in a new collecting tube and centrifuging at 1000 x g for 3 min. For the gel electrophoresis, 5 µl/lane of concentrated urine mixed in native Laemmli buffer (Biorad) were heated at 95°C for 3 min and separated in a "4-15% mini protean TGX" precast protein gel (Biorad). The run, performed with 1x SDS running buffer, lasted 45 min and was set at 160 V, 400 mA. Proteins were transferred on a 0.45 µm PVDF membrane (Sigma Aldrich) in semi dry mode using a "Trans-blot turbo transfer" system (Biorad) set at 25 V, 1 A for 30 min. After the membrane was blocked in 3.5 % milk-PBST for 1 hour at RT it was cut in a half between 75 and 50 kDa. The membrane part above 75 kDa was incubated in "goat anti rat IgG" (Thermo Fisher Scientific; 1:5k) while the part below 50 kDa was put in "sheep anti rat albumin" (Thermo Fisher Scientific; 1:30k). Both secondary antibodies were prepared in 3.5 % milk-PBST and let in incubation for 1 hour at RT on a rocking platform. After 3 washing rounds in PBS-T, each lasting 3 min, the two membrane parts were incubated in Pierce ECL substrate (Thermo Fisher Scientific) for 3 min in the dark. Immuno-positive signals were detected with "Imager 600" (Amersham).

3. Results

3.1 Validation of PLA_2R transgene expression vectors

Four transgene expression vectors, encoding either full-length human PLA_2R (Figure 11: EXP 1), full-length rat PLA_2R (Figure 11: EXP 4) or chimeric variants (Figure 11: EXP 2-3) combining rat and human sequence elements, were designed and validated in collaboration with GenOway (Lyon, France).

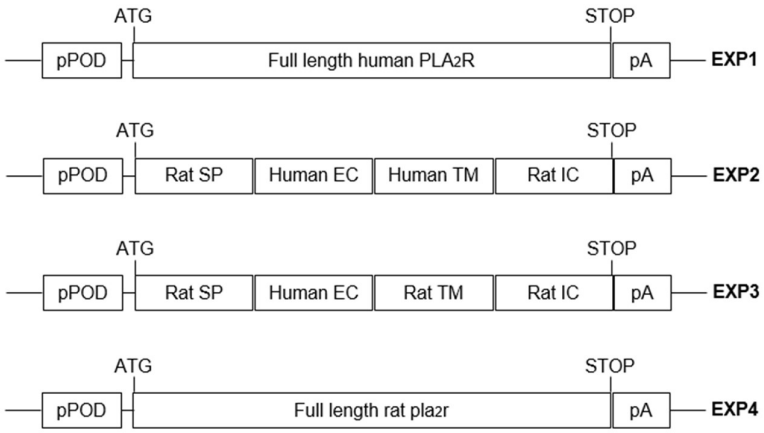


Figure 11: Schematic representation of PLA_2R expression vectors.
All vectors are expressed under the control of the podocin promoter (pPOD) and end with a poly-adenine tail (pA). Expression vectors 1 and 4 contain full length human and rat PLA_2R sequence respectively. Expression vectors 2 and 3 have a chimeric PLA_2R sequence with rat signal peptide (SP), human extracellular domain (EC) human/rat transmembrane domain (TM) and rat intracellular domain (IC).

The expression of the four transgene vectors was evaluated at RNA level in transfected rat fibroblasts (CRL-1764). The reversed transcribed cDNA was analysed by RT-PCR (Figure 12A, B), and showed that all expression vectors were successfully expressed at full length with no evidence of internal splicing both at 3' and 5' end. Transfected rat fibroblasts were also used to verify the expression of the four vectors at protein level. The anti PLA_2R commercial antibody (Sigma Aldrich) (Figure 13A) and the PLA_2R antibodies from human plasma (Figure 13C) succeeded to bind the full length human PLA_2R protein (EXP 1) and the chimeric PLA_2R protein in which extracellular and transmembrane domains derived from the human sequence (EXP 2).

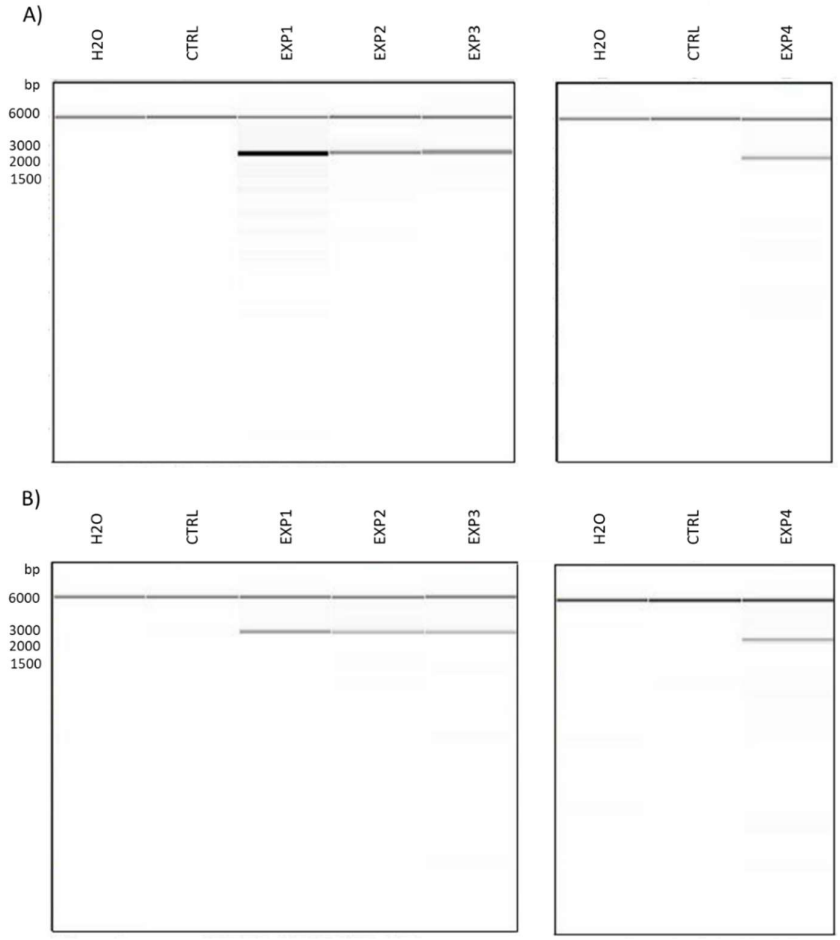


Figure 12: RT-PCR results.
A) *5' end B) 3' end of the cDNA derived from the four expression vectors (EXP 1-4) migrated as single bands at the expected high with no evidence of internal splicing. Negative controls, water (H_2O) and cDNA from non-transfected cells (CTRL), showed no contamination.*

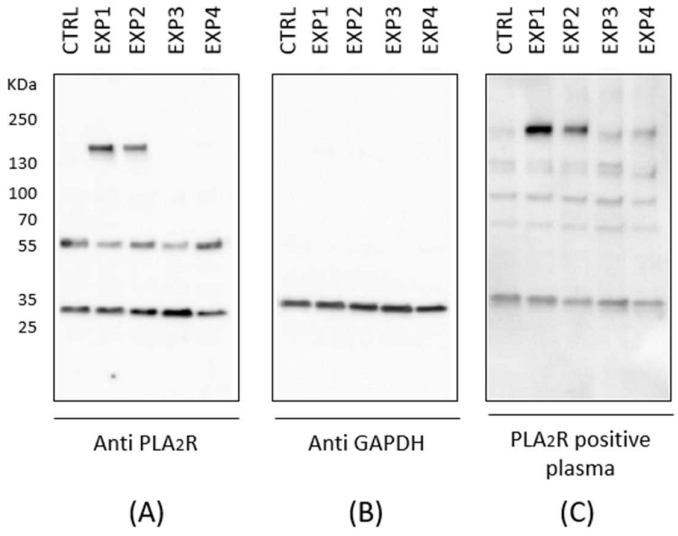


Figure 13: Western blot results.
Expression vectors 1 and 2 were recognised both by the commercial anti-PLA_2R antibody (A) and by PLA_2R antibody from human plasma (C). GAPDH was used as a loading control to normalize protein amount per lane (B). No PLA_2R signal was detected in non-transfected cells (CTRL). GAPDH: Glyceraldehyde-3-phosphate dehydrogenase.

The EXP 1 and EXP 2 vectors, which had been recognised by PLA_2R antibodies in western blot, were further analysed by FACS (fluorescent-activated cell sorting) to assess PLA_2R expression on the cell surface (Figure 14). No specific surface expression of PLA_2R was detected in HEK293 cells for either constructs. In contrast, a weak expression was observed in rat fibroblast cells (CRL1764), with a higher percentage of PLA_2R positive cells detected for EXP 2, the chimeric PLA_2R vector, compared to EXP 1, the full length PLA_2R vector.

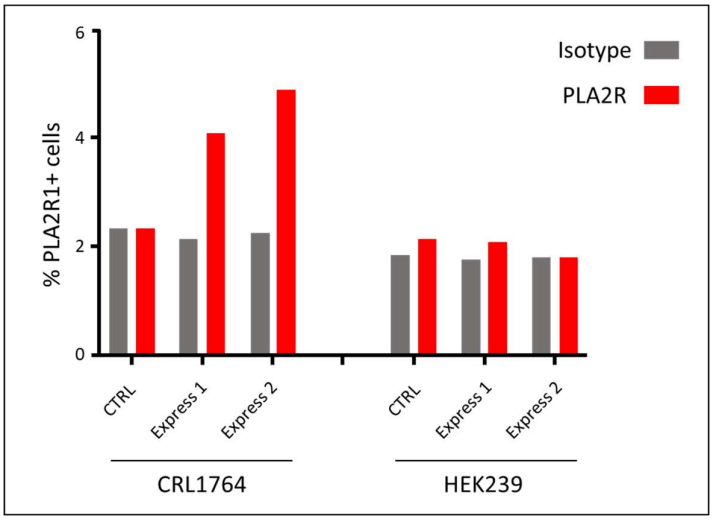


Figure 14: Fluorescence-activated cell sorting results.
PLA_2R expression of expression vectors 1 and 2 evaluated in transfected rat fibroblast (CRL1764) and in human embryonic kidney 293 cells (HEK293). Anti PLA_2R commercial antibody (red) detected the expression of both constructs only in rat cells. No signal was detected with the isotype antibody (grey).

In light of the in vitro tests assessing PLA_2R expression at the RNA, protein, and cell surface levels, the final transgene construct (Figure 15) selected for the pronuclear microinjection included: the human podocin promoter, the chimeric PLA_2R gene, an internal ribosome entry site (IRES) sequence and the td-Tomato reporter gene.

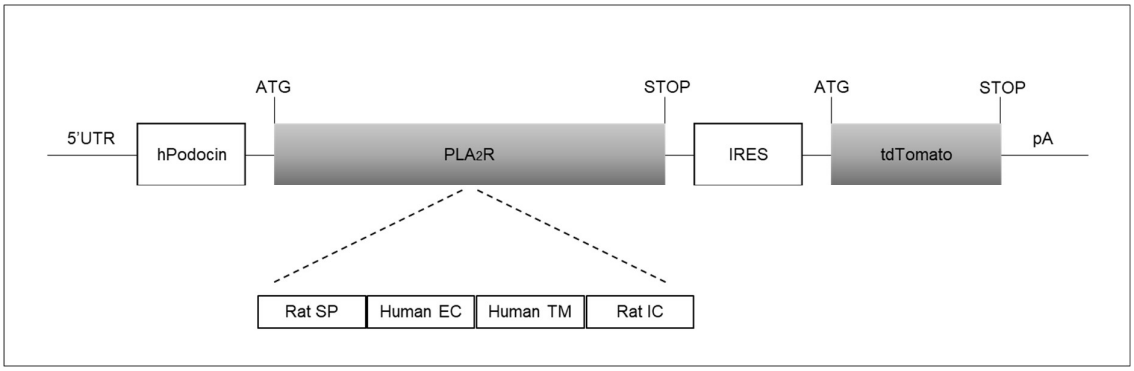


Figure 15: Schematic representation of chimeric PLA_2R-td-Tomato knock in construct.
SP: signal peptide. EC: extracellular domain. TM: transmembrane. IC: intracellular domain. IRES: internal ribosome entry site. pA: poly-adenine tail.

3.2 Genotyping of PLA_2R transgenic rats

The founder animals, two males and two females, presented a singular copy of the PLA_2R transgene (hemizygous genotype), as assessed by the genotyping and sequencing analysis carried out at GenOway (Lyon, France). The genotyping of the transgenic offspring, derived from the mating between founders and wild type rats, through PCR and agarose gel electrophoresis showed two DNA bands (Figure 16). In fact, all hemizygous rats were identified by discerning a band at 343 bp and one at 172 bp, representing the amplification of PLA_2R and quality control (ywhae gene) respectively. The specificity of the PLA_2R primer set, designed to bind the human sequence of the extracellular domain, was confirmed by the results seen in the wild type rats: presence of a singular band, for the quality control, with no band detectable at the PLA_2R migration high. The observed transgene transmission across the hemizygous offspring, deriving from hemizygous crossed with wild types (42 transgenic vs 59 wild type), did not significantly differ from the expected mendelian 1:1 ratio ($\chi^2 = 3, 50$; $p = 0, 05$).

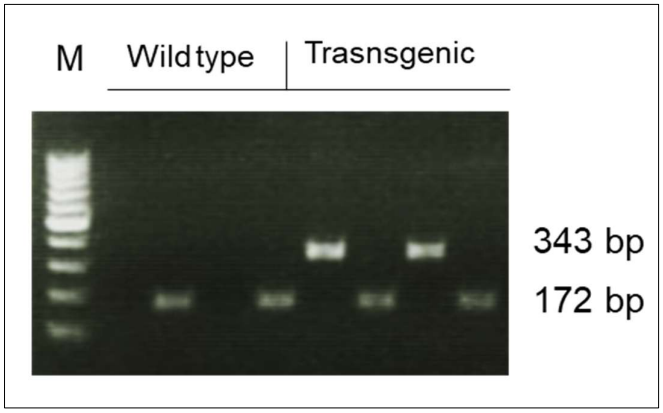


Figure 16: Genotyping results from wild type rats crossed with PLA_2R hemizygous. *All four animals are positive for ywhae quality control gene (172bp); transgenic animals show positivity at 343bp, band that represents pla2r. M: marker.*

Hemizygous rats, from different mothers, were mated to get an offspring characterized by two copies of the transgene (homozygous). To genotype the homozygous offspring, the standard PCR protocol was substituted with a real time-PCR based on SYBR greed detection chemistry. The robustness of the genotyping protocol was confirmed by the evaluation of the amplification efficiency of both PLA_2R and quality control primers. In fact, the slope of the standard curve (Figure 17), created plotting the Ct values with serial dilutions of transgenic rat DNA, showed an amplification efficiency (Efficiency = $(10^{\wedge\,(-1/\text{slope})} - 1) \times 100$) of 110% and 100% for PLA_2R and YWHAE primers respectively.

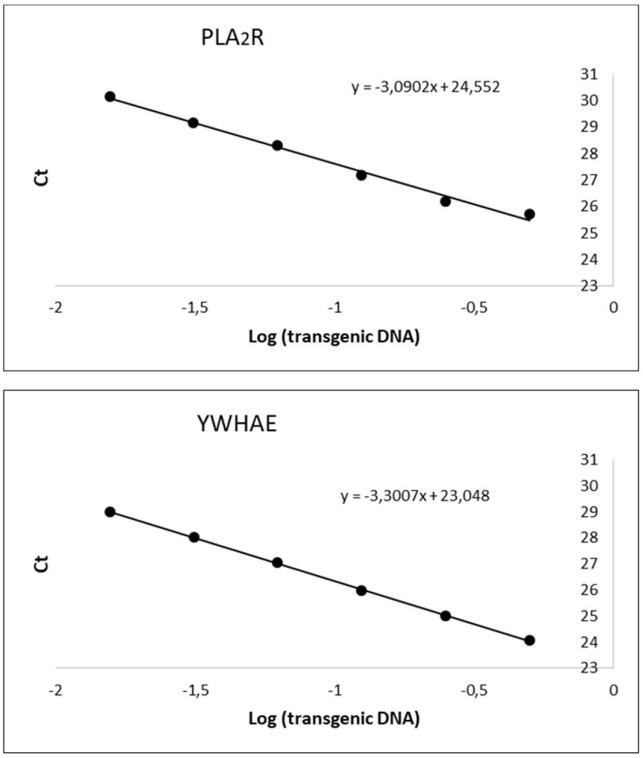


Figure 17: PCR efficiency curves.
Standard curve generated by plotting the log of DNA concentration against the cycle threshold values. Ct: cycle threshold.

The reliability of the protocol and the absence of unspecific amplifications was further confirmed by a melting curve experiment performed at the end of each PCR round (Figure 19). This experiment showed in fact only two peaks, one at temperature 80°C and the other at 85°C, corresponding to PLA_2R and ywhae amplification. No unspecific peak at different melting temperatures was seen for the test samples and in the no template control sample. The three different genotypes could be distinguished (Figure 18) setting a hemizygous rat, with a relative quantification of 1, as reference sample. Wild type animals showed no amplification for PLA_2R, with a relative quantification of 0, while hemizygous and homozygous presented a relative quantification of 1 and 2 respectively.

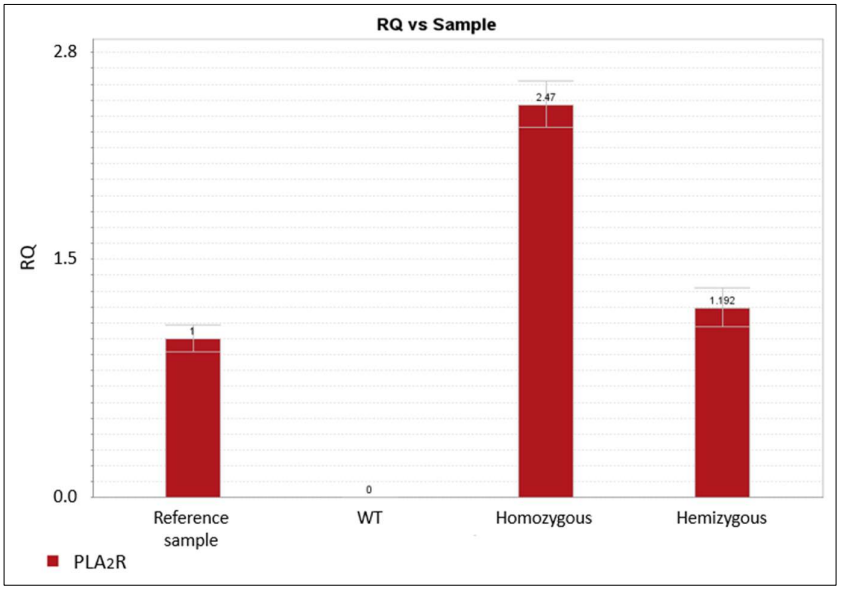


Figure 18: Relative quantification of PLA_2R transgene.
The relative quantification (RQ) of PLA_2R in wild type (WT), homozygous and hemizygous samples is zero, two and one respectively.

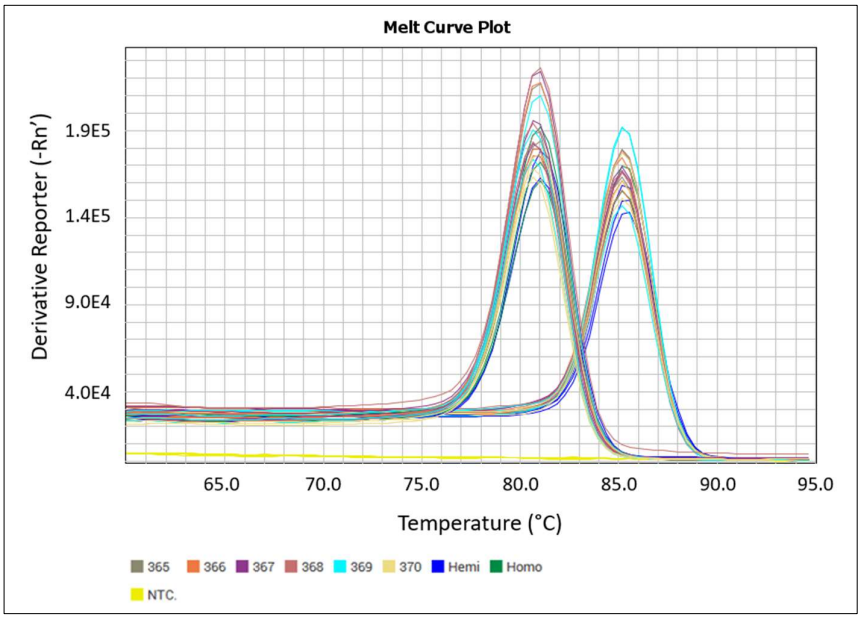


Figure 19: Melt curve graph.
Two peaks representing the melting temperature of PLA_2R (80°C) and of ywhae (85°C). The no template control (NTC) showed no peak meaning no contamination in the PCR mix.

3.3 Phenotyping of PLA_2R transgenic rats

The PLA_2R expression levels in PLA_2R transgenic male and female rats, was analysed at the age of eight weeks. Analysis of the RGE by western blot and densitometry evaluation, showed that PLA_2R expression seem to be higher in the homozygous rats compared to the hemizygous ones (Figure 20). Only one outlier with strong PLA_2R signal, was present among the hemizygous group. As expected, no PLA_2R positivity was detected in the RGE of wild type rats.



Figure 20: Evaluation of PLA_2R expression in rat glomerular extract.
Rat glomerular extract (RGE) from homozygous (T/T), hemizygous (T/+) and wild type (+/+) rats was analysed by western blot. Human PLA_2R antibodies positive serum was used as primary antibody to detect PLA_2R; GAPDH was used to check for the protein loading amount and normalize PLA_2R signal. Western blot bands' intensity was quantify with the software "Image studio lite 5.2". GAPDH: Glyceraldehyde-3-phosphate dehydrogenase.

The difference of PLA_2R expression between the three genotypes was observed also with immunofluorescence analysis (Figure 21). Conforming to western blot results, PLA_2R (green) showed a higher signal intensity in homozygous rats compared to the hemizygous in which the intensity was quite similar to that of a wild type rat. However, the PLA_2R expression level observed in the homozygous rats seemed to be not fully comparable to the one observed in humans. In addition it was observed that more green background is seen in the rat tubules compared to the human control. Whit this immunofluorescence analysis it was also possible to verify the correct PLA_2R localization in the podocytes. The green signal can in fact be seen along the capillaries in the outer aspect of the glomerular basement membrane (red).

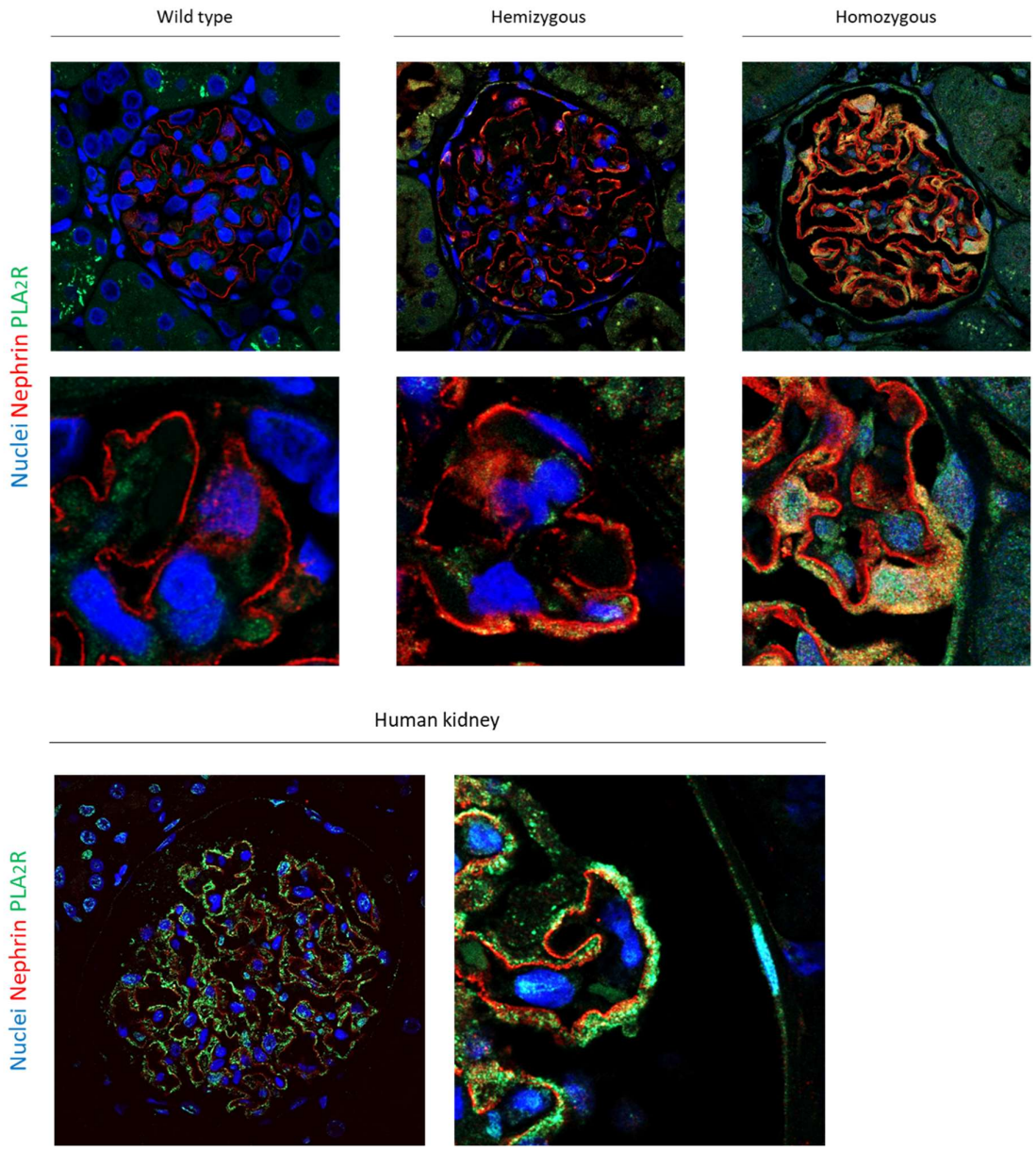


Figure 21: Evaluation of PLA_2R expression by immunofluorescence.
Kidney paraffin sections from representative wild type, hemizygous, homozygous rats and human stained for PLA_2R (green), nephrin (red) with nuclear counterstain (blue). PLA_2R expression, positive along the capillary loops, is higher in homozygous compared to hemizygous rats.

The PLA_2R expression didn't interfere with the normal morphology of the glomerulus. Through PAS staining (Figure 22), it was seen that the podocyte cells of transgenic animals appear normal and comparable to wild type. Moreover, the glomerular basement membrane stained homogenously pink and the capillary loops looked thin and well defined.

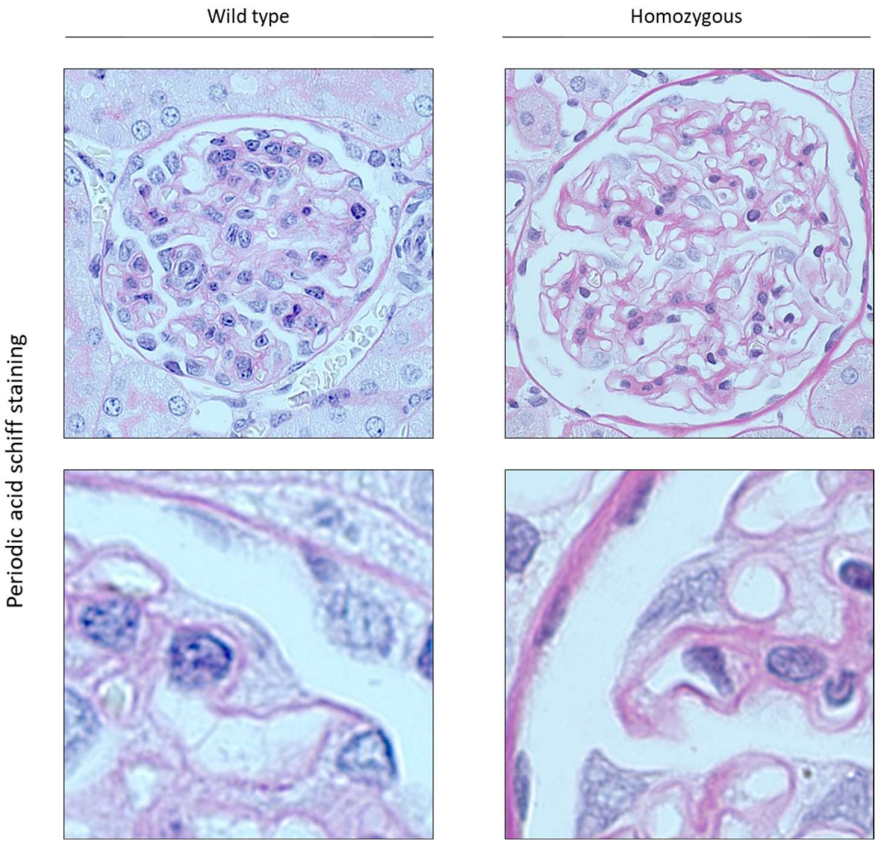


Figure 22: Periodic acid Schiff staining of rat glomeruli.
PAS staining of representative wild type and homozygous rats. No morphologic abnormalities are seen in the glomeruli of the transgenic rats.

The western blot analysis, performed on blood samples from 3 weeks old hemizygous (3 males, 2 females) and 8 to 9 weeks old homozygous (2 males, 2 females), showed that no animal developed antibodies directed against the human PLA_2R (Figure 23) following its expression on the podocytes.

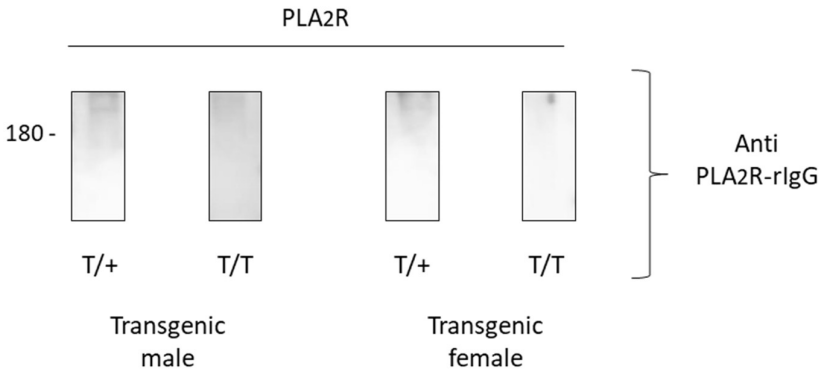


Figure 23: Assessment of spontaneous production of PLA_2R specific rat IgG.
Rat plasma was used as primary antibody in western blot to assess the presence of antibodies against PLA_2R. No anti PLA_2R antibodies were found in the blood of hemizygous (T/+) or homozygous (T/T) males and females.

Along with normal PAS staining, the functionality of the glomerular filtration barrier was assessed testing the transgenic animals for proteinuria. Albumin to creatinine ratios in 8 to 9 weeks old homozygous rats (5 males, 5 females) showed no relevant proteinuria (Figure 24) compared to wild type rats. This confirmed that hPLA$_2$R expression coexist with a healthy glomerulus.

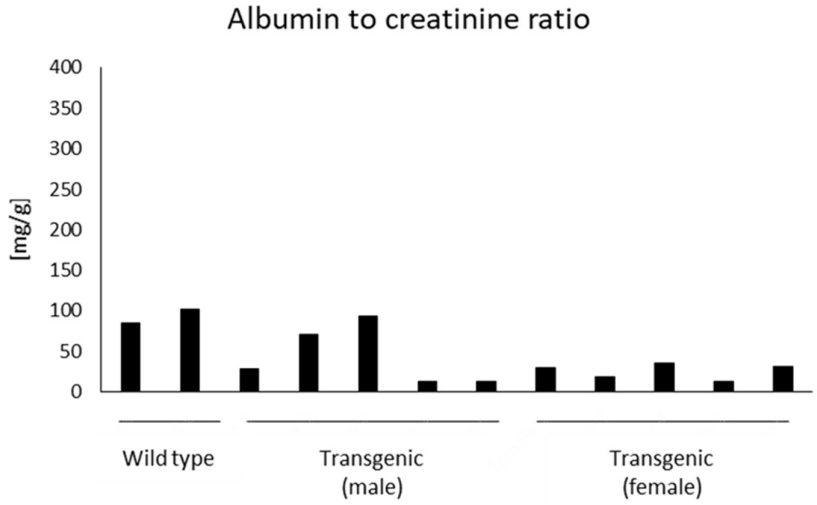


Figure 24: Albumin to creatinine ratio in rat urine.
Albumin to creatinine ratios of transgenic male and female rats are comparable to wild type rats.

3.4 Passive immunisation

3.4.1 Hemizygous rats

Ten hemizygous male rats, between seven and eight weeks old, were chosen to be immunised through the passive transfer of human anti PLA$_2$R antibodies. Since these animals were born from different mothers, they were equally assigned to experimental and control group to minimize the effect of external variables (maternal care, early life conditions, and genetic background).

Rat n°	**Sex**	**Weeks**	**Group**
01	Male	7-8	Experimental
02			
03			
04			
05			
06			Control
07			
08			
09			
10			

The passive immunisation of hemizygous rats was performed using a human plasma pool, made from MN patients positive for anti PLA_2R antibody. The plasma pool had a PLA_2R antibody titer of 460 RU/mL as determined by ELISA. After concentrating the PLA_2R antibody positive plasma pool to half volume, it was analysed by western blot. This analysis (Figure 25A) confirmed that the antibodies successfully bound PLA_2R under non-reducing conditions, while showing no reactivity with glomerular extracts from wild-type rats. Moreover, the results confirmed that the PLA_2R antibodies in the pool bound to the N-terminal region of PLA_2R, but also CTLD1-2 and CTLD7-8 subdomains. The results were negative for the CTLD8 domain. The healthy plasma (Figure 25B), used to immunise the control group, was tested with transgenic, wild type RGE and human glomerular extract (HGE) to confirm that the PLA_2R antibodies binding was indeed specific.

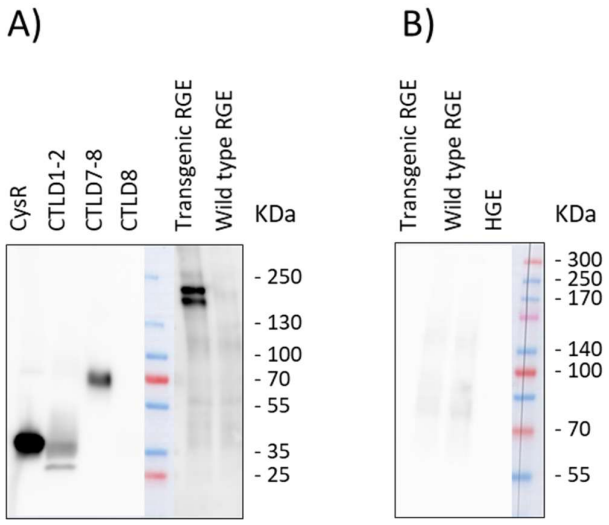


Figure 25: Evaluation of PLA_2R antibody positive plasma pool and healthy plasma reactivity. *A) PLA_2R antibody positive plasma pool and B) healthy plasma were tested as primary antibodies in western blot to evaluate their reactivity towards PLA_2R domains, RGE and HGE. CysR: cysteine rich domain. CTLD: C-type lectin-like domain. RGE: rat glomerular extract. HGE: human glomerular extract.*

All animals survived until the last day of the experiment except for control rat #09 which died because of an embolism occurred immediately after the second infusion.

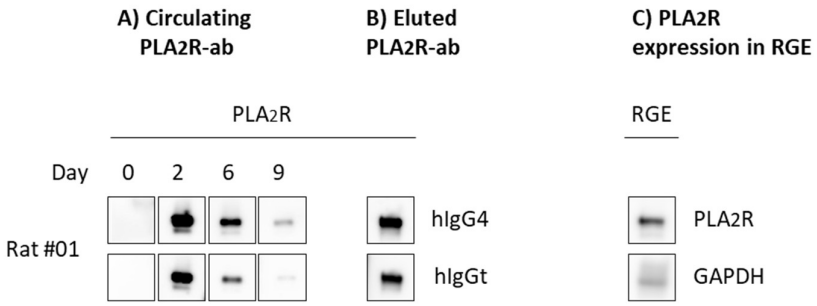
Western blot was used to detect circulating human anti PLA_2R antibodies in rat plasma at all time points. For the experimental group, no human PLA_2R specific IgG4 or IgGtot was detected in the plasma collected at day 0 before the immunisation (Figure 26A). A positivity for IgG4 and IgGtot appeared in the plasma collected one day after the first infusion (day 2). IgG4 remained

detectable until the end of the experiment (day 9), though with a decreasing trend, whereas total IgG declined more rapidly and was no longer detectable by day 6. Experimental rat #04 represented an exception to this trend, as anti PLA_2R antibodies in this animal remained at comparable levels across all time points following immunisation (Figure 26A). All control animals were negative for circulating PLA_2R specific IgG4 and IgGtot at all time points.

To check if the anti PLA_2R antibodies bound to the transgenic protein in vivo, glomeruli were isolated from kidney tissue collected after the harvesting at day 9. The glomeruli pellet was then used to perform an antibodies elution and the eluate was assessed as primary antibody by western blot to detect the presence of PLA_2R specific IgG4 and IgGtot.

The glomerular eluate of all experimental rats contained PLA_2R specific IgG4 and IgGtot (Figure 26B), exception made for rat # 04. In the case of this experimental animal, the negative result of the antibodies elution experiment was in line with the detection of constant amount of PLA_2R antibodies in circulation. Regarding the control group, the eluates from all rats didn't show positivity for PLA_2R specific IgG4 and IgGtot.

The PLA_2R expression of all ten rats was first tested on RGE by western blot. The RGE was analysed in non-reducing conditions and tested with human PLA_2R positive plasma. The membrane below 75KDa was incubated with anti GAPDH to normalize the PLA_2R signal with the total protein amount loaded per lane. Results were not positive for all test and control animals (Figure 26), such as rats #02, #04 and #05. In line with the observation that the PLA_2R expression in the hemizygous rats is very low when compared to the homozygous rats, the PLA_2R in most RGE gave a weak positivity (Figure 26C).



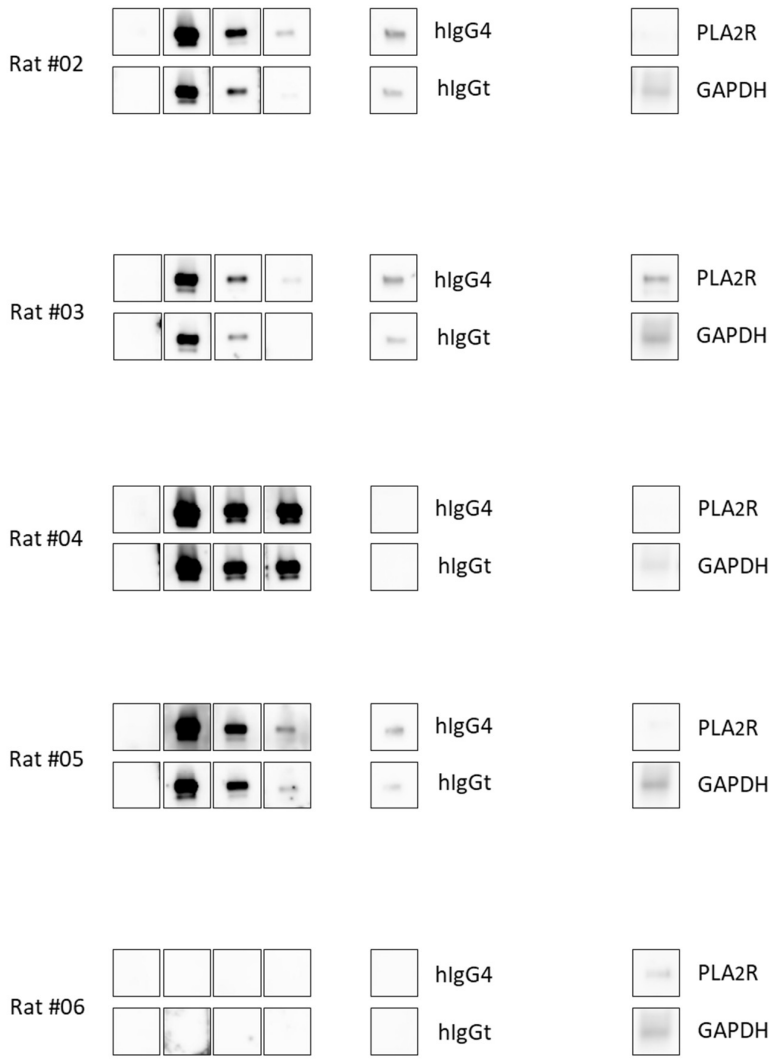


Figure 26: Western blot results.
A) Detection of human anti-PLA_2R IgG4 and total IgG in rat plasma collected at days 0, 2, 6, and 9. B) Detection of human anti-PLA_2R IgG4 and total IgG in rat glomerular eluate. C) Evaluation of PLA_2R expression in experimental rats (#01-05) and representative control #06 using RGE and human PLA_2R-ab positive serum. GAPDH signal from the same RGE samples was used as an internal loading control.

Immunofluorescence on paraformaldehyde-fixed kidney tissue (Figure 27) was performed alongside western blotting to assess PLA_2R expression in both experimental and control rats. For this staining the commercial anti PLA_2R antibody (Sigma Aldrich) was used. Results were positive only for the human kidney. No signal was observed in the wild type, experimental and control rat kidney tissues, confirming that the PLA_2R expression levels are low and below the technique detection limit.

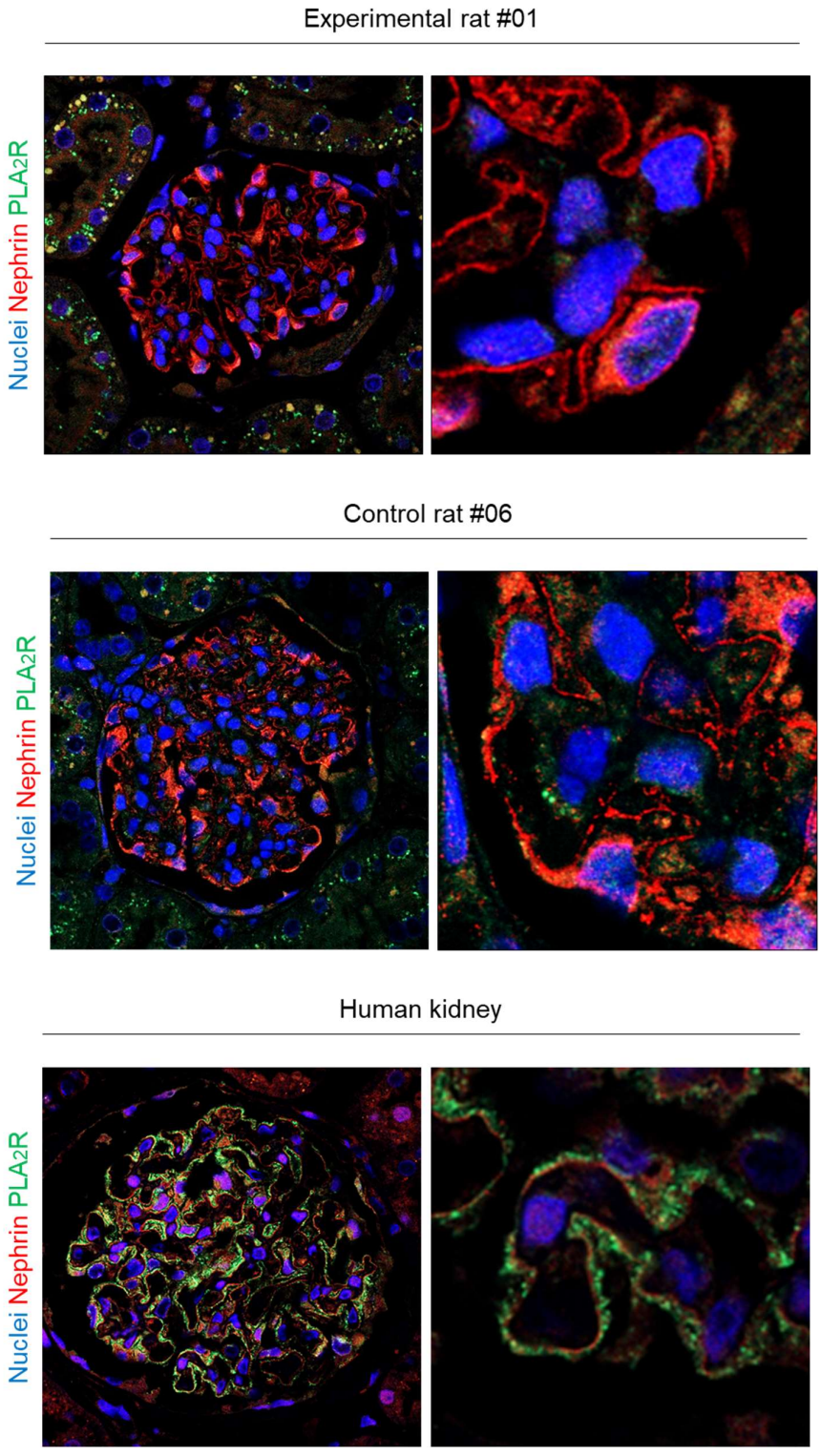


Figure 27: Evaluation of PLA_2R expression by immunofluorescence.
Kidney paraffin sections from representative experimental rat #01, representative control rat #06 and human kidney stained for PLA_2R (green), nephrin (red) with nuclear counterstain (blue).

Because of the low level of transgenic PLA_2R expression, the binding of anti-PLA_2R antibodies was only minimal. As a consequence the immunofluorescence staining for human total IgG (Figure 28) remained negative for all test and control rats.

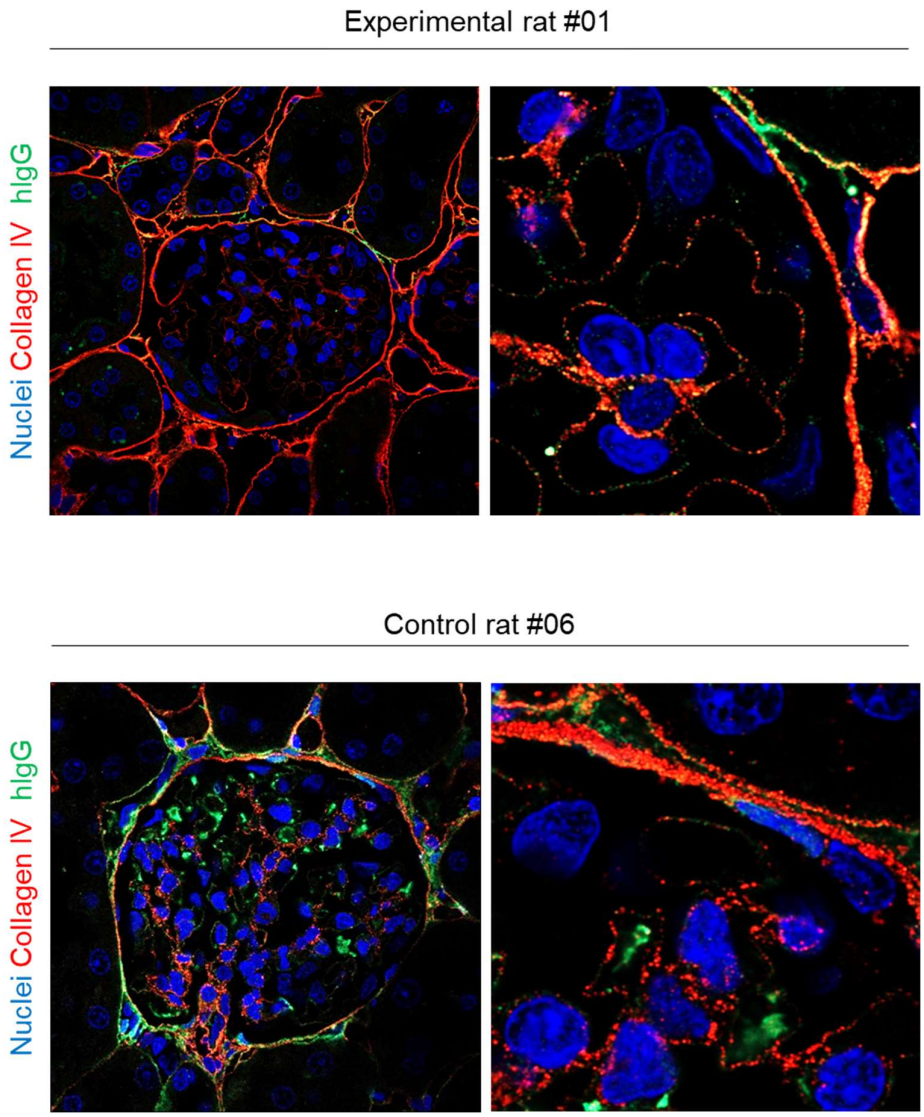


Figure 28: Evaluation of human IgG deposition by immunofluorescence.
Kidney paraffin sections from representative experimental rat #01 and control rat #06 stained for human IgG (green), collagen IV (red) with nuclear counterstain (blue).

No immune deposits or podocyte feet effacement were observed by electron microscopy (Figure 29). The absence of structural abnormalities in the glomeruli of experimental and control group was confirmed also by Periodic acid Schiff staining.

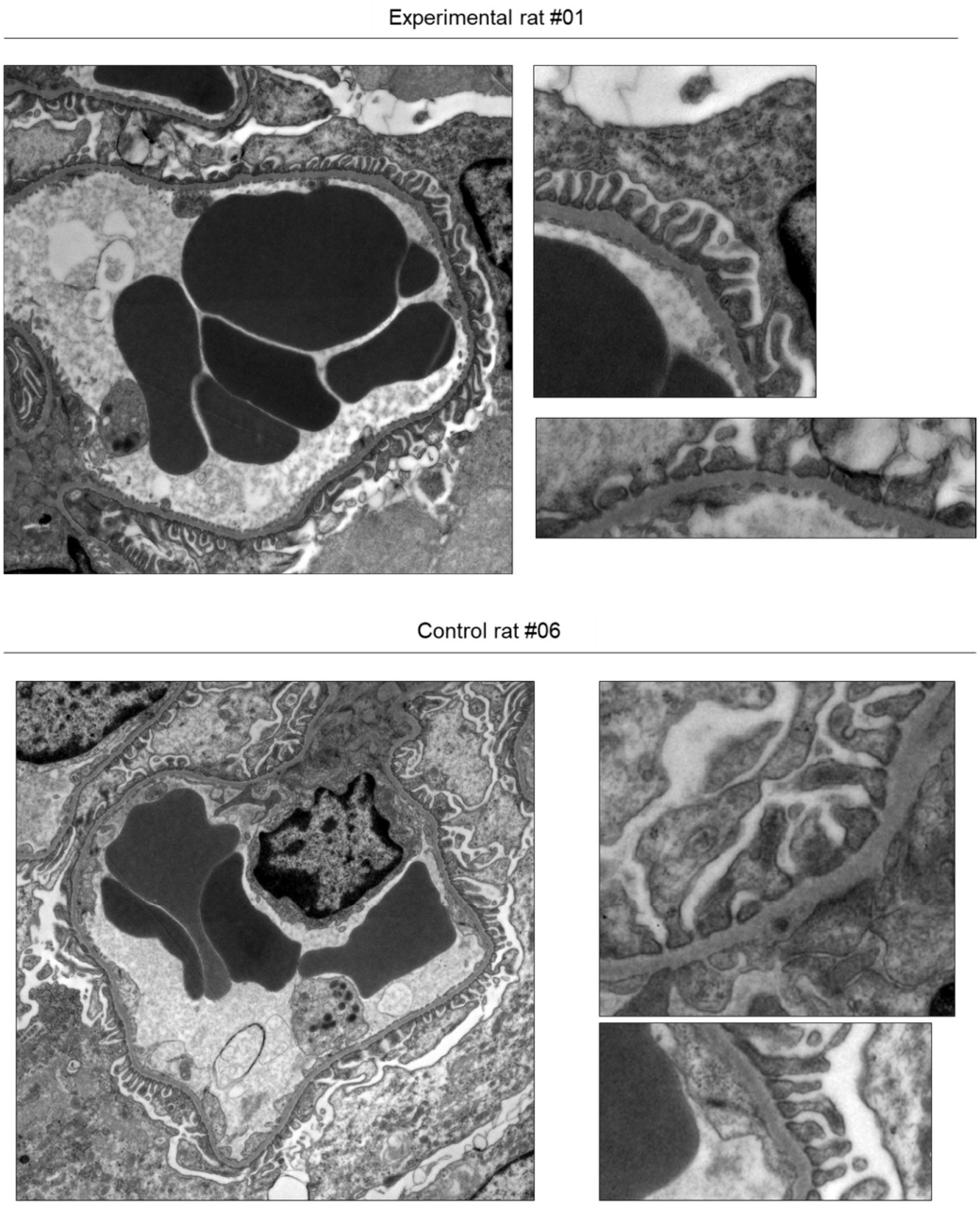


Figure 29: Electron microscopy picture of glomerulus.
Glomerular filtration barrier components present normal architecture in representative experimental rat #01 and control rat #06.

No increase in weight and oedema was observed in any animal. ACR measurement of each individual animal, did not show urine sample with proteinuric values (Figure 30A, B) and ACR values were comparable to the phenotyped animals that didn't receive any treatment. However, the experimental animals showed low-grade relative increase in ACR between day 0 and the other urine time points (Figure 30C). No such changes were observed in the control animals.

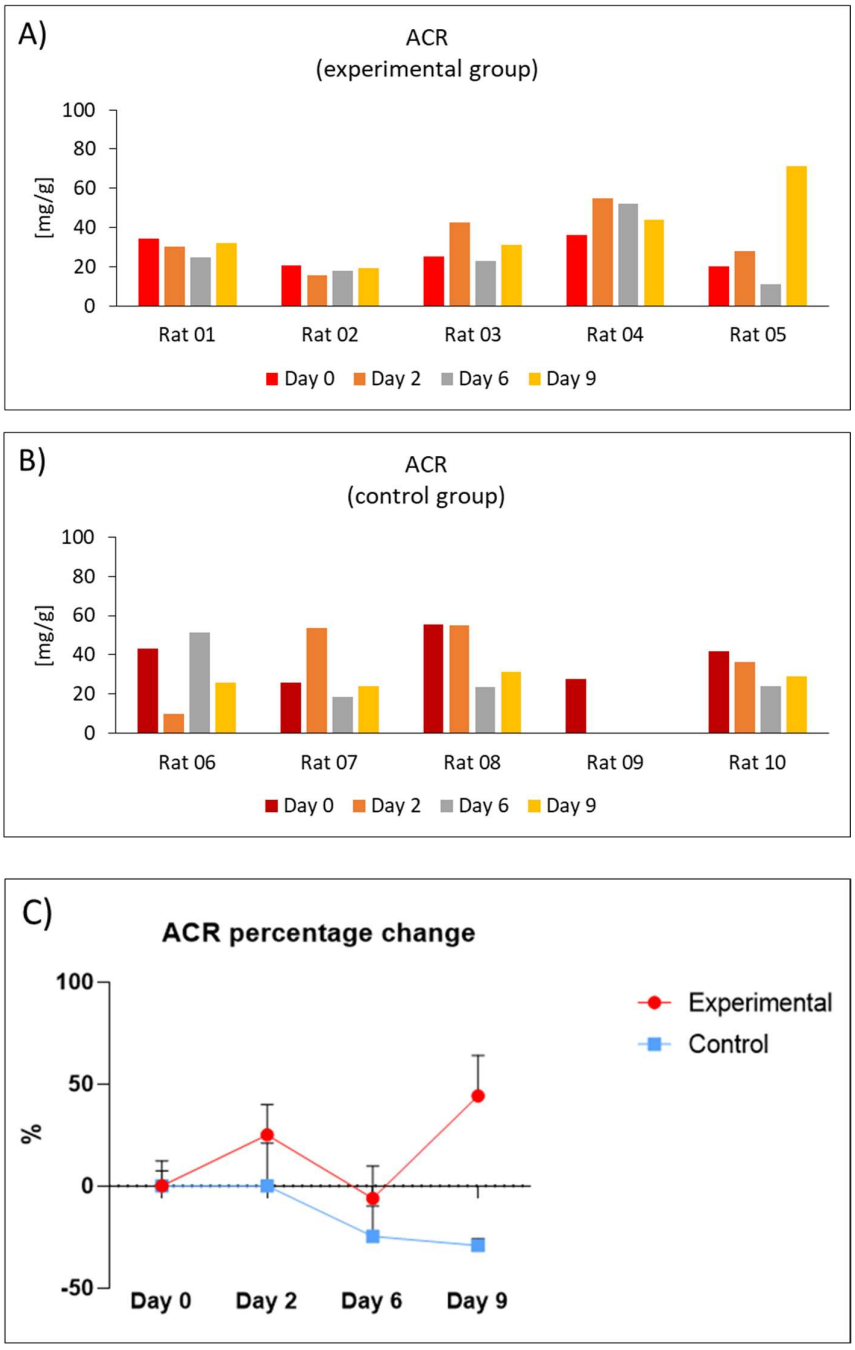


Figure 30: Urine analysis. *Individual albumin to creatinine ratio (ACR) in all time point urine of A) experimental and B) control groups. C) Average percentage change of ACR in experimental group (red) shows an increase at day 2 and 9; no increase seen in the control group (blue).*

3.4.2 Homozygous rats

Ten rats were genotyped as homozygous for the PLA_2R transgene and passively immunised with human PLA_2R antibodies. All animals were eight to nine weeks old at the beginning of the experiment. The immunisation was organised in experimental and control group each including three males and two females.

Rat n°	Sex	Weeks	Group
11	M	8-9	Experimental
12	M		
13	M		
14	F		
15	F		
16	M		Control
17	M		
18	M		
19	F		
20	F		

The immunisation scheme of the experiment was the same used with the hemizygous rats: two infusions with whole human plasma at day 0 and day 1. The experimental group was immunised with the same PLA_2R antibody positive plasma pool derived from patients with PLA_2R-ab positive MN that had been used in the hemizygous experiment. The control group received plasma from a healthy donor. Both infusions, PLA_2R antibody positive pool and healthy donor plasma, were concentrated to half volume. Prior to immunisation, the infusion mixes were tested by western blot to confirm the reactivity and specificity of the PLA_2R antibody positive plasma pool. The PLA_2R antibody positive plasma pool recognised human PLA_2R in the transgenic RGE and in the human glomerular extract (HGE), but only in non-reducing conditions. The intensity of the PLA_2R band observed in the human glomerular extract resulted higher compared to the one of the transgenic homozygous RGE. No binding was detected with the wild type RGE (Figure 31A). The healthy donor plasma used for the control group showed no binding activity (Figure 31B).

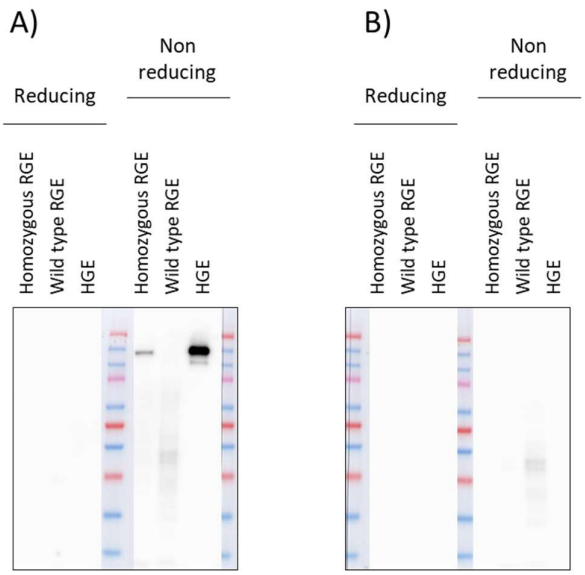


Figure 31: Evaluation of PLA_2R antibody positive plasma pool and healthy plasma reactivity.
A) PLA_2R antibody positive plasma pool and B) healthy plasma tested as primary antibodies by western blot to evaluate the specific reactivity with rat glomerular extract (RGE) and human glomerular extract (HGE). Anti-human IgG4 was used as secondary antibody.

No circulating PLA_2R specific IgG4 and IgGtot were detected in the experimental and control rats' plasma before the immunisation (day 0) (Figure 32). In two experimental animals, rats #11 and #14, the anti PLA_2R antibodies are present until day 9 showing a decreasing trend over the follow-up time in the experiment. In rats #12, #13 and #15 the anti PLA_2R antibodies are weakly or no more detectable at the last experiment day. When eluting antibodies from the isolated glomeruli, all experimental animals' eluates resulted positive for anti PLA_2R antibodies while all control animals 'eluates were negative.

Expression of transgenic human PLA_2R was assessed in RGE by western blot. The expression of human PLA_2R in the RGE was confirmed for all animals by the binding of PLA_2R antibodies from human plasma (Figure 32A). GAPDH signal intensity was comparable across samples, confirming similar loading amounts of RGE.

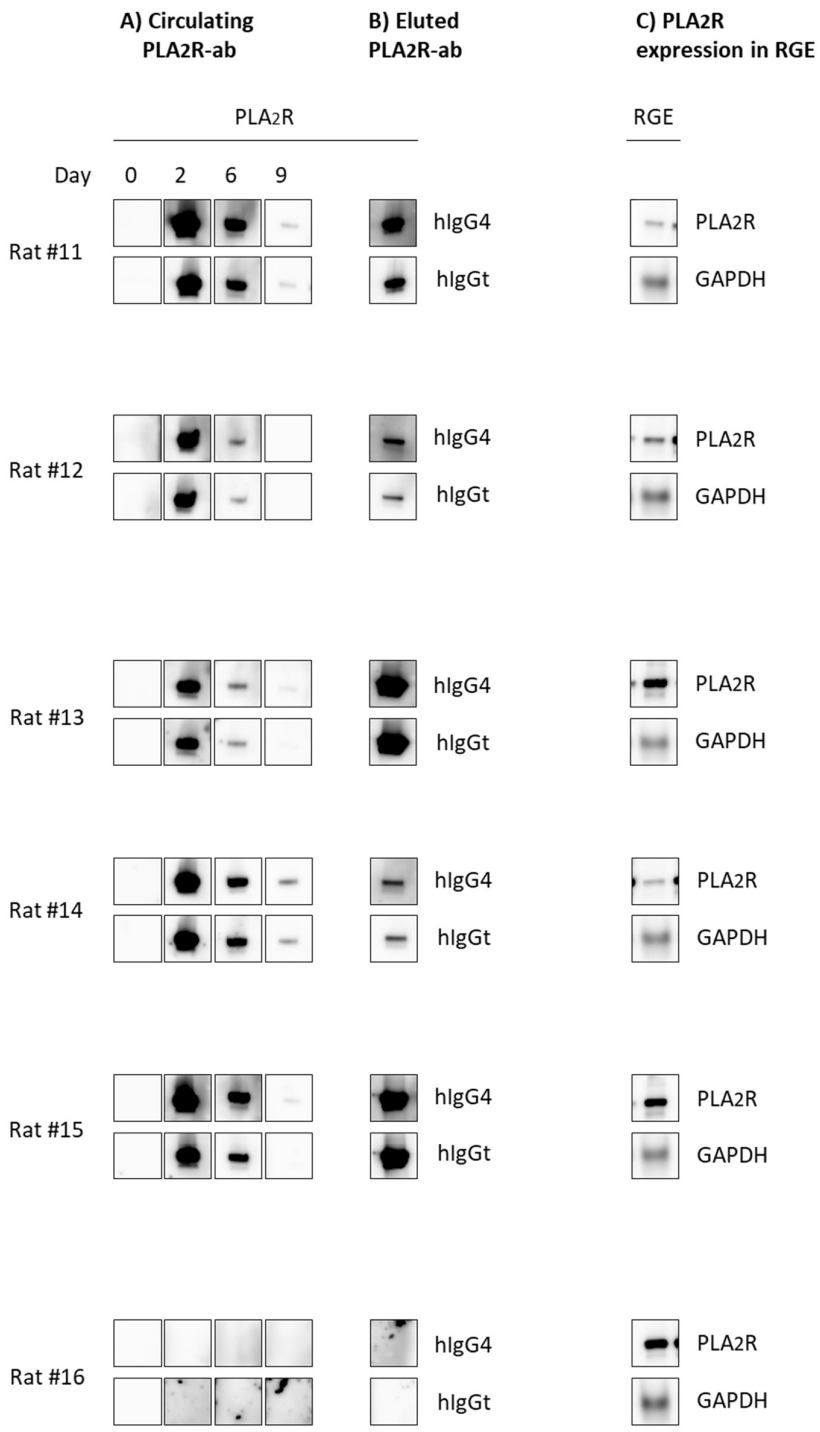


Figure 32: Western blot results.
A) Detection of human anti-PLA$_2$R IgG4 and total IgG in rat plasma collected at days 0, 2, 6, and 9. B) Detection of human anti-PLA$_2$R IgG4 and total IgG in rat glomerular eluate. C) Evaluation of PLA$_2$R expression in experimental rats (#11-15) and representative control #16 using RGE and human PLA$_2$R-ab positive serum. GAPDH signal from the same RGE samples was used as an internal loading control.

The evaluation of PLA_2R expression by means of immunofluorescence (Figure 33), showed positivity along the glomerular capillary loops.

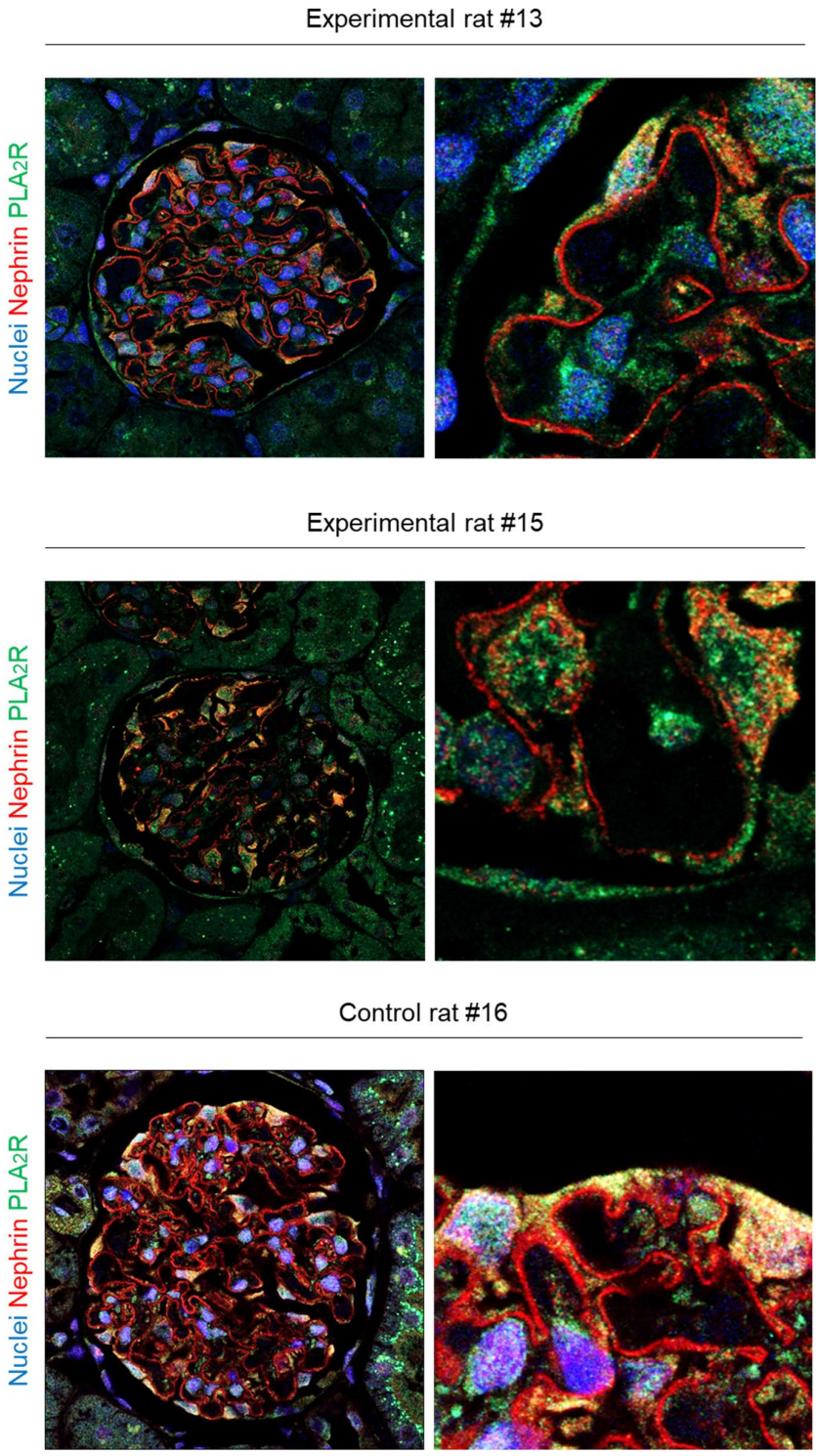
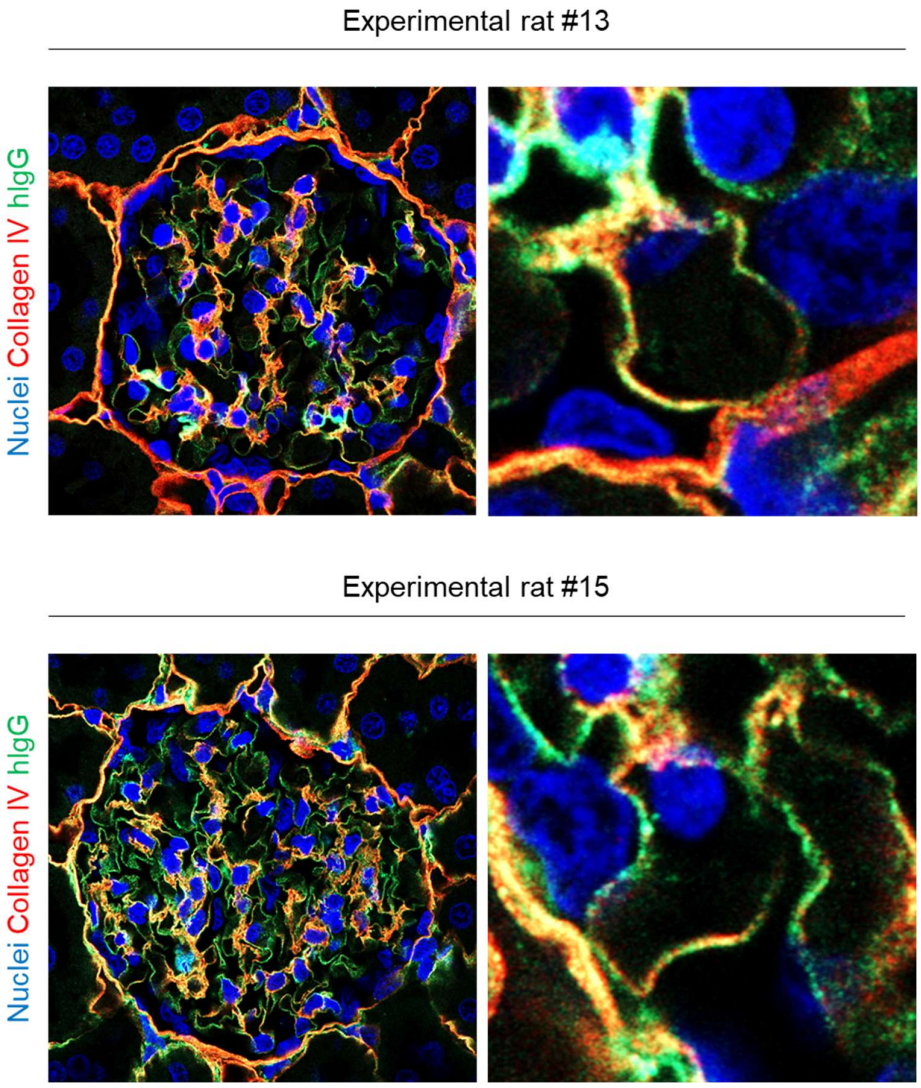


Figure 33: Evaluation of PLA_2R expression by immunofluorescence.
Kidney paraffin sections from representative experimental rats #13, #15 and control rat #16 stained for PLA_2R (green), nephrin (red) with nuclear counterstain (blue).

The immunofluorescence staining for human IgG revealed a low positivity (Figure 34), seemingly because the immune deposits were too small to be highlighted and could be misinterpreted with unspecific signal. Only the signals located in the sub-epithelial space were considered authentic.



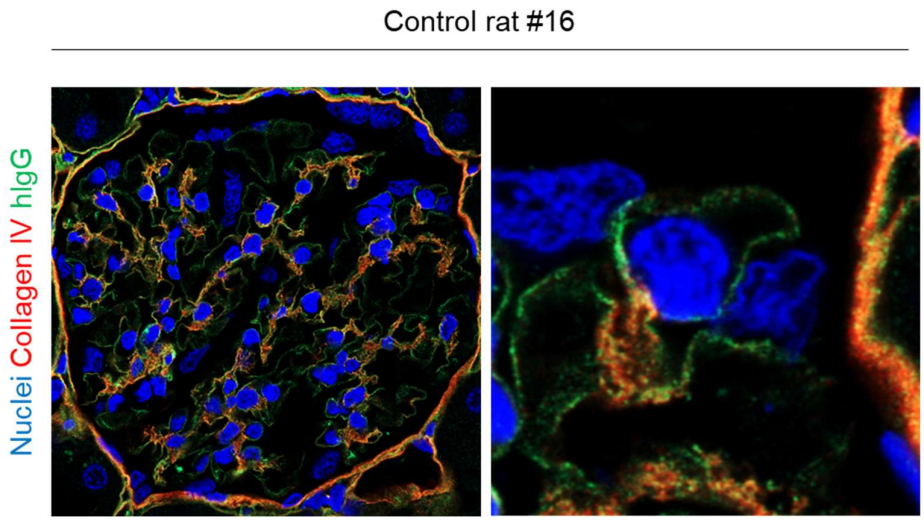
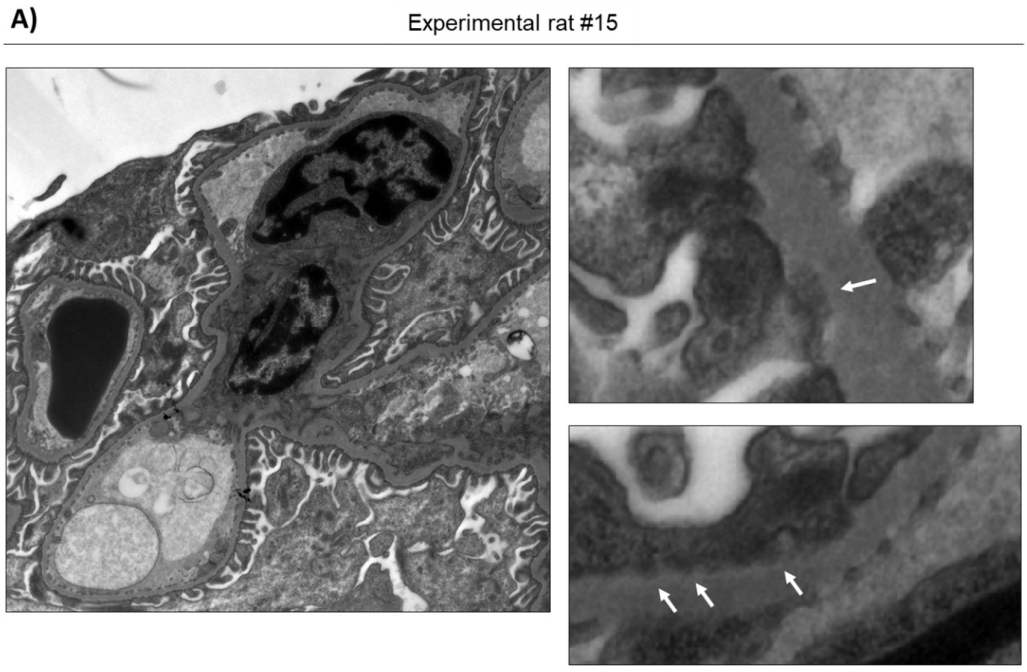
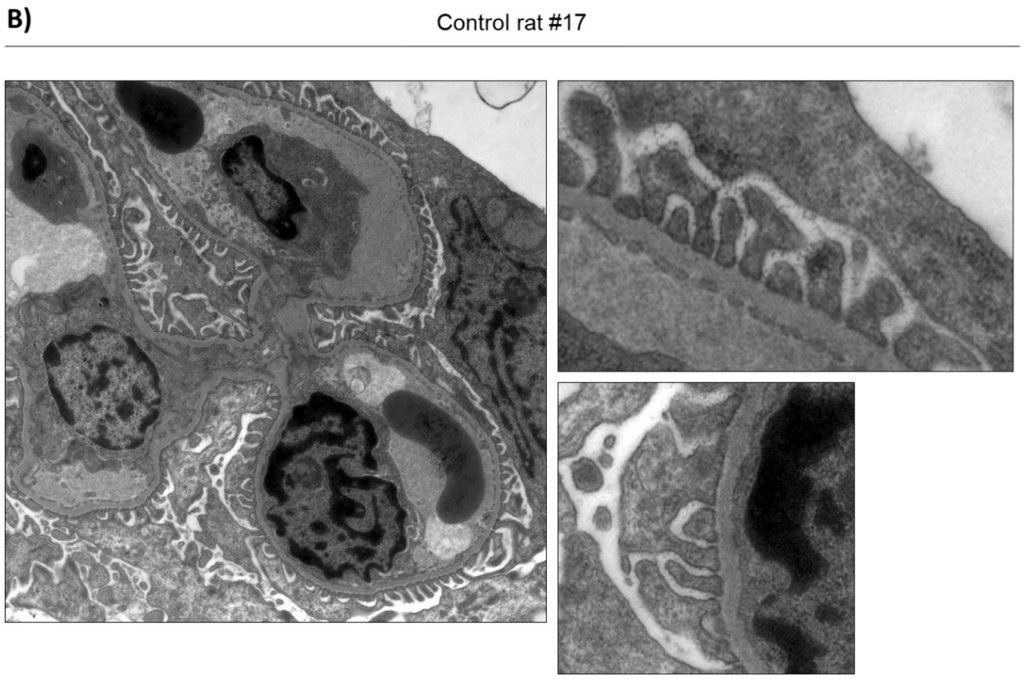


Figure 34: Evaluation of human IgG deposition by immunofluorescence.
Kidney paraffin sections from representative experimental rats #13, #15 and control rat #16 stained for human IgG (green), collagen IV (red) with nuclear counterstain (blue).

Sub-epithelial immune deposits in electron microscopy experiments were evident and could be seen as electron dense areas (Figure 35). The small size of the deposits, not yet surrounded by extracellular matrix, indicates changes representing the very early stages of the disease. Also, podocyte effacement was present along some areas of the glomerular basement membrane. No difference in the glomerulus structure was observed in the PAS staining.





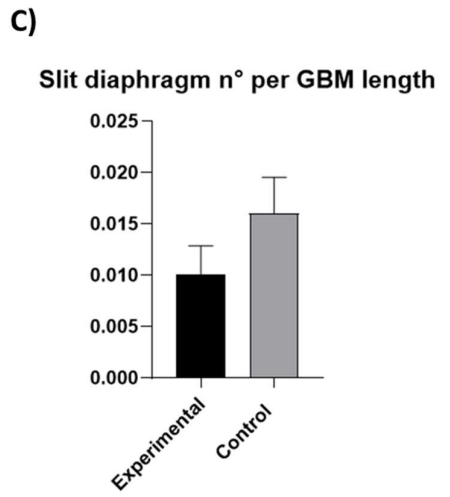


Figure 35: Electron microscopy picture of glomerulus and podocyte effacement evaluation. *A) Glomerular filtration barrier presents small electron dense deposits (white arrow) in representative experimental rat #15 B) normal architecture is seen in the representative control rat #17 C) experimental rat #15 showed a lower number of slit diaphragms, normalized to GBM length, compared to control animal #17.*

From the urine analysis, done by albumin ELISA and creatinine assay, no animal resulted proteinuric (Figure 36A, B). The absence of proteinuria was confirmed also by the lack of significant body weight gain and oedema. The only body weight difference observed was in fact the physiological one between males and females. The average percentage change of ACR (Figure 36C) showed an increase only at the last time point of the experiment, equally for experimental and control group.

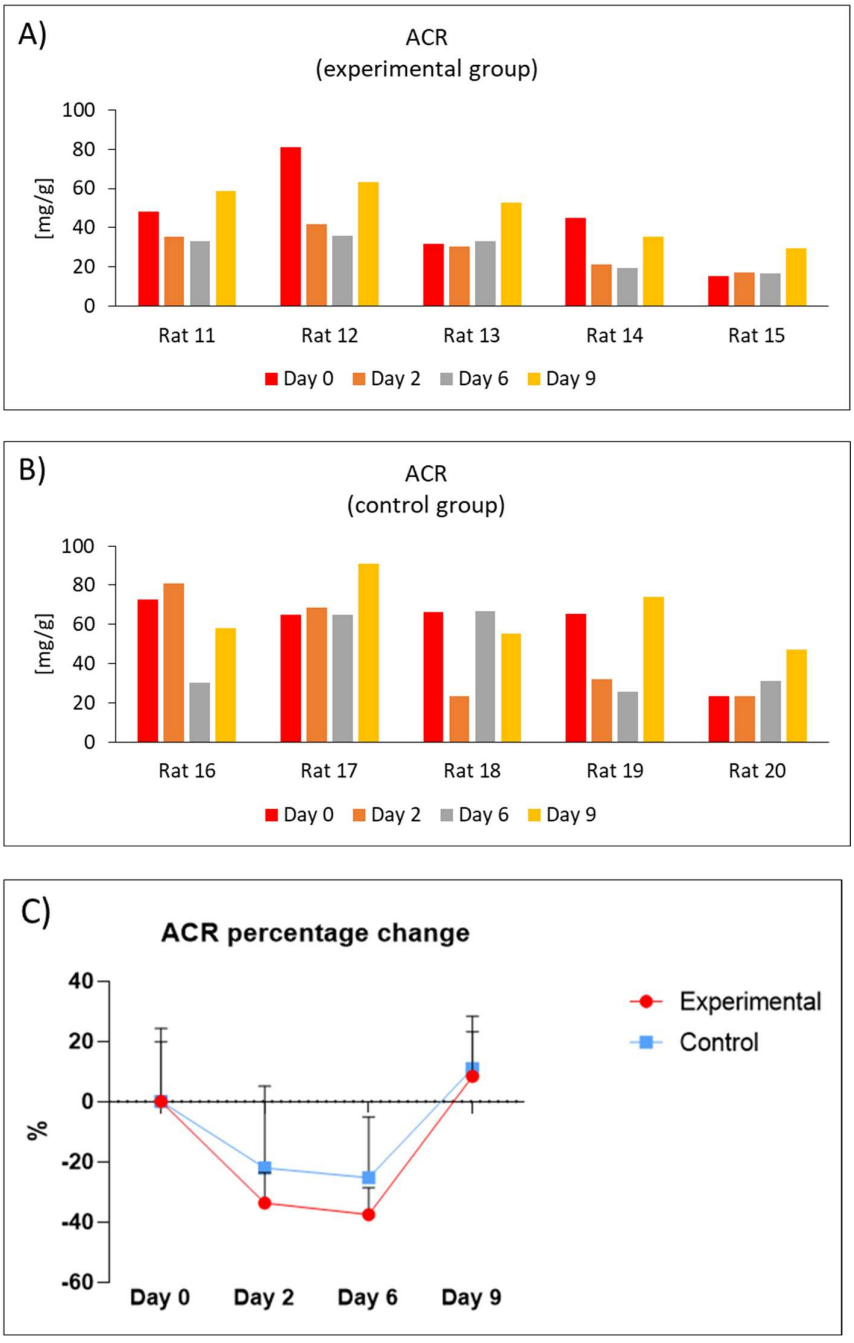


Figure 36: Urine analysis.
Individual albumin to creatinine ratio in all time point urine of experimental (A) and control (B) groups. Average percentage change of ACR (C) of experimental group (red) mirrors the control group trend (blue) showing an increase of ACR only at day 9. ACR: albumin to creatinine ratio.

3.5 Active immunisation

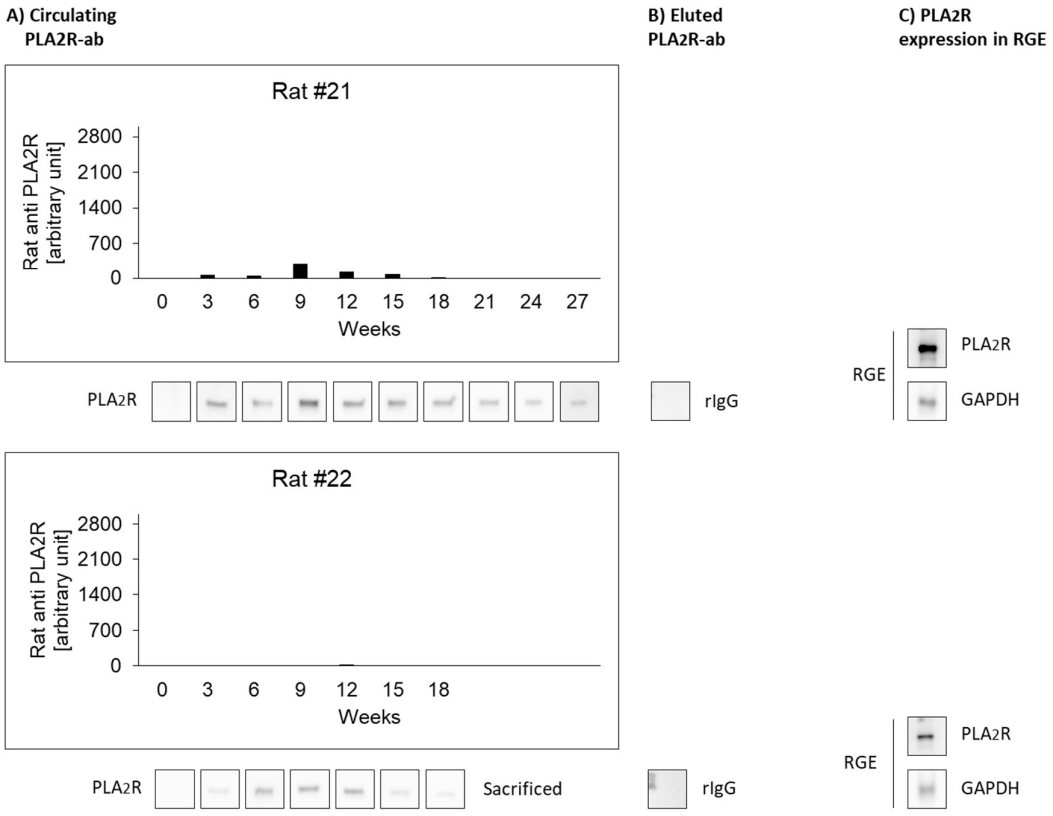
3.5.1 Hemizygous rats

Eight weeks old hemizygous rats were induced to produce antibodies against human PLA_2R by active immunisation. Eight rats were split into experimental and control group, each containing two males and two females. All animals received the immunisation mix every 3 weeks, for a total of 10 subcutaneous injections. An exception was made for rats #22 and #26 which were sacrificed beforehand to monitor the antibody deposition in the kidney. The injection mix of the experimental group was prepared with 10 µg of human PLA_2R extracellular domain diluted with equal amounts of sterile PBS and Freund's adjuvant. The control group received the same amount of immunisation buffer (PBS and adjuvant) without protein.

Rat n°	**Sex**	**Weeks**	**Group**
21	M	8	Experimental
22	F		
23	M		
24	F		
25	M		Control
26	F		
27	M		
28	F		

The presence of circulating PLA_2R specific rIgG (rat IgG) was determined by western blot and PLA_2R ELISA (Euroimmun). Western blot and PLA_2R ELISA results showed that none of the control animals produced PLA_2R specific rIgG (Figure 37A) and that there was a variation in the amount of antibodies produced among the experiemental animals. Both methodics, western blot and PLA_2R ELISA, confirmed that the antibodies started to appear between weeks 3 and 6. The animal that developped the highest amount of PLA_2R specific rIgG was rat #23 followed by rats #24, #21 and #22 (Figure 37A). In particular, rat #23 had a peak in antibody production around week 15, a trend not seen in rat #24 whose antibody production was contant. With the exception of animal #24 in week 27, the results of PLA2R-specific rIgG quantification were consistent between western blot and PLA2R ELISA. The discrepancy observed at this time point may be attributable to methodological issues, as not all western blot samples were analysed on the same gel. The evaluation of PLA_2R specific rIgG in the glomeruli eluate (Figure 37B) was in line with the results observed for the circulating antibodies. The elution was in fact positive only for the two rats that showed more antibodies in circulation, rats #23 and #24. The negative results of the

other two experimental animals may be due to the low amount of PLA_2R specific rIgG produced and available to bind the human protein in the glomerulus. All control animals didn't present PLA_2R specific rIgG in the glomeruli eluate. Next, the human PLA_2R expression on rat podocytes was evaluated by western blot using rat glomerular extract and by immune-fluorescence. Overall, PLA_2R expression was confirmed by western blot for all rats, except for one control animal.



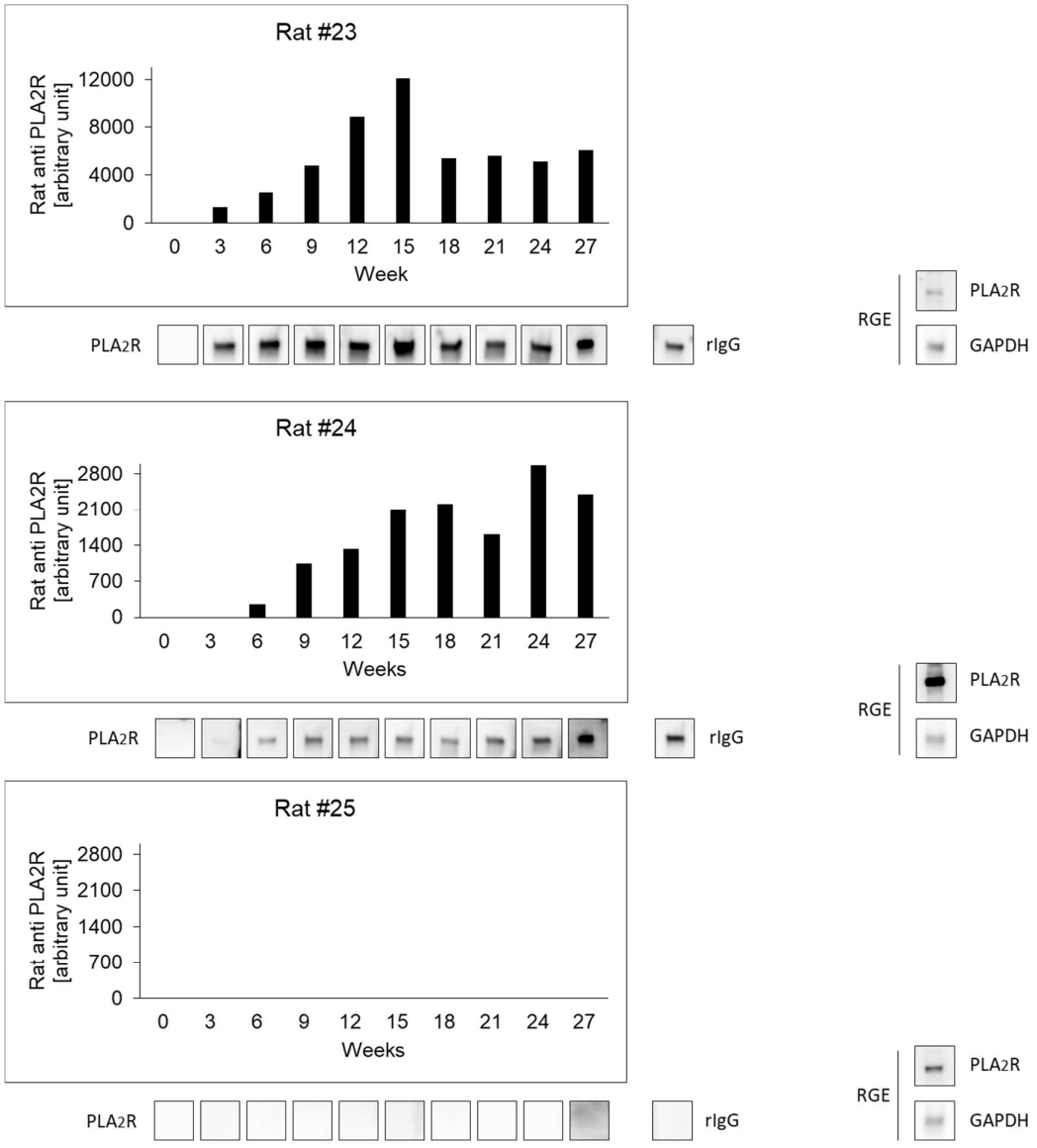


Figure 37: Western blot and PLA$_2$R ELISA results.
A) Detection of rat anti-PLA$_2$R IgG in rat plasma collected from week 0 to week 27 using western blot and PLA$_2$R specific ELISA. B) Detection of rat anti-PLA$_2$R IgG in rat glomerular eluate. C) Evaluation of PLA$_2$R expression in experimental rats (#21-24) and representative control #25 using RGE and human PLA$_2$R-ab positive serum. GAPDH signal from the same RGE samples was used as an internal loading control.

The immunofluorescence analysis performed on rat kidney paraffin sections, showed that it was not possible to detect a clear PLA$_2$R signal (Figure 38), probably due to the very low expression level of the protein.

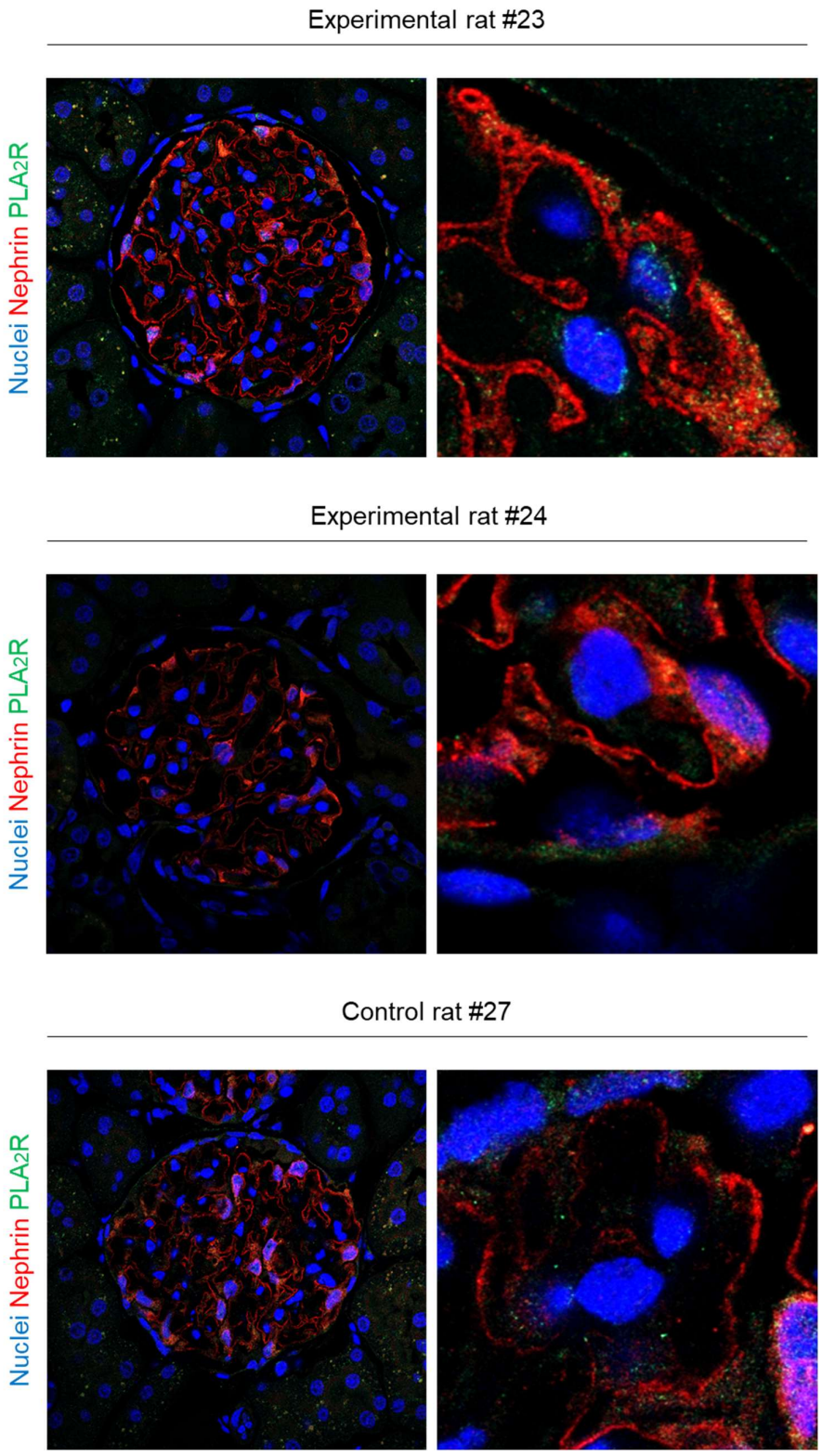
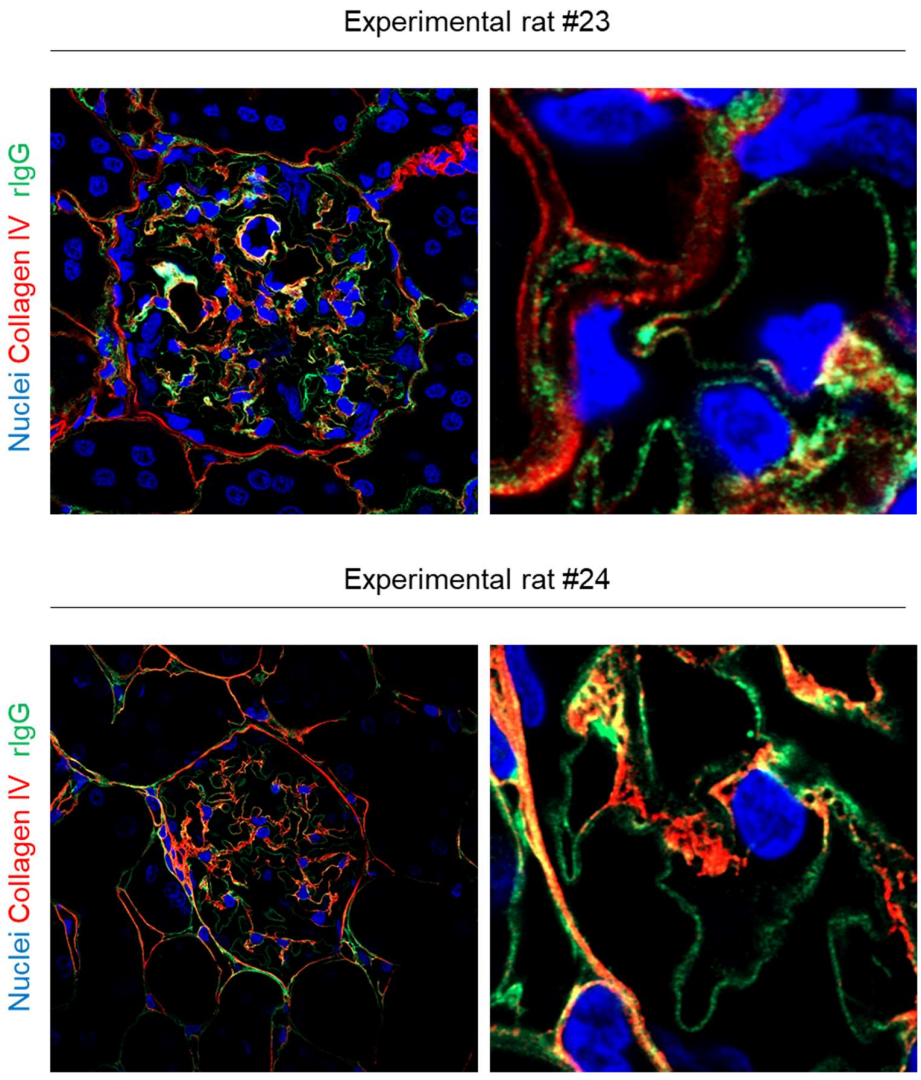


Figure 38: Evaluation of PLA_2R expression by immunofluorescence.
Kidney paraffin sections from representative experimental rats #23, #24 and control rat #27 stained for PLA_2R (green), nephrin (red) with nuclear counterstain (blue).

Subsequently, glomerular staining for rIgG was performed by immunofluorescence. Even though weak, a granular deposition of the rIgG (Figure 39) was observed along the GBM of the experimental animals #23 and #24. All the other experimental and control animals, showed a more uniform green signal, corresponding to a background staining.



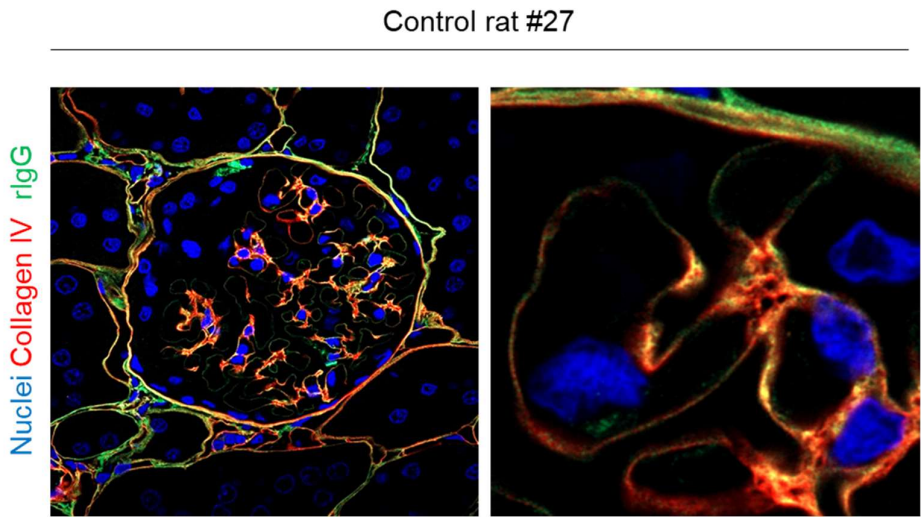
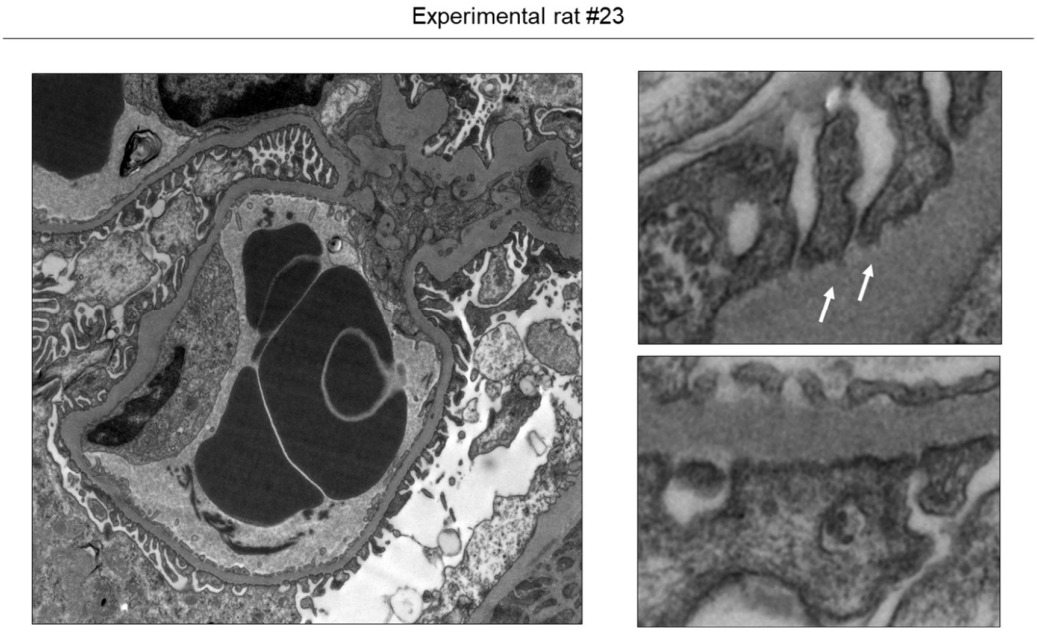


Figure 39: Evaluation of rIgG deposition by immunofluorescence.
Kidney paraffin sections from representative experimental rat #23, #24 and control rat #27 stained for rIgG (green), collagen IV (red) with nuclear counterstaining (blue).

Sub-epithelial deposition appears weak also in electron microscopy pictures (Figure 40), in line with the low expression of human PLA_2R. No glomerular basement membrane thickening nor podocyte effacement were discerned.



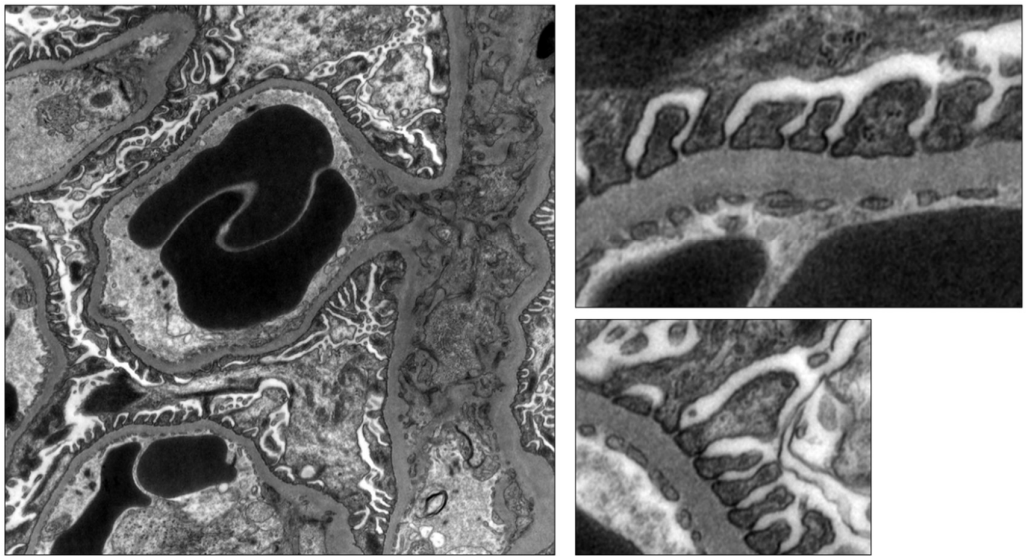
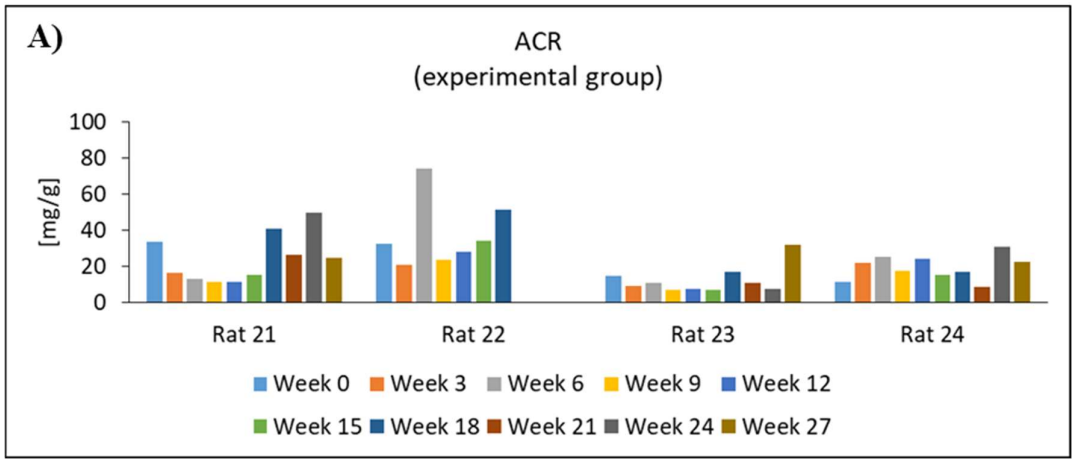


Figure 40: Electron microscopy picture of glomerulus.
Glomerular filtration barrier components present normal architecture in representative experimental rat #23 and control rat #27. Sparse small immune deposits are seen in experimental rat #23.

The urine albumin, normalised to creatinine for individual samples, showed that no experimental animal developed proteinuria. No significant differences in the albumin-to-creatinine ratio were detected at any time point between the experimental and control groups (Figures 41A, B). However, the experimental group (Figure 41C) showed an increase in average ACR percentage at weeks 6, 18, 24, and 27, whereas the control group doesn't shows such increase.



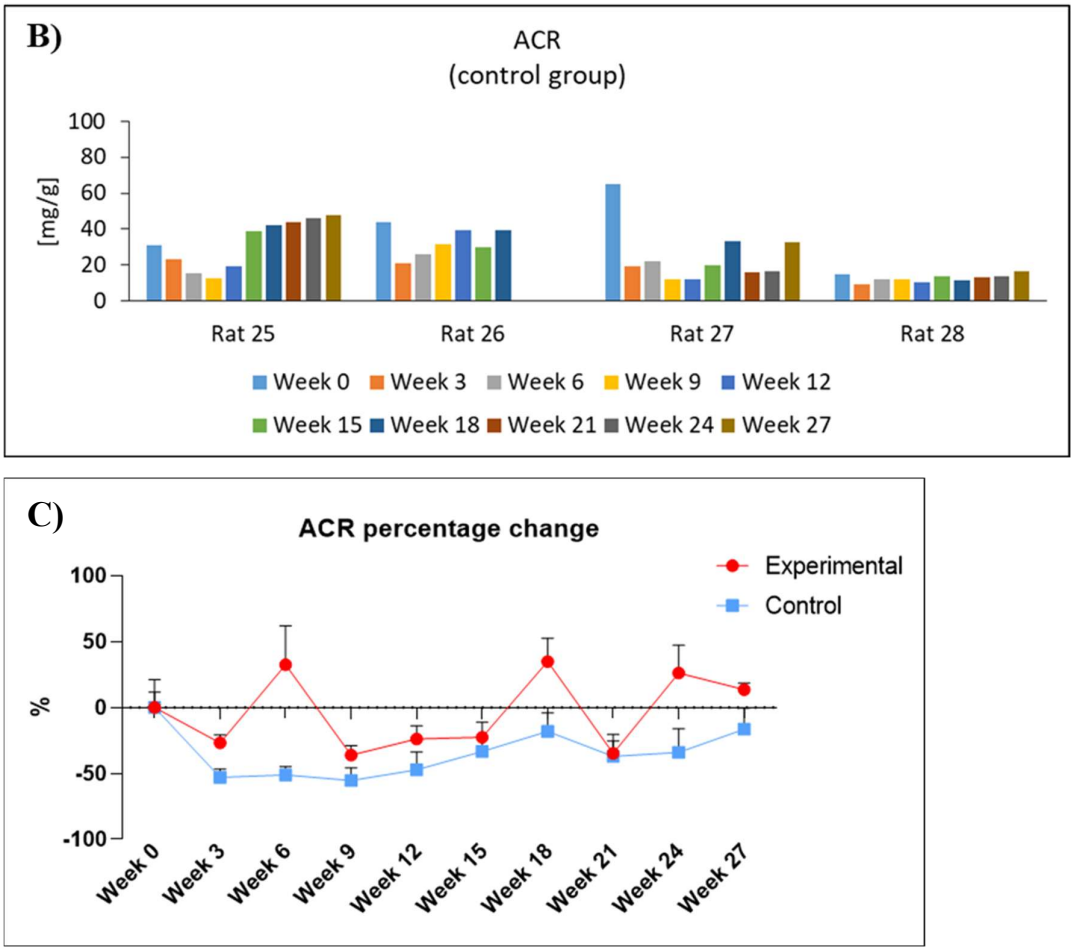


Figure 41: Urine analysis.

Individual albumin to creatinine ratio in all time point urine of A) experimental and B) control group. C) Average percentage change of ACR in experimental group (red) shows an increase at weeks 6, 18, 24 and 27; no increase is seen in the control group (blue). ACR: Albumin to Creatinine Ratio.

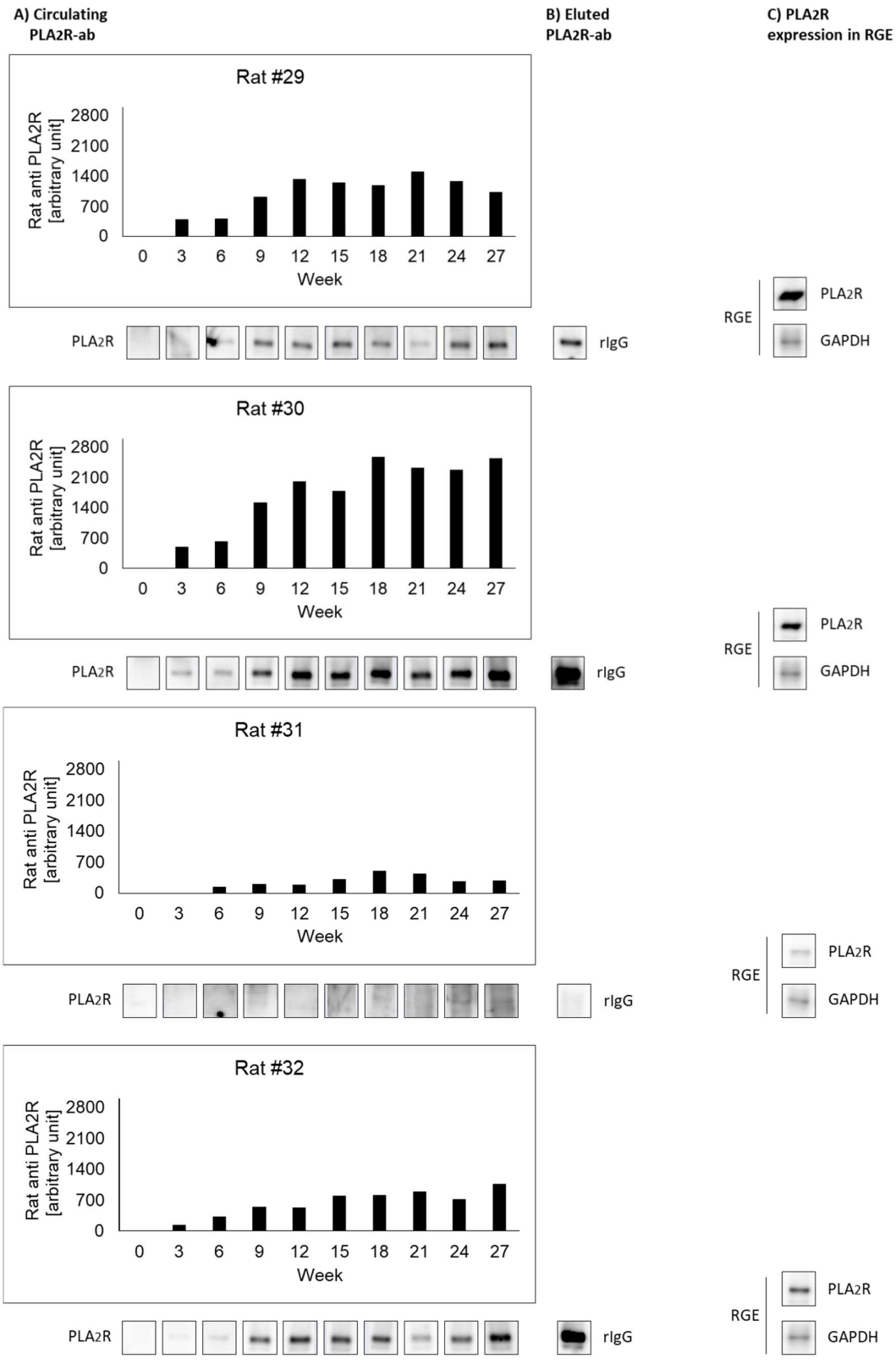
3.5.2 Homozygous rats

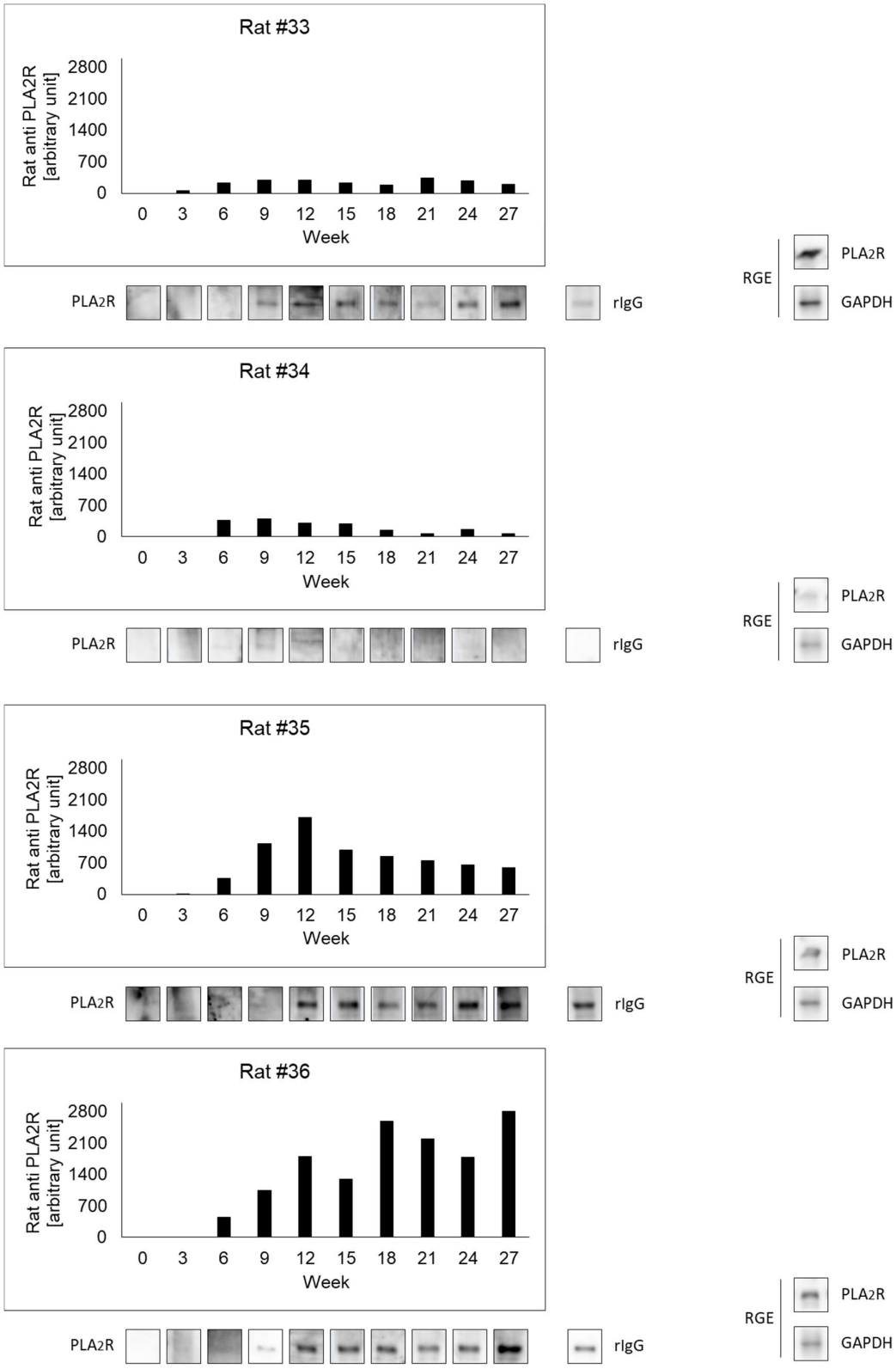
Fourteen homozygous rats, ten weeks old, were selected from the offspring of two distinguished mothers. Using the same scheme as the active immunisation on hemizygous rats, males and females were equally distributed to experimental and control groups. The experimental group included four males and four females, while the control group consisted of three males and three females. The immunisation protocol applied was identical to the one used with the hemizygous rats with the only difference being in the protein amount used for the immunisations. In fact, instead of 10 µg of human PLA_2R extracellular domain, 20 µg were used at each immunisation time point. The decision to increase the protein amount used to immunise the rats was made because of the low antibody levels detected in two of the rats immunised in the first set of

experiments (rats #21, #22 above). All rats survived for the entire 27 weeks duration of the experiment, except for control rat #41, which was euthanized after week 12.

Rat n°	Sex	Weeks	Group
29	M	10	Experimental
30	M		
31	M		
32	M		
33	F		
34	F		
35	F		
36	F		
37	M		Control
38	M		
39	M		
40	F		
41	F		
42	F		

The PLA_2R ELISA (Euroimmun) succeeded in detecting PLA_2R specific rIgG in all experimental animals (Figure 42A). Similarly to the immunisation carried out on hemizygous rats, circulating antibodies can be detected starting from weeks 3 and 6. A particularly stronger antibodies production was observed in rats #29, #30, #35 and #36. However, in the two experimental animals #31 and #34, the PLA_2R-ab were only detectable by ELISA and not by western blot. The low or undetectable amount of PLA_2R specific rIgG in the blood of these animals is in line with the antibodies elution experiment; in fact, no PLA_2R specific rIgG were detected in the eluate by western blot (Figure 42B). Positivity for PLA_2R specific rIgG in the glomerular eluate was confirmed in all the experimental animals in which circulating antibodies were detectable both by PLA_2R ELISA and western blot. All control animals showed no positivity for PLA_2R specific rIgG in circulation and in the glomerular eluate.
PLA_2R expression in podocytes was confirmed in all animals by western blot analysis using RGE (Figure 42C) and by immunofluorescence.


A) Circulating PLA2R-ab
B) Eluted PLA2R-ab
C) PLA2R expression in RGE
Rat #29
Rat #30
Rat #31
Rat #32
Rat anti PLA2R [arbitrary unit]
2800
2100
1400
700
0
0 3 6 9 12 15 18 21 24 27
Week
PLA2R
rIgG
RGE
PLA2R
GAPDH


Rat #33
Rat anti PLA2R [arbitrary unit]
2800
2100
1400
700
0
0 3 6 9 12 15 18 21 24 27
Week
PLA2R
rIgG
RGE
PLA2R
GAPDH
Rat #34
Rat anti PLA2R [arbitrary unit]
2800
2100
1400
700
0
0 3 6 9 12 15 18 21 24 27
Week
PLA2R
rIgG
RGE
PLA2R
GAPDH
Rat #35
Rat anti PLA2R [arbitrary unit]
2800
2100
1400
700
0
0 3 6 9 12 15 18 21 24 27
Week
PLA2R
rIgG
RGE
PLA2R
GAPDH
Rat #36
Rat anti PLA2R [arbitrary unit]
2800
2100
1400
700
0
0 3 6 9 12 15 18 21 24 27
Week
PLA2R
rIgG
RGE
PLA2R
GAPDH

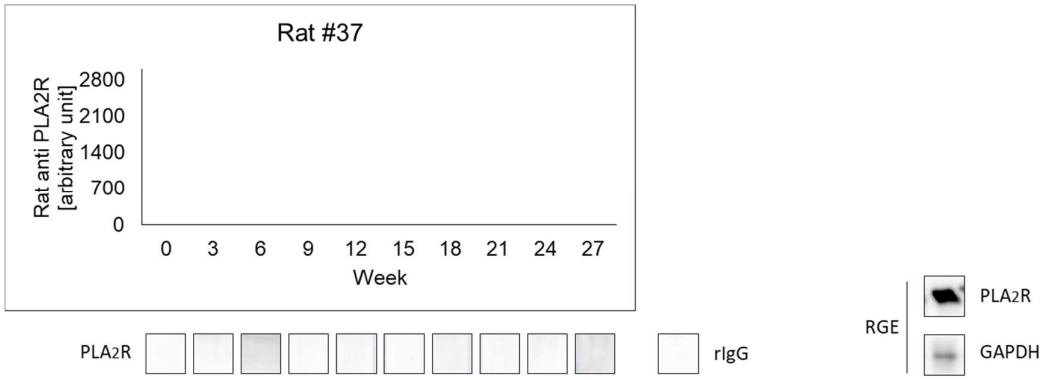
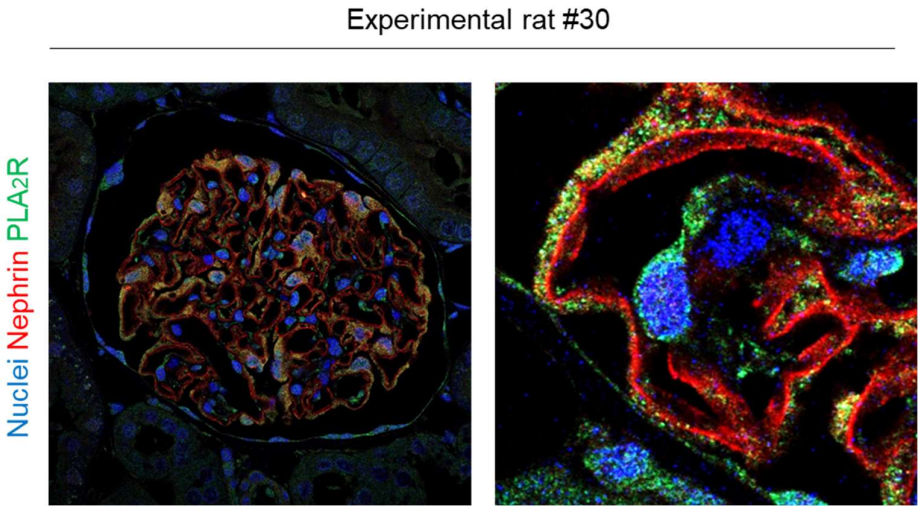


Figure 42: Western blot and PLA_2R ELISA results.
A) Detection of rat anti-PLA_2R IgG in rat plasma collected from week 0 to week 27 using western blot and PLA_2R specific ELISA. B) Detection of rat anti-PLA_2R IgG in rat glomerular eluate. C) Evaluation of PLA_2R expression in experimental rats (#29-36) and representative control #37 using RGE and human PLA_2R-ab positive serum. GAPDH signal from the same RGE samples was used as an internal loading control.

Unlike the active immunisation experiments with heterozygous animals, a clear and strong podocyte-specific signal was detected in the immunofluorescence analysis (Figure 43).



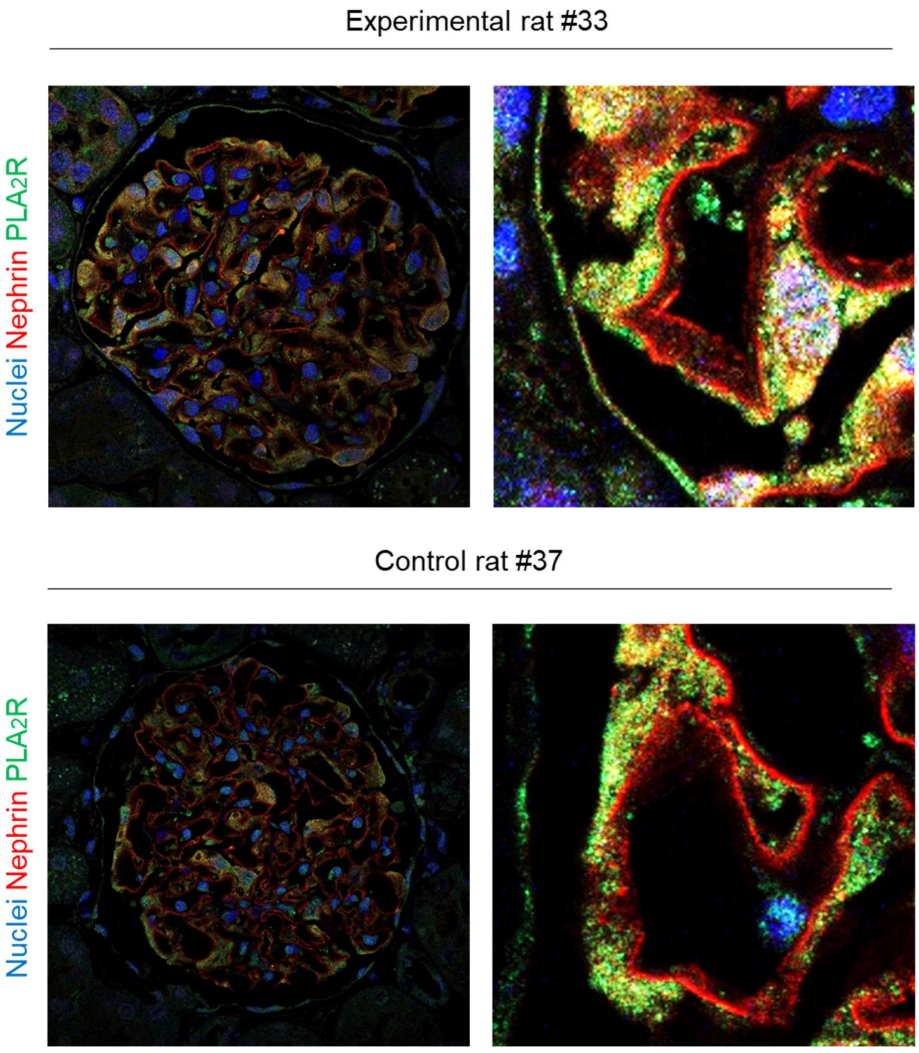


Figure 43: Evaluation of PLA_2R expression by immunofluorescence.
Kidney paraffin sections from representative experimental rats #30, #33 and control rat #37 stained for PLA_2R (green), nephrin (red) with nuclear counterstain (blue).

In addition to the production of PLA_2R specific rIgG, a weak antibody deposition was observed by immunofluorescence in the glomeruili of the experimental rats (Figure 44). Rats that produced more antibodies, such as rat #30, showed more small IgG deposits compared to rats with lower antibodies titer such as rat #33. In these animals with low antibody titer the rIgG signal along the GBM (laminin) resembled the more linear signal seen in the control rats.

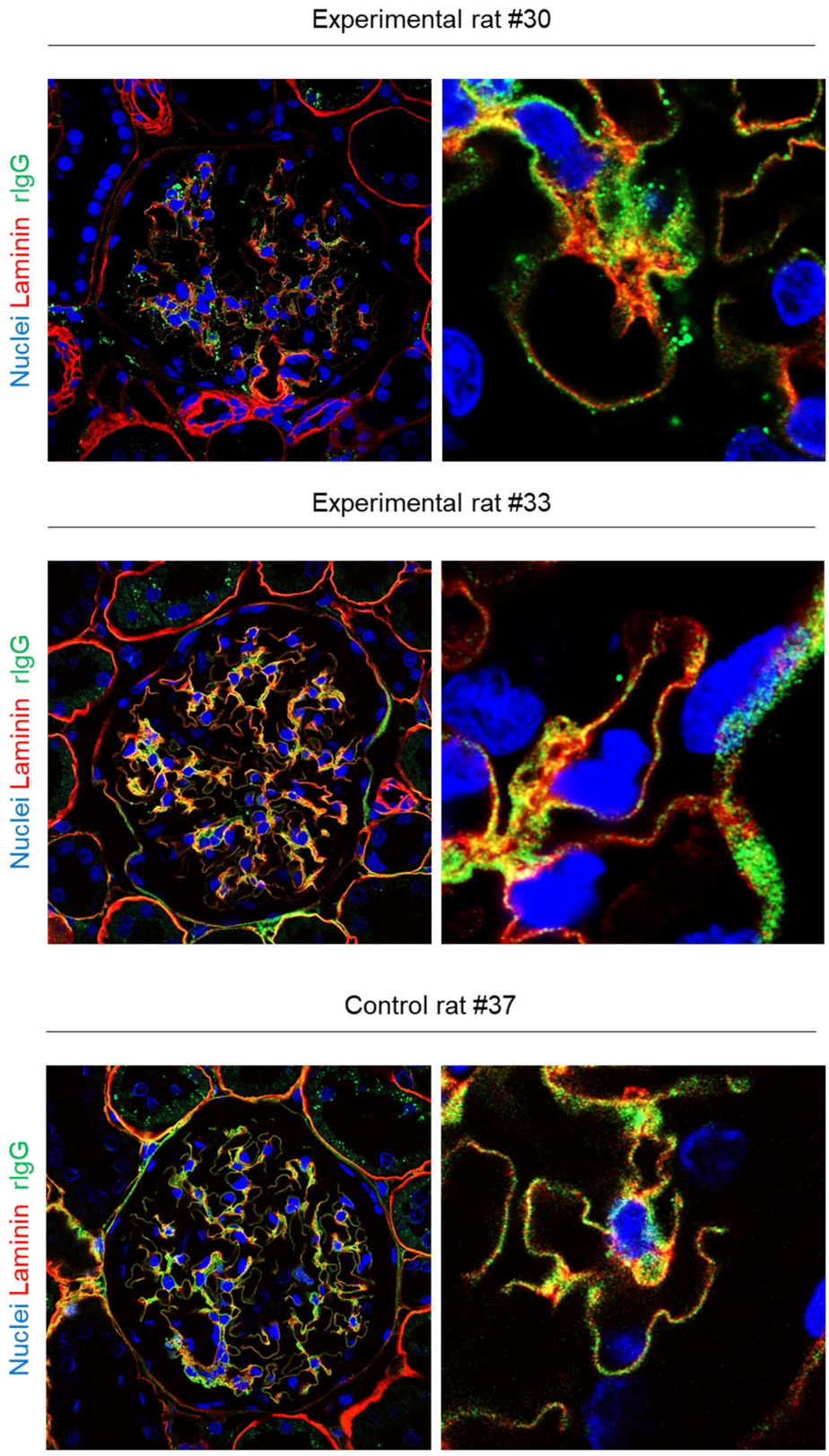
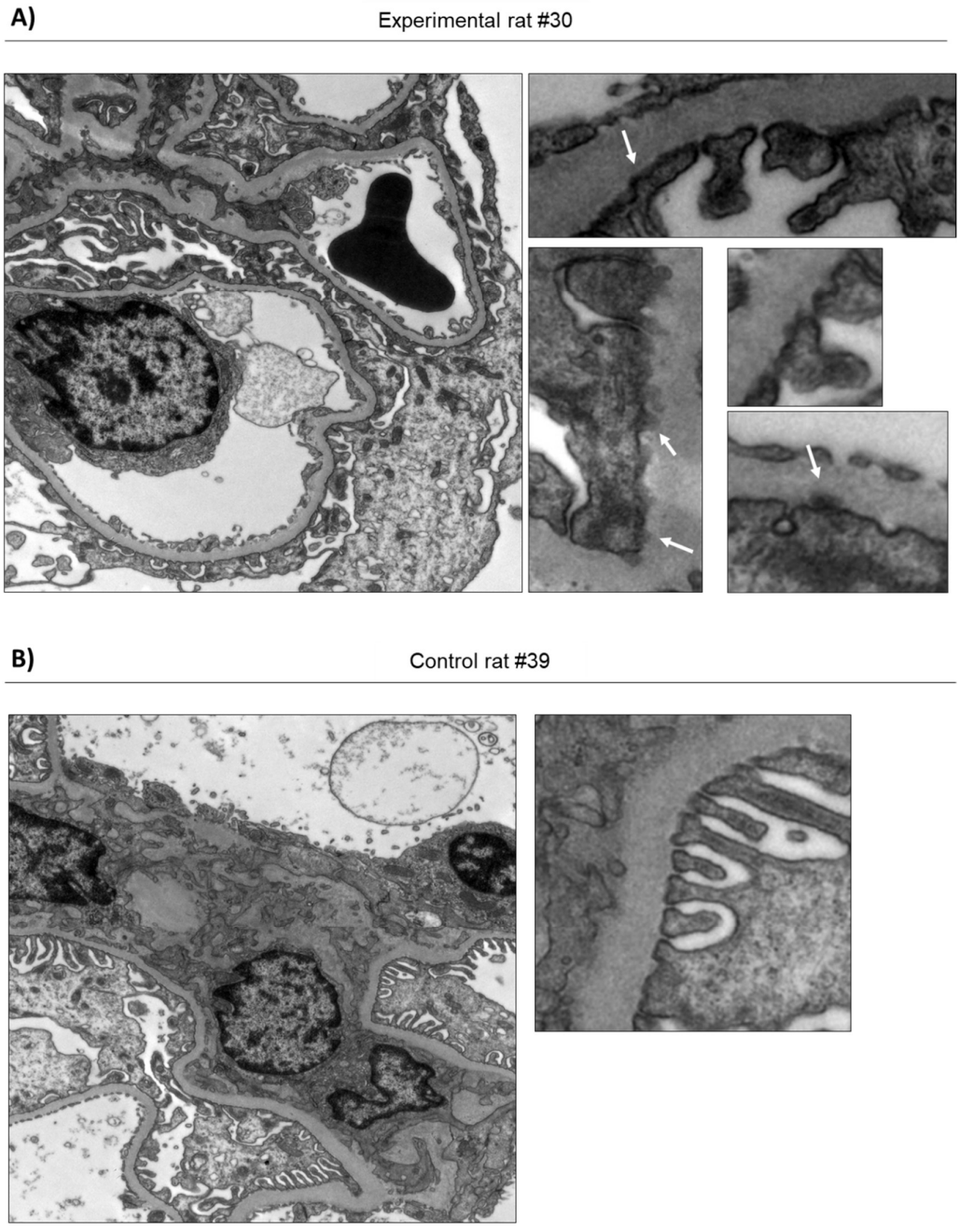


Figure 44: Evaluation of rat IgG deposition by immunofluorescence.
Kidney paraffin sections from representative experimental rats #30, #33 and control rat #37 stained for rIgG (green), laminin (red) with nuclear counterstain (blue).

Few small electron dense deposits were seen in experimental rat #30 (Figure 45A). These deposits are not homogenously distributed along the GBM and are small in size. No GBM thickening was observed. Experimental animal #30 showed a reduced number of slit diaphragms compared to control animal #39 (Figure 45C) as a sign of podocyte effacement.



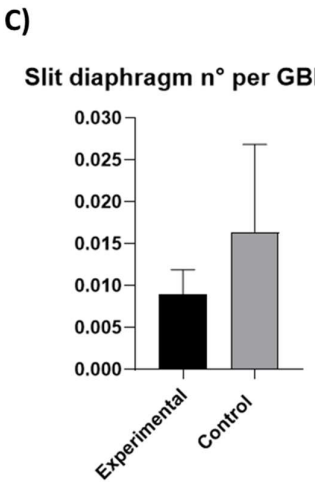


Figure 45: Electron microscopy of glomerulus and podocyte effacement evaluation.
A) Small electron-dense deposits (white arrow) in the GBM and podocyte effacement of representative experimental rat #30 B) normal filtration barrier morphology in representative control rat #39 C) experimental rat #30 showed a lower number of slit diaphragms, normalized to GBM length, compared to control animal #39.

The experimental rat #30, which showed a more evident rIgG deposition, was used to evaluate the rat complement deposition by immunofluorescence staining of rat IgG (green) and rat complement C3 (blue) (Figure 46). Apparent positive co-localization, suggested by the overlap of the green and blue channels, was examined individually using the single-channel images. However, despite the positivity for rat IgG along the GBM (red), no true co-localization of rat IgG and rat C3 could be confirmed.

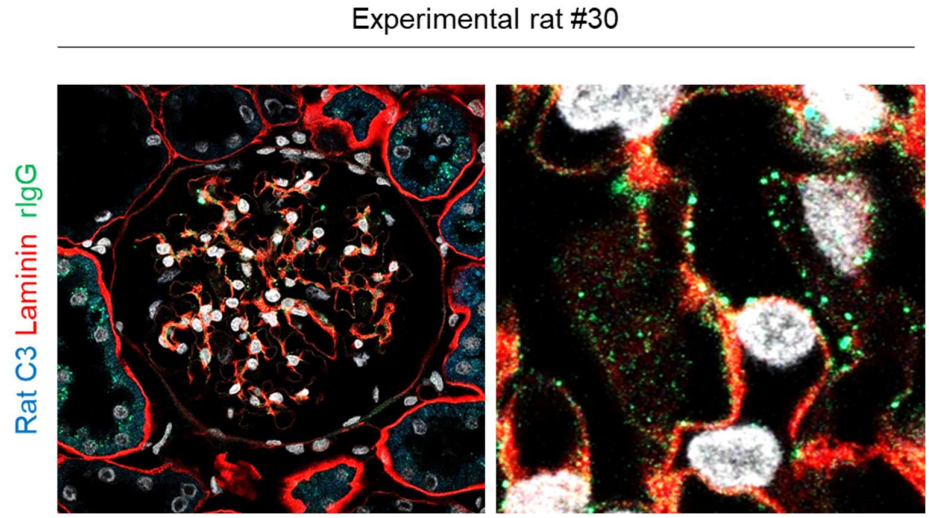


Figure 46: Evaluation of complement deposition in the glomerulus.
Kidney paraffin section of representative experimental rat #30 stained for rat C3 (blue), laminin (red), and rat IgG (green) with nuclear counterstain (white).

Lastly, proteinuria was analysed in all animals by albumin ELISA and creatinine assay. The fluctuation in the albumin to creatinine ratios could be seen both in experimental and control rats such as rat #30 and rat #37 respectively (Figure 47A, B). While no large proteinuria was observed, in some experimental animals proteinuria seems to increase over time (rats #30, 36).

The average percentage change of ACR (Figure 47C) showed an increase at the last time points, weeks 18-27, in both control and experimental groups.

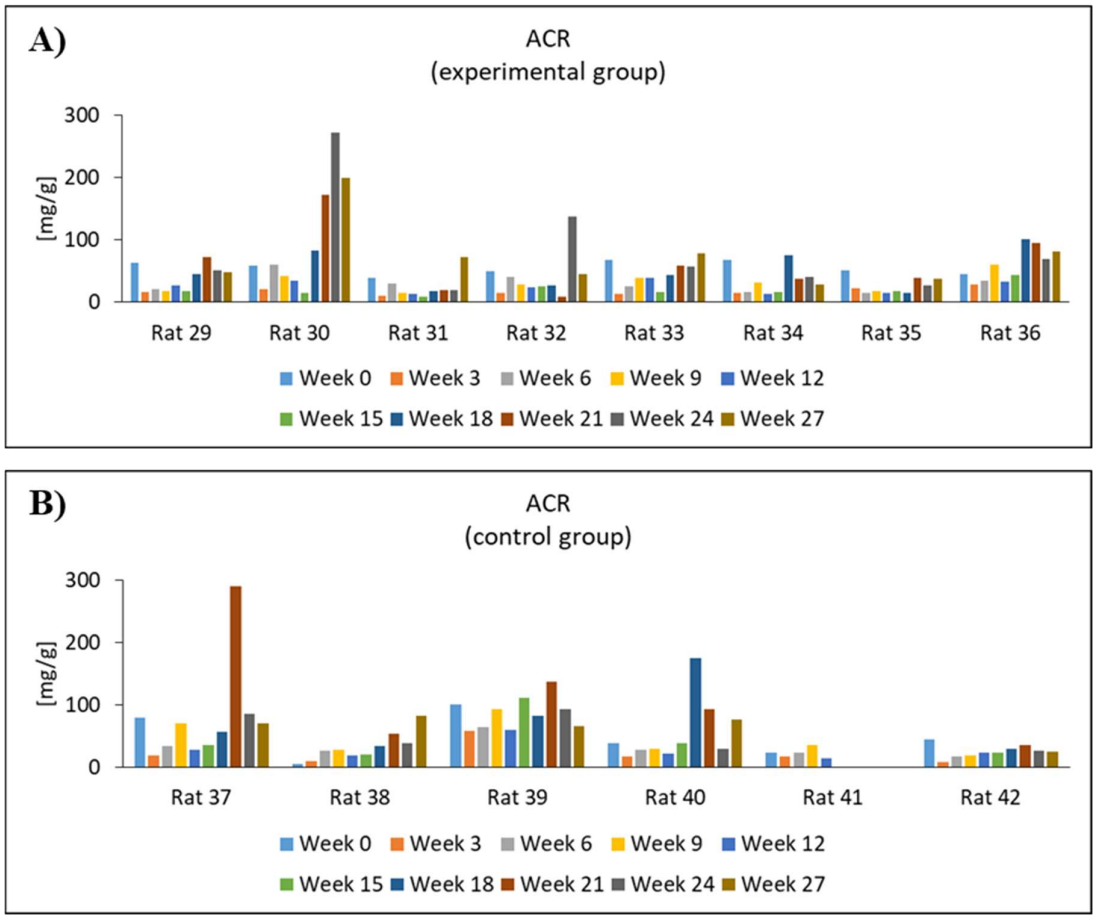


Figure 47: Urine analysis. *Individual albumin to creatinine ratio (ACR) in all time point urine of A) experimental and B) control groups. C) Average percentage change of ACR in experimental group (red) shows an increase at weeks 21, 24 and 27 while control group (blue) has an increase at weeks 18, 21, 24 and 27.*

4. Discussion

Membranous nephropathy is a rare antibody-mediated autoimmune disease of the kidney, characterized by the formation of immune deposits in the sub-epithelial space of the glomerular filtration barrier (Ronco et al., 2021; Hoxha et al., 2022). Majority of patients (70-80%) affected by MN develop antibodies which target PLA_2R, a transmembrane glycoprotein normally expressed on healthy podocytes (Beck et al., 2009; Q13018-Uniprot, 2023). The antibodies can bind also to other protein targets (endogenous or planted antigens). The deposition of antibodies results in the complement activation and the assembling of the membrane attack complex C5b-9 (Baker et al., 1989). The effect of complement activation, followed by events such as production of reactive oxygen species, cytoskeletal alterations, upregulation of tumour growth factor β and matrix metalloproteinase-9, leads to podocyte injury, impairment of the glomerular filtration barrier and consequent proteinuria. MN is indeed one of the most frequent causes of nephrotic syndrome in adults (Ronco et al., 2021). Two thirds of patients have a poor outcome showing persistent proteinuria which can eventually develop in end stage renal disease, the other third of patients undergoes a spontaneous remission of proteinuria and has a good outcome (Polanco, 2010; Sinico, 2016). At the time of the diagnosis, according to different criteria such as evaluation of PLA_2R-ab levels, eGFR and proteinuria, patients are addressed to a category of risk to develop progressive loss of kidney function. Based on the risk category they are in, patients can be assigned a supportive therapy (angiotensin converting enzyme inhibitors, angiotensin receptor blockers to reduce proteinuria, statins, diuretics etc.) or to an immunosuppressive therapy. Since immunosuppressive treatments have important and potentially detrimental side effects, it is extremely important to correctly predict the course of the disease in individual patients and consequently tailor the best treatment that avoids negative outcome and reduce therapy's side effects. Important notions about the patho-mechanisms of MN arose from studies in experimental animal models, especially studies in rat model of Heymann nephritis (Heymann et al., 1959). With this model, it was demonstrated that MN is an autoimmune condition, caused by autoantibodies that target podocyte antigens leading to the formation of immune complexes. Heymann nephritis model mirrored the morphological traits of MN in human: IgG deposition along the capillaries wall, thickening of the GBM and podocyte effacement. Moreover, this model succeeded in inducing proteinuria in the experimental rats and indicated the complement deposition has a crucial role in the disease pathogenesis. Despite the similarities between Heymann nephritis and MN, a key difference lays in the disease antigen:

megalin. Its human counterpart, LRP2 (low density lipoprotein receptor-related protein 2), is in fact not implicated in MN (Chung et al., 2022; Larsen et al., 2018).

The first human antigen was discovered in a prenatal case of MN (Debiec et al., 2002) caused by the trans-placental transfer of NEP (neutral endopeptidase) antibodies from a deficient mother to the foetus. Seven years later the most common antigen in MN, PLA_2R, was found (Beck et al., 2009). The discovery of PLA_2R as major antigen was of great help with the differentiation between idiopathic MN and secondary cases associated with other diseases; it also gave an important aid to improve the care of most of the patients because PLA_2R antibodies level correlate with the disease activity (Hoxha et al., 2014; Mahmud et al., 2019). After the discovery of PLA_2R, other important findings were made, including the identification of new endogenous and exogenous antigens, such as THSD7A and NELL-1 respectively. These two antigens are in fact the most common found in MN patients after PLA_2R (Tomas et al., 2014; Sethi et al., 2019). What these antigens have in common still remains an open question that requires further investigations. In parallel to the discovery of new antigens, different animal models were generated to replicate MN induced by PLA_2R antibodies (Meyer-Schwesinger et al., 2020; Reinhard et al., 2023; Tomas et al., 2023). This thesis project was designed to create a transgenic rat line expressing human PLA_2R specifically on the podocytes and use it to replicate the phenotype of idiopathic membranous nephropathy (iMN). Moreover, the model was conceived as a tool to study the patho-mechanisms of iMN and to eventually test new treatments. The use of transgenic animals was required since rats, as well as mice, don't express PLA_2R on the podocytes. Furthermore, inducing the expression of the human protein allows to perform experiments with human PLA_2R antibodies, since the binding affinity would be preserved. A MN model (Meyer-Schwesinger et al., 2020), established in transgenic mice expressing murine PLA_2R on podocytes, showed in fact that PLA_2R amino acid sequence identity between species is fundamental to preserve human IgG binding and thus to be able to induce the disease using human serum. In addition, rat was chosen as the species for generating a transgenic model because of its long standing use in experimental nephrology, most notably in the Heymann nephritis model. Furthermore, compared to mice, rats offer several advantages in terms of sample yield for molecular analysis. Their larger kidney size facilitates glomerular isolation and high quality histological analyses, while the increased blood and urine volumes allow repeated longitudinal sampling of proteinuria and circulating antibodies.

In order to optimize addressing, anchoring to the membrane, intracellular signalling and functionality of the transgenic protein, four different PLA_2R expression vectors were designed combining human and rat sequence for the signal peptide, transmembrane, intracellular and extracellular domains. To achieve a tissue and cell specific expression, the transgene expression

was put under the control of human podocin promoter. It was observed that all four expression vectors were successfully expressed at full length without the occurring of internal splicing.

The evaluation of the expression at protein level, confirmed that keeping the human sequence for the extracellular domain is essential to preserve the capacity of human antibodies to bind to the protein. In fact, this evaluation showed that the transgenic human PLA_2R, full length as well as the chimeric variant with the human transmembrane domain, was only recognised by the human anti-PLA_2R antibodies when in non-reducing conditions. This testify that the transgenic protein kept its three dimensional shape and thus the conformational epitopes. Based on the in vitro results, we concluded that the chimeric version of PLA_2R, comprising the rat signal peptide and intracellular domain combined with the human transmembrane and extracellular domains, was the most suitable candidate for generating the transgenic line. It ensured in fact proper targeting and functionality of PLA_2R in rat cells. To track the expression of the PLA_2R transgene a reporter gene, td-Tomato, was put after the PLA_2R stop codon and IRES sequence. Thanks to the IRES sequence, a singular mRNA is translated into two separated proteins to monitor PLA_2R expression while keeping the protein structure intact.

The PLA_2R transgene was randomly inserted into the rat genome through a pronuclear microinjection approach (GenOway, Lyon, France). For genotyping the hemizygous transgenic offspring, a standard PCR assay on crude tissue lysates was adopted, using one primer set specific for the transgenic PLA_2R and another (m-ywhae) as a positive control for the DNA integrity in cases of negative PLA_2R amplification. Homozygous animals were genotyped using purified DNA and a RT-PCR protocol, which allowed the discrimination of the transgene copy number. Following each RT-PCR run, a melt curve analysis was performed to rule out unspecific amplification.

The in vivo expression of human PLA_2R was assessed both in hemizygous and homozygous rats by means of western blot and immunofluorescence using human PLA_2R positive plasma and a commercial antibody. The expression appeared to be significantly higher in the homozygous animals compared to the hemizygous, although it didn't seem to reach the level or pattern typically observed in the human podocytes. Using immunofluorescence experiments, the podocyte specific expression of PLA_2R was confirmed and did not lead to any changes in the glomerular morphology. Indeed, from the observation of the PAS staining results, the glomerulus morphology of $hPLA_2R$ positive rats was comparable to that in wild type rats. Moreover, the preservation of an intact and functional structure of the glomerular filtration barrier was confirmed by urine physiologic values of albumin to creatinine ratio. A fundamental part of the transgenic animals' phenotyping was analysing rat plasma to exclude that $hPLA_2R$ positive rats recognise $hPLA_2R$

expressed on podocyte and produce antibodies against it spontaneously. Differently from another transgenic model expressing hPLA$_2$R (Tomas et al., 2023), in which transgenic mice spontaneously produce antibodies as soon as after three weeks of like, no hemizygous nor homozygous transgenic rats produced antibodies against hPLA$_2$R. Excluding spontaneous production of hPLA$_2$R specific rat rIgG was important for allowing active and passive immunisations organized as experimental vs control studies.

Passive immunisation

The passive transfer of human PLA$_2$R positive plasma was performed in five hemizygous males and five homozygous rats (three males, two females). The chosen rats were seven to nine weeks old when the experiment started and for each experimental animal a respective control rat of same sex and age was chosen. The experimental groups received a human plasma pool with high PLA$_2$R antibody titer, concentrated to half volume. The plasma pool used to treat the hemizygous and the homozygous was the same. The PLA$_2$R antibody positive plasma pool was shown to contain antibodies directed towards the main pathogenic epitopes in the CysR, CTLD1-2, CTLD7-8 domains. These antibodies were shown to be able to bind hPLA$_2$R in the RGE. The control animals received healthy plasma from one donor concentrated to half volume, which was shown to lack activity towards hPLA$_2$R in RGE. After the immunisation, rat plasma from all experimental time points was used as primary antibody in western blot to detect circulating anti hPLA$_2$R antibodies. In the experimental animals, traces of circulating hPLA$_2$R-IgG could be detected until day 9 when the experiment was concluded. This suggested that the antibodies were transferred in abundance and thus PLA$_2$R epitopes in the glomeruli were not in sufficient quantity to bind all antibodies. These antibodies showed a decreasing trend from day 2 to day 9 in all animals, with the exception of hemizygous rat #04 in which the amount of circulating antibodies stays constant until day 9. The successful elution of hPLA$_2$R-IgG from the isolated glomeruli of all experimental rats was the confirmation that human antibodies can bind the transgenic hPLA$_2$R not only in vitro but also in vivo. Considering that the elution failed in rat #04 it is possible that this animal was wrongly considered as hemizygous. The investigation of the hPLA$_2$R expression in RGE, confirmed that rat #04 could indeed be a wild type. All control animals resulted negative for circulating and eluted hPLA$_2$R-IgG. The low abundance of PLA$_2$R expression in hemizygous animals was confirmed by other experiments, showing no hPLA$_2$R-IgG deposition by immunofluorescence and no deposition by electron microscopy. While the PLA$_2$R expression was too low to allow significant hIgG deposition in the hemizygous animals, in the homozygous experimental rats, a weak hIgG deposition could be seen; the IgG deposition was confirmed by electron microscopy showing small

immune-dense areas on the sub-epithelial space of the GBM, corresponding to stage I MN according to Ehrenreich and Churg classification system. Podocyte effacement and feet process fusion could also be detected. However, none of the experimental animals developed significant proteinuria.

Active immunisation

The active immunisation was induced with the extracellular domain of $hPLA_2R$ in four hemizygous rats (two males, two females) and eight homozygous rats (four males, four females). For each round eight to ten weeks old animals were used. All twelve animals were accompanied by the respective control rats with same age and sex. The immunisation protocol applied was the same with the only difference being in the amount of $hPLA_2R$ protein used at each immunisation time point: the hemizygous rats received 10 µg while the homozygous received 20 µg. This choice was made since in the hemizygous experiments the levels of PLA_2R-ab developed were low and only some animals produced antibodies in a significant amount. Therefore, the higher amount of immunisation protein was chosen to possibly translate in a higher immune response and more antibodies production. The circulating $hPLA_2R$ specific rat IgG were analysed by western blot and by PLA_2R specific ELISA. All hemizygous rats belonging to the experimental group were positive for anti $hPLA_2R$-rIgG and only one rat had too low amount of anti $hPLA_2R$-rIgG to be detected by ELISA. Half of hemizygous experimental rats, one male and one female, produced considerably less antibodies compared to the others.

In the homozygous group, six out of eight experimental rats were positive for anti $hPLA_2R$-rIgG by western blot and ELISA; the remaining two animals showed antibodies only by ELISA. In both experimental groups, the anti $hPLA_2R$-rIgG production started between week 6 and week 9 after the first immunisation. Importantly, ELISA results showed that a greater number of experimental animals produced significant amount of anti PLA_2R antibody in the homozygous group immunised with higher protein doses, which allowed to speculate that the more protein used to immunise may lead to enhanced immune response. However, the amount of antibodies produced still showed large inter-individual variability.

The elution of anti PLA_2R rIgG from isolated glomeruli was not positive for all experimental animals. Elution was in fact positive only in 2/4 hemizygous and 6/8 homozygous animals. The amount of eluted antibodies for all experimental animals was proportional to the amount of circulating antibodies. No hemizygous or homozygous control rat was positive for circulating and eluted anti PLA_2R rIgG.

As seen in the passive transfer experiments, in the hemizygous animals the IgG depositions in the glomeruli was not detectable by immunofluorescence and extremely minor deposits were found by electron microscopy. These findings suggest that the PLA_2R expression in these animals was too low to detect eventual IgG deposits. Among the homozygous rats however, some animals showed a granular rIgG deposition along the GBM when analysed by immunofluorescence and small electron dense deposits by electron microscopy. Most importantly, one of these animals showed an increase of ACR from week 21 to week 27 when the experiment was concluded. The other animals, including control rats, didn't develop considerable proteinuria.

An immunofluorescence co-staining for rat complement C3 and rIgG was performed on the homozygous rat with the highest antibody titer, but no complement deposition was observed.

Overall, the results of these four rounds of experiments showed that signs of an early disease stage were achieved with the passive and active immunisation of homozygous rats. The main limitations that may had prevented the complete development of the disease and proteinuria are: $hPLA_2R$ expression, lack of complement deposition and genetic background of the animal strain. The $hPLA_2R$ expression is higher in animals with two transgene copies, however it still seems not comparable to the expression levels in the human glomerulus. One strategy to compensate this limitation could be to have more $hPLA_2R$ antibodies in circulation available to bind the protein in vivo. This strategy could be applied especially for the passive immunisation experiment in homozygous rats, in which the $hPLA_2R$-IgG had a clear decrease at the last experiment time points. Albeit still detectable in the circulation, it is possible that more antibodies may be needed to saturate the $hPLA_2R$ available to bind in the glomerulus. An approach may be to isolate the IgG from the PLA_2R antibody positive plasma pool and concentrate them until a higher titer of antibodies is achieved. For the active immunisation the solution could be using more $hPLA_2R$ protein to immunise the animals.

The absence of complement deposition is a critical point for developing proteinuria. Other MN animal models in which proteinuria was achieved showed the complement activation and co-localisation with anti-PLA_2R IgG. In passively immunised transgenic BALB/c mice expressing $mPLA_2R$, IgG and complement deposition (C3) were accompanied with oxidative stress and resulted in nephrotic range proteinuria (Meyer-Schwesinger et al., 2020). Various complement components were found also in transgenic BALB/c mice expressing human PLA_2R on the podocytes (Tomas et al., 2023). It has to be pointed out that these two models are based on a mice strain which is an excellent responder to immunisation since Th2 cells are easily activated (Nakamura, 2013). Complement activation was shown also in Heymann Nephritis rat models, using various strains that include also Sprague-Dawley (Pippin et al., 2009). In other Heymann

Nephritis model though, proteinuria was achieved without the assembling of the membrane attack complex suggesting that other early complement components, the immune-complexes size or $CD4^+$ and $CD8^+$ T cells play an important role too (Spicer et al., 2007). The inability to develop proteinuria could be linked also to the intrinsic resistance of the Sprague Dawley background. A passive immunisation conducted on different rodents (Tomas et al., 2017), showed that the genetic background is crucial for the induction of proteinuria. C57BL/6, DBA/J1 mice and Sprague Dawley rats didn't develop proteinuria after the immunisation with anti THSD7A-IgG even though these antibodies were able to bind the antigen in the GBM. On the other hand, BALB/c mice developed the proteinuric phenotype. In another study, Sprague Dawley rats immunised with modified rat kidney fraction 3, not only showed IgG deposition but developed also proteinuria (Barbas et al., 2004). Only a small number of experimental rats though, two out of eight, rats became proteinuric.

Translating these observations to the MN rat model established with this project, the negative results for C3 deposition added to the very small size of immune deposits give an explanation to the absence of proteinuria. An assessment of immune cells infiltration and subset characterisation would be helpful to have a better understanding of the leading causes that brought to the absence of important morphologic changes in the glomerular filtration barrier and eventually propose new alternatives to improve the animal model.

Although this model did not fully replicate the features of idiopathic membranous nephropathy and only reproduced an early stage of the disease, it still represents a valuable tool for the future investigations into the antibody–antigen interactions and the mechanisms that bring to the disease development. In addition, it may provide a mean to explore novel therapeutic strategies, such as targeting antigen-specific B cells, accelerating the clearance of pathogenic circulating antibodies with engineered molecules, or blocking the antibody–antigen interaction using small molecules such as Fab fragments.

5. Summary

Membranous nephropathy is a rare antibody mediated autoimmune disease of the kidney that represents one of the main causes of nephrotic syndrome in adults. The disease can arise without other secondary causes (idiopathic MN) or it can be associated to other diseases such as infections, cancer, other autoimmune diseases (secondary MN). The autoantibodies developed can target endogenous antigens expressed on the podocytes or exogenous ones. Among these antigens, PLA_2R is the most common found in 70-80% of MN patients. Membranous nephropathy disease is characterised by the granular deposition of autoreactive IgG, mainly IgG4, in the sub-epithelial space between podocytes and GBM; in these deposits complement components are found, which are involved in induction of structural changes of the glomerular filtration barrier that lead to proteinuria. All patients diagnosed with MN are given a supportive therapy. The patients at high risk of developing ESRD are treated with immunosuppressive therapy. All the treatments available nowadays are followed by diverse side effects and not always guarantee a positive outcome.

This thesis project aimed to establish a MN model using transgenic rats expressing human PLA_2R specifically on podocytes which would allow in the future to better investigate the patho-mechanisms of the disease and test antigen specific treatments in vivo. Two approaches were used to induce the disease:

- Passive immunisation using whole plasma from patients positive for PLA_2R antibodies
- Active immunisation injecting the animals with the extracellular domain of PLA_2R.

Both protocols were applied in hemizygous and homozygous rats. With these experiments, it was possible to show that human IgG can bind $hPLA_2R$ in vivo and form small deposits. Actively immunised rats successfully produced antibodies against PLA_2R which were found in the sub-epithelial deposits. However, given the low PLA_2R expression, only glomerular morphologic changes of an early stage of the disease were achieved (small immune deposits, weak podocytes ´foot effacement) without development of proteinuria. The plausible reasons that influenced the lack of proteinuria and the progression of more severe structural changes are the low PLA_2R expression, immune deposits size and the absence of complement deposition. These issues can be addressed adjusting the immunisation protocol in order to increase the amount of PLA_2R specific IgG available to bind the protein in the glomerulus by the administration of higher amounts of human anti-PLA_2R IgG and PLA_2R protein. More investigations need to be done to understand why these protocols failed in the rat complement activation.

Membranöse Nephropathie ist eine seltene, antikörpervermittelte Autoimmunerkrankung der Niere und eine der Hauptursachen des nephrotischen Syndroms bei Erwachsenen. Die Krankheit kann ohne andere sekundäre Ursachen auftreten (idiopathische MN) oder mit anderen Krankheiten wie Infektionen, Krebs oder anderen Autoimmunerkrankungen assoziiert sein (sekundäre MN). Die entwickelten Autoantikörper können sich gegen endogene, auf den Podozyten exprimierte oder exogene Antigene richten. Unter diesen Antigenen ist PLA_2R das am häufigsten vorkommende und wird bei 70–80 % der MN-Patienten gefunden. Die Erkrankung Membranöse Nephropathie ist durch granuläre Ablagerungen von autoreaktivem IgG, hauptsächlich IgG4, im subepithelialen Raum zwischen Podozyten und GBM gekennzeichnet; in diesen Ablagerungen finden sich Komplementkomponenten, die an der Induktion struktureller Veränderungen der glomerulären Filtrationsbarriere beteiligt sind, die zu Proteinurie führen. Alle Patienten mit der Diagnose MN erhalten eine unterstützende Therapie. Patienten mit hohem Risiko für die Entwicklung einer terminalen Niereninsuffizienz werden mit immunsuppressiven Therapien behandelt. Alle heute verfügbaren Behandlungen gehen mit vielfältigen Nebenwirkungen einher und garantieren nicht immer einen positiven Ausgang.
Ziel dieses Dissertationsprojekts war die Etablierung eines MN-Modells mit transgenen Ratten, die humanes PLA_2R spezifisch auf Podozyten exprimieren. Dies soll zukünftig eine bessere Erforschung der Pathomechanismen der Erkrankung und die Erprobung antigenspezifischer Behandlungen in vivo ermöglichen. Zur Induktion der Erkrankung wurden zwei Ansätze verfolgt:
– Passive Immunisierung mit Vollplasma von Patienten mit positiven PLA_2R-Antikörpern
– Aktive Immunisierung durch Injektion der extrazellulären Domäne von PLA_2R an die Tiere.
Beide Protokolle wurden an hemizygoten und homozygoten Ratten angewendet. Mit diesen Experimenten konnte gezeigt werden, dass humanes IgG in vivo an $hPLA_2R$ binden und kleine Ablagerungen bilden kann. Aktiv immunisierte Ratten produzierten erfolgreich Antikörper gegen PLA_2R, die in den subepithelialen Ablagerungen nachgewiesen wurden. Aufgrund der geringen PLA_2R-Expression wurden jedoch nur glomeruläre morphologische Veränderungen eines frühen Krankheitsstadiums (geringe Immunablagerungen, schwache Auslöschung der Podozytenfüße) ohne Entwicklung einer Proteinurie erreicht. Die plausiblen Gründe für das Ausbleiben der Proteinurie und das Fortschreiten schwerwiegenderer struktureller Veränderungen sind die geringe PLA_2R-Expression, die Größe der Immunablagerungen und das Fehlen von Komplementablagerungen. Diesen Problemen kann durch eine Anpassung des Immunisierungsprotokolls begegnet werden, um die Menge an PLA_2R-spezifischem IgG, das zur Bindung des Proteins im Glomerulus zur Verfügung steht, durch die Verabreichung höherer

Mengen an humanem Anti-PLA_2R-IgG und PLA_2R-Protein zu erhöhen. Es bedarf weiterer Untersuchungen, um zu verstehen, warum diese Protokolle bei der Komplementaktivierung bei Ratten versagten.

6. List of abbreviations

Abbreviation	Meaning
ACR	Albumin to creatinine ratio
ADH	Antidiuretic hormone
ANP	Atrial natriuretic peptide
BALB/c	Bagg albino mice
Bip	Binding immunoglobulin protein
bp	Base pair
BSA	Bovine serum albumin
CRISPR/Cas9	clustered regularly interspaced short palindromic repeats and CRISPR-associated protein 9
CTLD	C-type lectin domain
CTNT1	Contactin 1
Cys-R	Cysteine rich
DRAQ5	Deep Red Anthraquinone 5
ECL	Enhanced chemiluminescence
EDTA	Ethylenediaminetetraacetic acid
ELISA	Enzyme-linked immunosorbent assay
ESRD	End stage renal disease
EtOH	Ethanol
EXT1/2	Exostosin ½
FACS	Fluorescence-activated cell sorting
GAPDH	Glyceraldehyde-3-phosphate dehydrogenase
GBM	Glomerular basement membrane
GFR	Glomerular filtration rate
Grp94	Glucose regulated protein 94
GWAS	Genome wide association study

HEK	Human embryonic kidney
HGE	Human glomerular extract
HLA	Human leukocyte antigen
HRP	Horseradish peroxidase
HTRA1	High temperature requirement A
IFT	Immunofluorescence test
IRES	Internal ribosome entry site sequence
IRF4	Interferon regulatory factor-4
LRP2	Low density lipoprotein receptor-related protein 2
MBL	Mannose binding lectin
MHC	Major Histocompatibility Complex
MMP9	Matrix metalloproteinase-9
MN	Membranous nephropathy
MWCO	Molecular weight cutoff
NCAM1	Neural cell adhesion molecule 1
NELL-1	NEL-like protein 1
NEPH1	Podocin
NF-KB1	Nuclear factor Kappa B subunit-1
NIAT	Non-immunosuppressive antiproteinuric treatment
NTNG1	Netrin G1
PAS	Periodic acid Schiff
PBS	Phosphate buffered saline
PCR	Polymerase chain reaction
PLA_2R	Phospholipase A2 receptor
PVDF	Polyvinylidene fluoride
RAAS	Renin-angiotensin-aldosterone system
RAP	Receptor associate protein
RGE	Rat glomerular extract

ROS	Reactive oxygen species
RPF	Renal plasma flow
RT	Room temperature
SD	Sprague-Dawley
SDS-PAGE	Sodium Dodecyl Sulphate–Polyacrylamide Gel Electrophoresis
SEMA3B	Semaphoring-3B
SNPs	Single nucleotide polymorphisms
$sPLA_2$	Secreted phospholipase A2
SYNPO	Synaptopodin
TAE	Tris-acetate-ethylenediaminetetraacetic acid
TGF-β	Tumour growth factor β
THBS1	Thrombospondin 1
THSD7A	Thrombospondin type1 domain containing 7A
TMB	Tetramethylbenzidine
TSP-1	Thrombospondin type 1
T/T	Homozygous
T/+	Hemizygous
YWHAE	Tyrosine 3-monooxygenase/tryptophan 5-monooxygenase activation protein epsilon

7. List of figures

Figure 1: Schematic representation of the glomerular filtration barrier. 8
Figure 2: Criteria to assess risk for loss of kidney function. 11
Figure 3: Therapy assignment according to risk category. 12
Figure 4: PCR profile. 30
Figure 5: Primers used for the genotyping of hemizygous rats. 31
Figure 6: PLA_2R primer used for the genotyping of homozygous rats. 33
Figure 7: RT-PCR profile. 33
Figure 8: RT-PCR dissociation curve. 34
Figure 9: Schematic representation of active immunisation timeline. 35
Figure 10: Schematic representation of passive immunisation timeline. 36
Figure 11: Schematic representation of PLA_2R expression vectors. 45
Figure 12: RT-PCR results. 46
Figure 13: Western blot results. 46
Figure 14: Fluorescence-activated cell sorting results. 47
Figure 15: Schematic representation of chimeric PLA_2R-td-Tomato knock in construct. ..47
Figure 16: Genotyping results from wild type rats crossed with PLA_2R hemizygous. rats. 48
Figure 17: PCR efficiency curves. 49
Figure 18: Relative quantification of PLA_2R transgene. 50
Figure 19: Melt curve graph. 50
Figure 20: Evaluation of PLA_2R expression in rat glomerular extract. 51
Figure 21: Evaluation of PLA_2R expression by immunofluorescence. 52
Figure 22: Periodic acid Schiff staining of rat glomeruli. 53
Figure 23: Assessment of spontaneous production of PLA_2R specific rat IgG. 53
Figure 24: Albumin to creatinine ratio in rat urine. 54
Figure 25: Evaluation of PLA_2R antibody positive plasma pool and healthy plasma reactivity. 55
Figure 26: Western blot results. 57
Figure 27: Evaluation of PLA_2R expression by immunofluorescence. 58
Figure 28: Evaluation of human IgG deposition by immunofluorescence. 59
Figure 29: Electron microscopy picture of glomerulus 60
Figure 30: Urine analysis. 61

Figure 31: Evaluation of PLA$_2$R antibody positive plasma pool and healthy plasma reactivity. 63
Figure 32: Western blot results. 64
Figure 33: Evaluation of PLA$_2$R expression by immunofluorescence. 65
Figure 34: Evaluation of human IgG deposition by immunofluorescence. 67
Figure 35: Electron microscopy picture of glomerulus and podocyte effacement evaluation 68
Figure 36: Urine analysis. 69
Figure 37: Western blot and PLA$_2$R ELISA results. 72
Figure 38: Evaluation of PLA$_2$R expression by immunofluorescence. 73
Figure 39: Evaluation of rIgG deposition by immunofluorescence. 75
Figure 40: Electron microscopy picture of glomerulus. 76
Figure 41: Urine analysis. 77
Figure 42: Western blot and PLA$_2$R ELISA results. 81
Figure 43: Evaluation of PLA$_2$R expression by immunofluorescence. 82
Figure 44: Evaluation of rat IgG deposition by immunofluorescence. 83
Figure 45: Electron microscopy of glomerulus and podocyte effacement evaluation. 85
Figure 46: Evaluation of complement deposition in the glomerulus. 85
Figure 47: Urine analysis. 86

8. Bibliography

Adams, R., et al. "Extending the halflife of a fab fragment through generation of a humanized anti-human serum albumin Fv domain: an investigation into the correlation between affinity and serum half-life. MAbs 2016; 8: 1336–46." *DOI* 10.19420862.2016: 1185581.

Adler, S. T. E. P. H. E. N. "Integrin receptors in the glomerulus: potential role in glomerular injury." *American Journal of Physiology-Renal Physiology* 262.5 (1992): F697-F704.

Alfaleh, M. A., et al. "Phage display derived monoclonal antibodies: from bench to bedside. Front Immunol 11: 1986." (2020).

Al-Rabadi, Laith Farah, et al. "Serine protease HTRA1 as a novel target antigen in primary membranous nephropathy." *Journal of the American Society of Nephrology* 32.7 (2021): 1666-1681.

Anatomy and Physiology. J. Gordon Betts, Kelly A. Young, James A. Wise, Eddie Johnson, Brandon Poe, Dean H. Kruse, Oksana Korol, Jody E. Johnson, Mark Womble, Peter DeSaix, 2013, *OpenStax*, https://openstax.org/books/anatomy-and-physiology/pages/references.

Ancian, Philippe, et al. "The human 180-kDa receptor for secretory phospholipases A2: molecular cloning, identification of a secreted soluble form, expression, and chromosomal localization." *Journal of Biological Chemistry* 270.15 (1995): 8963-8970.

Arif, Ehtesham, and Deepak Nihalani. "Glomerular filtration barrier assembly: an insight." *Postdoc journal: a journal of postdoctoral research and postdoctoral affairs* 1.4 (2013): 33.

Ayoub, Isabelle, et al. "Establishing a case for anti-complement therapy in membranous nephropathy." *Kidney International Reports* 6.2 (2021): 484-492.

Baker, P. J., et al. "Depletion of C6 prevents development of proteinuria in experimental membranous nephropathy in rats." *The American journal of pathology* 135.1 (1989): 185.
Banerjee, Ashis. *Clinical Physiology*. Cambridge University Press, 2005.

Barabas, Arpad Z., et al. "Production of Heymann nephritis by a chemically modified renal antigen." *International journal of experimental pathology* 85.5 (2004): 277-285.

Bech, Anneke P., et al. "Association of anti-PLA2R antibodies with outcomes after immunosuppressive therapy in idiopathic membranous nephropathy." *Clinical Journal of the American Society of Nephrology* 9.8 (2014): 1386-1392.

Beck Jr, Laurence H., et al. "M-type phospholipase A2 receptor as target antigen in idiopathic membranous nephropathy." *New England Journal of Medicine* 361.1 (2009): 11-21.

Beck, Laurence H., and David J. Salant. "Membranous nephropathy: from models to man." *The Journal of clinical investigation* 124.6 (2014): 2307-2314.

Brown Jr, Arnold L. "The structure of the nephron." *Medical Clinics of North America* 50.4 (1966): 927-935.

Burbelo, Peter D., et al. "Detection of PLA2R autoantibodies before the diagnosis of membranous nephropathy." *Journal of the American Society of Nephrology* 31.1 (2020): 208-217.

Cattran, Daniel. "Management of membranous nephropathy: when and what for treatment." *Journal of the American Society of Nephrology* 16.5 (2005): 1188-1194.

Caza, Tiffany N., et al. "NELL1 is a target antigen in malignancy-associated membranous nephropathy." *Kidney international* 99.4 (2021): 967-976.

Caza, Tiffany N., et al. "Neural cell adhesion molecule 1 is a novel autoantigen in membranous lupus nephritis." *Kidney international* 100.1 (2021): 171-181.

Chen, Ashton, et al. "Idiopathic membranous nephropathy in pediatric patients: presentation, response to therapy, and long-term outcome." *BMC nephrology* 8 (2007): 1-6.

Chung, Edmund YM, et al. "Membranous nephropathy: clearer pathology and mechanisms identify potential strategies for treatment." *Frontiers in Immunology* 13 (2022): 1036249.

Couser, W. G., et al. "Experimental glomerulonephritis in the isolated perfused rat kidney." *The Journal of clinical investigation* 62.6 (1978): 1275-1287.

Couser, William G. "Primary membranous nephropathy." *Clinical Journal of the American Society of Nephrology* 12.6 (2017): 983-997.

Couser, William G. "Primary membranous nephropathy." *Clinical Journal of the American Society of Nephrology* 12.6 (2017): 983-997.

Cupps, T. R., L. C. Edgar, and A. S. Fauci. "Suppression of human B lymphocyte function by cyclophosphamide." *Journal of immunology (Baltimore, Md.: 1950)* 128.6 (1982): 2453-2457.

Cybulsky, Andrpy V., et al. "Complement-induced glomerular epithelial cell injury. Role of the membrane attack complex in rat membranous nephropathy." *The Journal of clinical investigation* 77.4 (1986): 1096-1107.

Cybulsky, ANDREY V., et al. "Complement C5b-9 complex activates phospholipases in glomerular epithelial cells." *American Journal of Physiology-Renal Physiology* 257.5 (1989): F826-F836.

Cybulsky, Andrey V., Richard J. Quigg, and David J. Salant. "Experimental membranous nephropathy redux." *American Journal of Physiology-Renal Physiology* 289.4 (2005): F660-F671.

Cybulsky, A. V., et al. "A role for thromboxane in complement-mediated glomerular injury." *The American journal of pathology* 128.1 (1987): 45.

Cybulsky, Andrey V., et al. "Complement C5b-9 membrane attack complex increases expression of endoplasmic reticulum stress proteins in glomerular epithelial cells." *Journal of Biological Chemistry* 277.44 (2002): 41342-41351.

Cybulsky, Andrey V., et al. "Role of the endoplasmic reticulum unfolded protein response in glomerular epithelial cell injury." *Journal of Biological Chemistry* 280.26 (2005): 24396-24403.

Daehn, Ilse S., and Jeremy S. Duffield. "The glomerular filtration barrier: a structural target for novel kidney therapies." *Nature Reviews Drug Discovery* 20.10 (2021): 770-788.

Dahan, Karine, et al. "Rituximab for severe membranous nephropathy: a 6-month trial with extended follow-up." *Journal of the American Society of Nephrology* 28.1 (2017): 348-358.

Davies, C. de L., et al. "Comparison of IgG diffusion and extracellular matrix composition in rhabdomyosarcomas grown in mice versus in vitro as spheroids reveals the role of host stromal cells." *British journal of cancer* 86.10 (2002): 1639-1644.

Debiec, Hanna, et al. "Antenatal membranous glomerulonephritis due to anti–neutral endopeptidase antibodies." *New England Journal of Medicine* 346.26 (2002): 2053-2060.

East, Lucy, and Clare M. Isacke. "The mannose receptor family." *Biochimica et Biophysica Acta (BBA)-General Subjects* 1572.2-3 (2002): 364-386.

Ebefors, Kerstin, Lovisa Bergwall, and Jenny Nyström. "The glomerulus according to the mesangium." *Frontiers in Medicine* 8 (2022): 740527.

ENSG00000165973-NELL1/tissue/kidney. Accessed February 10, 2025.

Farquhar, Marilyn G., et al. "The Heymann nephritis antigenic complex: megalin (gp330) and RAP." *Journal of the American Society of Nephrology* 6.1 (1995): 35-47.

Faul, Christian, et al. "The actin cytoskeleton of kidney podocytes is a direct target of the antiproteinuric effect of cyclosporine A." *Nature medicine* 14.9 (2008): 931-938.

Faulds, Diana, and Eugene M. Sorkin. "Abciximab (c7E3 Fab) A Review of its Pharmacology and Therapeutic Potential in Ischaemic Heart Disease." *Drugs* 48 (1994): 583-598.

Fehmi, Janev, et al. "Contactin-1 links autoimmune neuropathy and membranous glomerulonephritis." *PloS one* 18.3 (2023): e0281156.

Fervenza, F.C. et al.”Rituximab treatment of idiopathic membranous nephropathy” Fervenza, Fernando C., et al. "Rituximab or cyclosporine in the treatment of membranous nephropathy." *New England Journal of Medicine* 381.1 (2019): 36-46.

Finch, Natalie C., et al. "The unique structural and functional characteristics of glomerular endothelial cell fenestrations and their potential as a therapeutic target in kidney disease." *American Journal of Physiology-Renal Physiology* 325.4 (2023): F465-F478.

Fresquet, Maryline, et al. "Identification of a major epitope recognized by PLA2R autoantibodies in primary membranous nephropathy." *Journal of the American Society of Nephrology* 26.2 (2015): 302-313.

Fung, John J., et al. "Use of OKT3 with ciclosporin and steroids for reversal of acute kidney and liver allograft rejection." *Nephron* 46.Suppl. 1 (1987): 19-33.

Gallardo, Pedro A., and Carlos P. Vio. "Functional anatomy of the kidney." *Renal Physiology and Hydrosaline Metabolism*. Cham: Springer International Publishing, 2022. 7-28.

Glassock, Richard J. "Diagnosis and natural course of membranous nephropathy." *Seminars in nephrology*. Vol. 23. No. 4. WB Saunders, 2003.

Gogesch, Patricia, et al. "The role of Fc receptors on the effectiveness of therapeutic monoclonal antibodies." *International Journal of Molecular Sciences* 22.16 (2021): 8947.

Golbus, Ashley L., et al. "Immunosuppressive regimens in porcine transplantation models." *Transplantation Reviews* 36.4 (2022): 100725.

Grumont, Raelene J., and Steve Gerondakis. "Rel induces interferon regulatory factor 4 (IRF-4) expression in lymphocytes: modulation of interferon-regulated gene expression by rel/nuclear factor κB." *The Journal of experimental medicine* 191.8 (2000): 1281-1292.

H. Nakamura, BALB/c Mouse, Editor(s): Stanley Maloy, Kelly Hughes, Brenner's Encyclopedia of Genetics (Second Edition),Academic Press,2013,Pages 290-292,ISBN 9780080961569, https://doi.org/10.1016/B978-0-12-374984-0.00133-9.

Haddad, George, et al. "Altered glycosylation of IgG4 promotes lectin complement pathway activation in anti-PLA2R1–associated membranous nephropathy." *The Journal of clinical investigation* 131.5 (2021).

Harvey, Scott J., et al. "Disruption of glomerular basement membrane charge through podocyte-specific mutation of agrin does not alter glomerular permselectivity." *The American journal of pathology* 171.1 (2007): 139-152.

Herwig, Johanna, et al. "Thrombospondin type 1 domain–containing 7A localizes to the slit diaphragm and stabilizes membrane dynamics of fully differentiated podocytes." *Journal of the American Society of Nephrology* 30.5 (2019): 824-839.

Heymann, Walter, et al. "Production of nephrotic syndrome in rats by Freund's adjuvants and rat kidney suspensions." *Proceedings of the Society for Experimental Biology and Medicine* 100.4 (1959): 660-664.

Heymann, Walter, et al. "Production of nephrotic syndrome in rats by Freund's adjuvants and rat kidney suspensions." *Proceedings of the Society for Experimental Biology and Medicine* 100.4 (1959): 660-664.

Howman, Andrew, et al. "Immunosuppression for progressive membranous nephropathy: a UK randomised controlled trial." *The Lancet* 381.9868 (2013): 744-751.

Hoxha, Elion, et al. "An indirect immunofluorescence method facilitates detection of thrombospondin type 1 domain–containing 7A–specific antibodies in membranous nephropathy." *Journal of the American Society of Nephrology* 28.2 (2017): 520-531.

Hoxha, Elion, et al. "Phospholipase A2 receptor autoantibodies and clinical outcome in patients with primary membranous nephropathy." *Journal of the American Society of Nephrology* 25.6 (2014): 1357-1366.

Hoxha, Elion, et al. "Phospholipase A2 receptor autoantibodies and clinical outcome in patients with primary membranous nephropathy." *Journal of the American Society of Nephrology* 25.6 (2014): 1357-1366.

Hoxha, Elion, et al. "PLA2R antibody levels and clinical outcome in patients with membranous nephropathy and non-nephrotic range proteinuria under treatment with inhibitors of the renin-angiotensin system." *PloS one* 9.10 (2014): e110681.

Hoxha, Elion, Linda Reinhard, and Rolf AK Stahl. "Membranous nephropathy: new pathogenic mechanisms and their clinical implications." *Nature Reviews Nephrology* 18.7 (2022): 466-478.

Jacobs, Roland, et al. "Detection and quantification of rituximab in the human urine." *Journal of Immunological Methods* 451 (2017): 118-121.

Janeway, Charles A., et al. *Immunobiologie*. De Boeck Supérieur, 2009.

Kaufman, Daniel P., Hajira Basit, and Stephen J. Knohl. "Physiology, glomerular filtration rate." (2018).

Kerjaschki, Dontscho, and Marilyn Gist Farquhar. "The pathogenic antigen of Heymann nephritis is a membrane glycoprotein of the renal proximal tubule brush border." *Proceedings of the National Academy of Sciences* 79.18 (1982): 5557-5561.

Kerjaschki, D. O. N. T. S. C. H. O., A. A. R. O. Miettinen, and MARILYN GIST Farquhar. "Initial events in the formation of immune deposits in passive Heymann nephritis. gp330-anti-gp330 immune complexes form in epithelial coated pits and rapidly become attached to the glomerular basement membrane." *The Journal of experimental medicine* 166.1 (1987): 109-128.

Kerjaschki, Dontscho, and Thomas James Neale. "Molecular mechanisms of glomerular injury in rat experimental membranous nephropathy (Heymann nephritis)." *Journal of the American Society of Nephrology* 7.12 (1996): 2518-2526.
Kidney International, Volume 73, Issue 1, (2008): 117 – 125.

Kitzler, Thomas M., et al. "Complement modulates the function of the ubiquitin–proteasome system and endoplasmic reticulum-associated degradation in glomerular epithelial cells." *Biochimica et Biophysica Acta (BBA)-Molecular Cell Research* 1823.5 (2012): 1007-1016.

Köhler, Georges, and Cesar Milstein. "Continuous cultures of fused cells secreting antibody of predefined specificity." *nature* 256.5517 (1975): 495-497.

Larsen, Christopher P., et al. "LDL receptor-related protein 2 (megalin) as a target antigen in human kidney anti-brush border antibody disease." *Journal of the American Society of Nephrology* 29.2 (2018): 644-653.

Le Quintrec, Moglie, et al. "Contactin-1 is a novel target antigen in membranous nephropathy associated with chronic inflammatory demyelinating polyneuropathy." *Kidney International* 100.6 (2021): 1240-1249.

Lennon, Rachel, Michael J. Randles, and Martin J. Humphries. "The importance of podocyte adhesion for a healthy glomerulus." *Frontiers in endocrinology* 5 (2014): 160.

Liu, Hua, et al. "Cytochrome P450 2B1 mediates complement-dependent sublytic injury in a model of membranous nephropathy." *Journal of Biological Chemistry* 285.52 (2010): 40901-40910.

Liu, Justin KH. "The history of monoclonal antibody development–progress, remaining challenges and future innovations." *Annals of medicine and surgery* 3.4 (2014): 113-116.
Liu, Ting, et al. "NF-κB signaling in inflammation." *Signal transduction and targeted therapy* 2.1 (2017): 1-9.

Lonberg, Nils. "Human antibodies from transgenic animals." *Nature biotechnology* 23.9 (2005): 1117-1125.

Lu, Jing, et al. "Regulatory effects of IRF4 on immune cells in the tumor microenvironment." *Frontiers in immunology* 14 (2023): 1086803.

Madrazo-Ibarra, Antonio, and Pradeep Vaitla. "Histology, nephron." *StatPearls [Internet]*. StatPearls Publishing, 2023.

Mahmud, Maida, et al. "Role of phospholipase A2 receptor 1 antibody level at diagnosis for long-term renal outcome in membranous nephropathy." *PLoS One* 14.9 (2019): e0221293.

Malik, B., and A. Ghatol. "Understanding How Monoclonal Antibodies Work.[Updated 2023 Jun 26]." *StatPearls [Internet]. Treasure Island (FL): StatPearls Publishing* (2023).

Marinaki, S., C. Skalioti, and J. N. Boletis. "B cell depletion: rituximab in glomerular disease and transplantation." *Nephron Extra* 3.1 (2013): 125-130.

McCafferty, John, et al. "Phage antibodies: filamentous phage displaying antibody variable domains." *nature* 348.6301 (1990): 552-554.

McGrogan, Anita, Casper FM Franssen, and Corinne S. de Vries. "The incidence of primary glomerulonephritis worldwide: a systematic review of the literature." *Nephrology Dialysis Transplantation* 26.2 (2011): 414-430.

McMillan, James I., et al. "Characterization of a glomerular epithelial cell metalloproteinase as matrix metalloproteinase-9 with enhanced expression in a model of membranous nephropathy." *The Journal of clinical investigation* 97.4 (1996): 1094-1101.

Meyer-Schwesinger, Catherine, et al. "A novel mouse model of phospholipase A2 receptor 1-associated membranous nephropathyámimics podocyte injury in patients." *Kidney International* 97.5 (2020): 913-919.

Michel, C. C., and F. E. Curry. "Microvascular permeability." *Physiological reviews* (1999).
Miner, Jeffrey H. "The glomerular basement membrane." *Experimental cell research* 318.9 (2012): 973-978.

Meyer-Schwesinger, Catherine, et al. "Ubiquitin C-terminal hydrolase-l1 activity induces polyubiquitin accumulation in podocytes and increases proteinuria in rat membranous nephropathy." *The American journal of pathology* 178.5 (2011): 2044-2057.

Mitchell, Simon, Jesse Vargas, and Alexander Hoffmann. "Signaling via the NFκB system." *Wiley Interdisciplinary Reviews: Systems Biology and Medicine* 8.3 (2016): 227-241.

Mudge, Stuart J., et al. "Activation of nuclear factor-κB by podocytes in the autologous phase of passive Heymann nephritis." *Kidney international* 59.3 (2001): 923-931.

Neale, T. James, et al. "Proteinuria in passive Heymann nephritis is associated with lipid peroxidation and formation of adducts on type IV collagen." *The Journal of clinical investigation* 94.4 (1994): 1577-1584.

Neale, T. James, et al. "Reactive oxygen species and neutrophil respiratory burst cytochrome b558 are produced by kidney glomerular cells in passive Heymann nephritis." *Proceedings of the National Academy of Sciences* 90.8 (1993): 3645-3649.

Noble, Bernice, et al. "Factors influencing susceptibility of LEW rats to Heymann nephritis." *Clinical Immunology and Immunopathology* 30.2 (1984): 241-254.

Ogobuiro, Ifeanyichukwu, and Faiz Tuma. "Physiology, renal." (2019).
Ohlson, Maria, Jenny Sörensson, and Börje Haraldsson. "Glomerular size and charge selectivity in the rat as revealed by FITC-Ficoll and albumin." *American Journal of Physiology-Renal Physiology* 279.1 (2000): F84-F91.

Pan, Yangbin, et al. "sPLA2 IB induces human podocyte apoptosis via the M-type phospholipase A2 receptor." *Scientific Reports* 4.1 (2014): 6660.

Passot, C., et al. "Influence of FCGRT gene polymorphisms on pharmacokinetics of therapeutic antibodies, MAbs 5 (4)(2013) 614–619."

Patrakka, Jaakko, and Karl Tryggvason. "New insights into the role of podocytes in proteinuria." *Nature Reviews Nephrology* 5.8 (2009): 463-468.

Pavenstadt, Hermann, Wilhelm Kriz, and Matthias Kretzler. "Cell biology of the glomerular podocyte." *Physiological reviews* 83.1 (2003): 253-307.

Pavenstadt, Hermann, Wilhelm Kriz, and Matthias Kretzler. "Cell biology of the glomerular podocyte." *Physiological reviews* 83.1 (2003): 253-307.

Penny, Mark J., Rochelle A. Boyd, and Bruce M. Hall. "Permanent CD8+ T cell depletion prevents proteinuria in active Heymann nephritis." *The Journal of experimental medicine* 188.10 (1998): 1775-1784.

Perkinson, D. T., et al. "Membrane attack complex deposition in experimental glomerular injury." *The American journal of pathology* 120.1 (1985): 121.

Polanco, Natalia, et al. "Spontaneous remission of nephrotic syndrome in idiopathic membranous nephropathy." *Journal of the American Society of Nephrology* 21.4 (2010): 697-704.
Pippin, Jeffrey W., et al. "DNA damage is a novel response to sublytic complement C5b-9–induced injury in podocytes." *The Journal of clinical investigation* 111.6 (2003): 877-885.

Pippin, Jeffrey W., et al. "Inducible rodent models of acquired podocyte diseases." *American Journal of Physiology-Renal Physiology* 296.2 (2009): F213-F229.

Ponticelli, Claudio, et al. "A randomized trial of methylprednisolone and chlorambucil in idiopathic membranous nephropathy." *New England Journal of Medicine* 320.1 (1989): 8-13.

Ponticelli, Claudio, et al. "Controlled trial of methylprednisolone and chlorambucil in idiopathic membranous nephropathy." *New England Journal of Medicine* 310.15 (1984): 946-950.

Quan, Xiao-ying, et al. "Revisited cyclophosphamide in the treatment of lupus nephritis." *BioMed Research International* 2022.1 (2022): 8345737.

Quinteros, Daniela A., et al. "Therapeutic use of monoclonal antibodies: general aspects and challenges for drug delivery." *Nanostructures for drug delivery*. Elsevier, 2017. 807-833.

Quiza, Cesar G., Peter L. Leenaerts, and Bruce M. Hall. "The role of T cells in the mediation of glomerular injury in Heymann's nephritis in the rat." *International immunology* 4.4 (1992): 423-432.

Ramachandran, R., et al. "Temporal association between PLA2R antibodies and clinical outcomes in primary membranous nephropathy." *Kidney international reports* 3.1 (2018): 142-147.

Ravindran, Aishwarya, et al. "Proteomic analysis of complement proteins in membranous nephropathy." *Kidney international reports* 5.5 (2020): 618-626.

Reinhard, Linda, et al. "Clinical relevance of domain-specific phospholipase A2 receptor 1 antibody levels in patients with membranous nephropathy." *Journal of the American Society of Nephrology* 31.1 (2020): 197-207.

Reinhard, Linda, et al. "Netrin G1 is a novel target antigen in primary membranous nephropathy." *Journal of the American Society of Nephrology* 33.10 (2022): 1823-1831.

Reinhard, Linda, et al. "Pathogenicity of human anti-PLA2R1 antibodies in minipigs: a pilot study." *Journal of the American Society of Nephrology* 34.3 (2023): 369-373.

Reitsma, Sietze, et al. "The endothelial glycocalyx: composition, functions, and visualization." *Pflügers Archiv-European Journal of Physiology* 454 (2007): 345-359.

Remuzzi, Giuseppe, et al. "Rituximab for idiopathic membranous nephropathy." *The Lancet* 360.9337 (2002): 923-924.

Richards, J. M., N. J. Vogelzang, and J. A. Bluestone. "Neurotoxicity after treatment with muromonab-CD3." *The New England Journal of Medicine* 323.7 (1990): 487-488.

Rinschen, Markus M., et al. "A multi-layered quantitative in vivo expression atlas of the podocyte unravels kidney disease candidate genes." *Cell reports* 23.8 (2018): 2495-2508.

Ronco, P., Beck, L., Debiec, H., Fervenza, F. C., Hou, F. F., Jha, V.& Wetzels, J. (2021). Membranous nephropathy. *Nature reviews Disease primers*, *7*(1), 69.

Rovin, Brad H., et al. "KDIGO 2021 clinical practice guideline for the management of glomerular diseases." *Kidney international* 100.4 (2021): S1-S276.

Ryman, Josiah T., and Bernd Meibohm. "Pharmacokinetics of monoclonal antibodies." *CPT: pharmacometrics & systems pharmacology* 6.9 (2017): 576-588.

Salant, DAVID J., et al. "A new role for complement in experimental membranous nephropathy in rats." *The Journal of clinical investigation* 66.6 (1980): 1339-1350.

Salant, David J., Richard J. Quigg, and Andrey V. Cybulsky. "Heymann nephritis: mechanisms of renal injury." *Kidney international* 35.4 (1989): 976-984.

Santoro, Domenico, et al. "Contactin 1, a potential new antigen target in membranous nephropathy: a case report." *American Journal of Kidney Diseases* 80.2 (2022): 289-294.

Saran, Anita M., et al. "Complement mediates nephrin redistribution and actin dissociation in experimental membranous nephropathy." *Kidney international* 64.6 (2003): 2072-2078.

Satchell, Simon C., and Filip Braet. "Glomerular endothelial cell fenestrations: an integral component of the glomerular filtration barrier." *American Journal of Physiology-Renal Physiology* 296.5 (2008): F947-F956.

Scolari, Francesco, et al. "Rituximab or cyclophosphamide in the treatment of membranous nephropathy: the RI-CYCLO randomized trial." *Journal of the American Society of Nephrology* 32.4 (2021): 972-982.

Scott, Rizaldy P., and Susan E. Quaggin. "The cell biology of renal filtration." *Journal of cell biology* 209.2 (2015): 199-210.

Seifert, Larissa, et al. "The classical pathway triggers pathogenic complement activation in membranous nephropathy." *Nature Communications* 14.1 (2023): 473.

Seifert, Larissa, et al. "The most N-terminal region of THSD7A is the predominant target for autoimmunity in THSD7A-associated membranous nephropathy." *Journal of the American Society of Nephrology* 29.5 (2018): 1536-1548.

Seitz-Polski, Barbara, et al. "Epitope spreading of autoantibody response to PLA2R associates with poor prognosis in membranous nephropathy." *Journal of the American Society of Nephrology* 27.5 (2016): 1517-1533.

Sekula, Peggy, et al. "Genetic risk variants for membranous nephropathy: extension of and association with other chronic kidney disease aetiologies." *Nephrology Dialysis Transplantation* 32.2 (2017): 325-332.

Sethi, Sanjeev, et al. "Neural epidermal growth factor-like 1 protein (NELL-1) associated membranous nephropathy." *Kidney international* 97.1 (2020): 163-174.

Sethi, Sanjeev, et al. "Semaphorin 3B–associated membranous nephropathy is a distinct type of disease predominantly present in pediatric patients." *Kidney international* 98.5 (2020): 1253-1264.

Shah, Monarch, Andrew DeLaat, and Corey Cavanaugh. "Treatment of membranous nephropathy: Perspectives on current and future therapies." *Frontiers in Nephrology* 3 (2023): 1110355.

Shankland, Stuart J., et al. "Differential expression of transforming growth factor-β isoforms and receptors in experimental membranous nephropathy." *Kidney international* 50.1 (1996): 116-124.

Sharma, Prerna, et al. "Therapeutic antibodies in medicine." *Molecules* 28.18 (2023): 6438.

Simmonds, M. J., and S. C. L. Gough. "The HLA region and autoimmune disease: associations and mechanisms of action." *Current genomics* 8.7 (2007): 453-465.

Sinico, R. A., et al. "Immunology of membranous nephropathy: from animal models to humans." *Clinical & Experimental Immunology* 183.2 (2016): 157-165.

Sörensson, Jenny, Maria Ohlson, and Börje Haraldsson. "A quantitative analysis of the glomerular charge barrier in the rat." *American Journal of Physiology-Renal Physiology* 280.4 (2001): F646-F656.

Soriano, Roberto M., Dana Penfold, and Stephen W. Leslie. "Anatomy, abdomen and pelvis, kidneys." (2018).

Spicer, S. Timothy, et al. "Induction of passive Heymann nephritis in complement component 6-deficient PVG rats." *The Journal of Immunology* 179.1 (2007): 172-178.
Stahl, Phillip R., et al. "THSD7A expression in human cancer." *Genes, Chromosomes and Cancer* 56.4 (2017): 314-327.

Stanescu, Horia C., et al. "Risk HLA-DQA1 and PLA2R1 alleles in idiopathic membranous nephropathy." *New England Journal of Medicine* 364.7 (2011): 616-626.

Takano, Tomoko, and Andrey V. Cybulsky. "Complement C5b-9-mediated arachidonic acid metabolism in glomerular epithelial cells: role of cyclooxygenase-1 and-2." *The American journal of pathology* 156.6 (2000): 2091-2101.

Tapia, Carolina, and Khalid Bashir. "Nephrotic syndrome." (2017).

Teisseyre, Maxime, et al. "Rituximab immunomonitoring predicts remission in membranous nephropathy." *Frontiers in Immunology* 12 (2021): 738788.

The Human Protein Atlas. NELL1. Available at: www.proteinatlas.org/
Tomas, Nicola M., et al. "Podocyte expression of human phospholipase A2 receptor 1 causes immune-mediated membranous nephropathy in mice." *Kidney international* 103.2 (2023): 297-303.

Tomas, Nicola M., et al. "Thrombospondin type-1 domain-containing 7A in idiopathic membranous nephropathy." *New England Journal of Medicine* 371.24 (2014): 2277-2287.
Tomas, Nicola M., et al. "A heterologous model of thrombospondin type 1 domain-containing 7A-associated membranous nephropathy." *Journal of the American Society of Nephrology* 28.11 (2017): 3262-3277.

Topham, Peter S., et al. "Complement-mediated injury reversibly disrupts glomerular epithelial cell actin microfilaments and focal adhesions." *Kidney international* 55.5 (1999): 1763-1775.

Tryggvason, Karl, Jaakko Patrakka, and Jorma Wartiovaara. "Hereditary proteinuria syndromes and mechanisms of proteinuria." *New England Journal of Medicine* 354.13 (2006): 1387-1401.
UniProt: the universal protein knowledgebase in 2023. *Nucleic acids research*, 2023, 51.D1: D523-D531.

Van den Brand, Jan AJG, et al. "Long-term outcomes in idiopathic membranous nephropathy using a restrictive treatment strategy." *Journal of the American Society of Nephrology* 25.1 (2014): 150-158.

Van den Brand, Jan AJG, et al. "Safety of rituximab compared with steroids and cyclophosphamide for idiopathic membranous nephropathy." *Journal of the American Society of Nephrology* 28.9 (2017): 2729-2737.

Van Den Hoven, M. J., et al. "Reduction of anionic sites in the glomerular basement membrane by heparanase does not lead to proteinuria." *Kidney international* 73.3 (2008): 278-287.

Verma, Priyanshu R., and Praful Patil. "Nephrotic syndrome: A review." *Cureus* 16.2 (2024).

Von Haxthausen, Franziska, et al. "Antigen-specific IgG subclasses in primary and malignancy-associated membranous nephropathy." *Frontiers in immunology* 9 (2018): 3035.

Xenaki, Katerina T., Sabrina Oliveira, and Paul MP van Bergen En Henegouwen. "Antibody or antibody fragments: implications for molecular imaging and targeted therapy of solid tumors." *Frontiers in immunology* 8 (2017): 1287.

Xie, Jingyuan, et al. "The genetic architecture of membranous nephropathy and its potential to improve non-invasive diagnosis." *Nature communications* 11.1 (2020): 1600.

Xu, Jie, et al. "The fate of immune complexes in membranous nephropathy." *Frontiers in Immunology* 15 (2024): 1441017.

Zhang, Mu-fan, et al. "Clinical and prognostic significance of glomerular C1q deposits in primary MN." *Clinica Chimica Acta* 485 (2018): 152-157.

Zvaritch, Elena, Gérard Lambeau, and Michel Lazdunski. "Endocytic Properties of the M-type 180-kDa Receptor for Secretory Phospholipases A2 (∗)." *Journal of Biological Chemistry* 271.1 (1996): 250-257.

9. Note of thanks

I would like to thank all the people who guided and supported me throughout my PhD journey:

First, I would like to express my deepest gratitude to my first mentor, Professor Dr. Rolf AK Stahl, who sadly passed away too early before this work could be completed. He always believed in me and instilled in me the passion for asking new questions keeping high the curiosity above all.

A special thanks and a lot of gratitude goes to Professor Dr. Elion Hoxha, who kindly took over Professor Stahl's role and guided me with patience, insightful ideas and stimulating discussions. His support helped me to grow not only as a researcher but also as a thinker.

I am also very grateful to my supervisor, Dr. Linda Reinhard, for her support with everyday challenges in the laboratory, professional guidance and valuable suggestions.

My heartfelt thanks goes to all the members of my working group, technicians and students, who not only gave me professional help but also emotional support to fill every day in the lab with smiles and friendship. I would like to thank the animal facility staff of the University Medical Center Hamburg-Eppendorf, who welcomed me into a kind and supportive team and assisted me with professionalism and dedication through every challenge.

Finally, I owe the deepest gratitude to my family and friends for their love, encouragement and wise advice throughout this journey.

10. Curriculum Vitae

Personal informations	Name	Nicoletta Ferru
	Date of birth	10.01.1993
	Place of birth	Cagliari, Italy
Education	2012-2016	Bachelor of science, Università degli studi di Cagliari
	2016-2018	Master of science, Università degli studi di Cagliari
	11/2018-01/2019	Internship at Mount Sinai Hospital, Toronto
Work experience	2020-2025	Non-medical PhD program, University medical center Hamburg-Eppendorf

Publications

Reinhard L, Machalitza M, Wiech T, Gröne HJ, Lassé M, Rinschen M, **Ferru N**, Bräsen JH, Drömann F, Rob PMaria, Sethi S, Hoxha E, Stahl RAK (2022): Netrin G1 Is a Novel Target Antigen in Primary Membranous Nephropathy. *Journal of the American Society of Nephrology* 33(10): p 1823-1831, October 2022. | DOI: 10.1681/ASN.2022050608

Reinhard L, Wiech T, Reitmeier A, Lassé M, Machalitza M, Heumann A, **Ferru N**, Loreth D, Schröder ML, Hutzfeldt A, Stahl FR, Peine S, Gröne HJ, Meyer-Schwesinger C, Rinschen MM, Stahl RAK, Hoxha E (2023): Pathogenicity of Human Anti-PLA_2R1 Antibodies in Minipigs: A Pilot Study. *Journal of the American Society of Nephrology* 34(3): p 369-373, March 2023. | *DOI:* 10.1681/ASN.0000000000000068

Machalitza M, Debiec H, Krümpelmann B, **Ferru N**, Kilictas ME, Huber TB, Reinhard L, Wiech T, Ronco P, Hoxha E (2025): PCDH7-antibodies and PCDH7 immune deposits are mostly found in patients with PLA2R1- or NELL1-associated membranous nephropathy. *Kidney International* Research LetterVolume 107, Issue 1p188-191January 2025 | DOI: 10.1016/j.kint.2024.10.012

11. Statutory declaration

Eidesstattliche Versicherung

Ich versichere ausdrücklich, dass ich die Arbeit selbständig und ohne fremde Hilfe, insbesondere ohne entgeltliche Hilfe von Vermittlungs- und Beratungsdiensten, verfasst, andere als die von mir angegebenen Quellen und Hilfsmittel nicht benutzt und die aus den benutzten Werken wörtlich oder inhaltlich entnommenen Stellen einzeln nach Ausgabe (Auflage und Jahr des Erscheinens), Band und Seite des benutzten Werkes kenntlich gemacht habe. Das gilt insbesondere auch für alle Informationen aus Internetquellen. Soweit beim Verfassen der Dissertation KI-basierte Tools („Chatbots“) verwendet wurden, versichere ich ausdrücklich, den daraus generierten Anteil deutlich kenntlich gemacht zu haben. Die „Stellungnahme des Präsidiums der Deutschen Forschungsgemeinschaft (DFG) zum Einfluss generativer Modelle für die Text- und Bilderstellung auf die Wissenschaften und das Förderhandeln der DFG“ aus September 2023 wurde dabei beachtet. Ferner versichere ich, dass ich die Dissertation bisher nicht einem Fachvertreter an einer anderen Hochschule zur Überprüfung vorgelegt oder mich anderweitig um Zulassung zur Promotion beworben habe. Ich erkläre mich damit einverstanden, dass meine Dissertation vom Dekanat der Medizinischen Fakultät mit einer gängigen Software zur Erkennung von Plagiaten überprüft werden kann.

Unterschrift: .....